Encapsulation of T4 Bacteriophage in Electrospun Biopolymers

by

Reza Korehei

MSc., University of British Columbia, 2007

A THESIS SUBMITTED IN PARTIAL FULFILLMENT OF

THE REQUIREMENTS FOR THE DEGREE OF

DOCTOR OF PHILOSOPHY

in

THE FACULTY OF GRADUATE STUDIES

(Forestry)

THE UNIVERSITY OF BRITISH COLUMBIA

(Vancouver)

April 2013

© Reza Korehei, 2013

Abstract

Packaging foods with antibacterial electrospun fibrous mats, in particular the incorporation of bacteria specific viruses such as bacteriophages may address concerns triggered by recent waves of bacterial food contamination. To this end several methods for incorporating or encapsulating T4 bacteriophage into electrospun fibres were investigated. The incorporation of T4 bacteriophage using simple suspension electrospinning lead to major losses in T4 bacteriophage activity, with more than five-orders of magnitude decrease in activity being observed. Improved T4 bacteriophage viability was obtained using two newly developed electrospinning processes, emulsion and coaxial electrospinning. In emulsion electrospinning, T4 bacteriophage was pre-encapsulated in an alginate reservoir via an emulsification process and subsequently electrospun into fibres. The emulsion electrospun fibres exhibited only two-orders of magnitude decrease in T4 bacteriophage activity. By contrast, complete T4 bacteriophage activity was maintained when coaxial electrospinning was employed. In the coaxial electrospinning process, a core/shell fibre structure was formed where the T4 bacteriophage was allocated to the fibre core, protected by the outer polymer shell. Depending on the polymer system used the rate of T4 bacteriophage release from the coaxial electrospun fibres varied. When hydrophilic poly(ethylene oxide) (PEO) was used as the polymer shell layer, immediate release of T4 bacteriophage was observed upon exposure to buffer. Increasing the PEO molecular weight increased the electrospun fibre diameter and viscosity of the releasing medium, which resulted in relatively slower T4 bacteriophage release profiles. Similarly, the blending of cellulose diacetate (CDA) with PEO dramatically decreased the release behaviour. Depending on the PEO/CDA ratio, post-release electrospun fibre morphology varied from discontinuous fibres to minimally swollen fibres, consistent with the release profiles.

In the PEO fibres the mechanism of T4 bacteriophage release is likely through solvent activation/polymer dissolution, while in the PEO/CDA blends a more diffusion control mechanism likely prevails. The Encapsulation of T4 bacteriophage within the electrospun fibres also improved T4 bacteriophage storability; full T4 bacteriophage activity was maintained for more than a month at +4 °C, as compared to only hours for non-encapsulated phage. These results are significant in the context of controlling and preventing bacterial infections in perishable foods during refrigerated storage.

Table of Contents

List of Tables

List of Figures

List of Symbols and Abbreviations

°C	Degrees Celsius
Alg	Alginate
AOT	Sodium bis(2-ethylhexyl) sulfosuccinate
BSA	Bovine serum albumin
$CaCl_2$	Calcium Chloride
CDA	Cellulose diacetate
CFU	Colony forming units
$CHCl_3$	Chloroform
DCM	Dichloromethane
DMF	N,N,-dimethyl formamide
DMSO	Dimethyl sulfoxide
DS	Degree of substitution
DSC	Differential scanning calorimetry
E. coli B	Escherichia coli B strain
ES	Electrospinning
FITC	Fluorescein isothiocyanate
FTIR	Fourier Transform Infrared
H_2O	Water
HPLC	High pressure liquid chromatography
LCSM	Laser confocal scanning microscopy
MeOH	Methanol
mg	Milligram

mL	Millilitre
M_n	Number-averaged molecular weight
M_w	Weight-averaged molecular weight
NaOH	Sodium hydroxide
nm	Nanometer
O/W	Oil-in-water
PBS	Phosphate buffered saline
PCL	Poly (caprolactone)
PDI	Polydispersity index
PEO	Poly (ethylene oxide)
PFU	Plaque forming unit
PLGA	poly(D,L-lactic acid-*co*-glycolic acid)
PLLA	poly(D,L-lactic acid)
PMMA	poly(methyl methacrylate)
PVA	poly(vinyl alcohol)
SDS	Sodium dodecyl sulfate
SEM	Scanning electron microscopy
SM	storage medium buffer
TEM	Transition electron microscope
TSA	Tryptic soy agar
TSB	Tryptic soy broth
T_g	Glass transition temperature
TGA	Thermogravimetric analysis

THF	Tetrahydrofuran
T_m	Melting transition temperature
UV	Ultraviolet
W/O	Water-in-oil
XRD	X-ray diffraction
μg	Microgram
μL	Microlitre
μm	Micrometer

Acknowledgements

I would like to begin by expressing my deep gratitude to my advisor, Dr. John Kadla, for being my mentor as I pursued my Ph.D., for the encouragement and guidance he gave me at challenging milestones in my project. I would also like to acknowledge the support of my advisory committee members Dr. Frank Ko and Dr. Helen Burt, for devoting time to helping me in many aspects of my research project.

I would also like to convey my special thanks to all my examination committee members Dr. Phil Evans, Dr. Tim Durance, Dr. Jay Kizhakkedathu and Dr. Sam Hudson for their valuable time and support. I would also like to thank Dr. Shawn Mansfield and all the staff in the Department of Wood Science for their friendly support during my lab work. I will always be extremely grateful to my lab mates in the biomaterial group and my heartfelt thanks for Mrs. Ana Xavier for her friendship and support during challenging times. I would also like to thank Dr. Mansel Griffiths from University of Guelph and his lab members for training and providing materials and also NSERC Sentinel Bioactive Paper Network in Canada for their financial support of this project.

My parents deserve special mention for their inseparable support and prayers. My late father, in the first place was the person who put the fundament of my learning character, showed me the joy of intellectual pursuit when I was a child. My mother is the one who sincerely raised me with her caring and gentle love. I also want to thank Shirin and Ali for being supportive and caring siblings. Words fail me to express my appreciation to my wife Helia whose love and persistent confidence in me, has taken the load off my shoulder. I owe her for great support and taking care of our children, Shanai and Arshan while I was engaged in this study. Without her support I would never have succeeded and I hope she enjoys the effort being completed. I would also thank Jalali's family for letting me take her hand in marriage, and accepting me as a member of the family.

To my wife Helia

Chapter 1: Introduction

1.1 Historical and practical explanation of the electrospinning process

Electrospinning is a process that employs electrostatic forces to draw continuous fibres from polymer solutions or melts (i.e. molten solutions). Electrospun fibres have a very small diameter, typically in the range of nano- or micrometers (Seeram 2005; Andrady 2008). In the electrospinning process, a spinneret containing a polymer solution or melt is charged to create an electric potential on the order of 10 kV. The spinneret is typically separated at a fixed distance from a grounded conductive collector as shown in **Figure 1.1.** Initially, the competition between the repulsion of charges and the surface tension stretches the solution into a conical shape referred to as a Taylor Cone (Taylor 1964). If the potential is increased above a critical value the repulsion of charges accumulating on the fluid surface overcomes the surface tension, and a straight jet is emitted from the Taylor cone. Then after a short distance, the initially straight jet segment generally becomes unstable and displays bending, undulating movements as it passes toward the collector. Bending the jet in the instability region decreases the jet diameter and therefore increases the surface area of the fibre. The dramatic increase in the surface area of the jet results in rapid solvent evaporation and solidification of the fibre jet as it travels toward the collector. The fibre jet is deposited as a nonwoven web on the collector, from which it is retrieved. The fibres obtained under the best electrospinning condition are generally of circular cross-section, continuous and bead free (Reneker 1996; Huanga 2003). Electrospinning from a molten precursor is a similar process except there is no solvent evaporation (Khurana 2003).

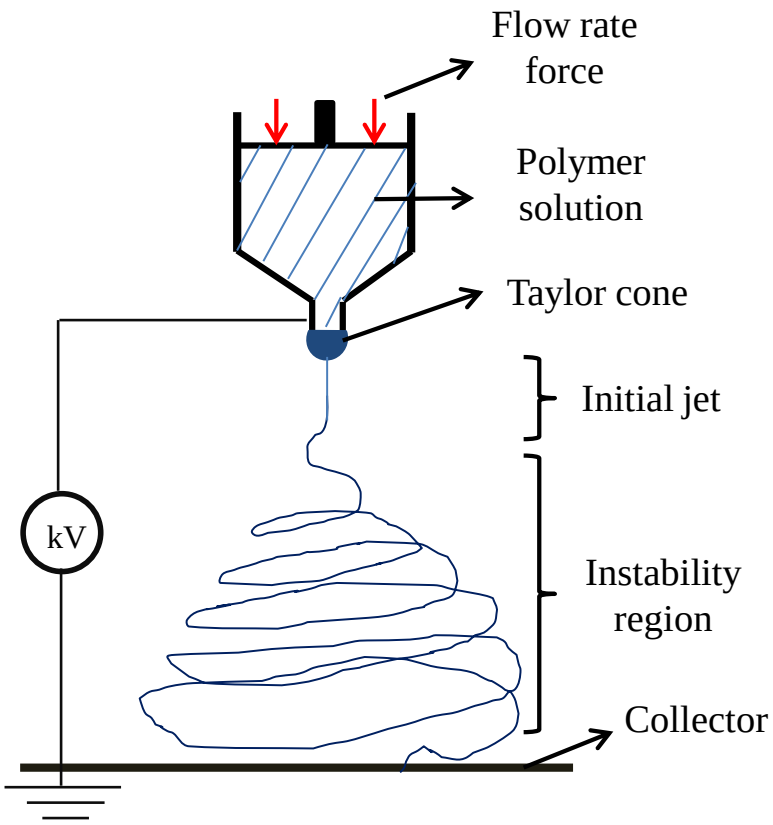

Figure 1-1: Schematic representation of the electrospinning process.

Anton Formhals carried out the earliest experiments in developing the electrospinning process toward commercialization (Formhals 1934). Formhals used the electrospinning setup to generate filaments from cellulose acetate/acetone solution for the fabrication of textile yarns. From 1934 to 1944, Formhals published a series of patents, improving his experimental setup and describing the process of polymer filament production using electrostatic forces (Formhals 1934). In 1964 the theoretical underpinnings of electrospinning were developed by Geoffrey Ingram Taylor (Taylor 1964). Taylor mathematically modeled the shape of the cone formed by the fluid droplet

under the effect of an electric field, for which this characteristic droplet shape is now named ("Taylor cone"). In 1971, shortly after Taylor's work, interest shifted away from a mathematical understanding of the electrospinning process to testing the effect of varying polymer solution and processing parameters (i.e., solution viscosity, polymer concentration, polymer molecular weight, flow rate, and voltage). Baumgarten (Baumgarten 1971) began to build the relationships between individual parameters and the structural properties of electrospun fibres. A major finding was that increasing the viscosity of a polymer solution results in enhancement of fibre diameter according to an exponential power law of ~0.5 (Baumgarten 1971).

The next critical step in the evolution of modern electrospinning occurred in 1981 when Larrondo and Manley demonstrated the production of fibres from molten polymers such as polypropylene using an electrostatic force (Larrondo 1981a). The fibre diameters from melt electrospinning were much higher than those obtained from the electrospinning of polymer solution (above 50 micrometers in diameter). The large fibre diameter was attributed to the high viscosity of the polymer melt. They also discovered that the fibre diameter is inversely related to the melt temperature.

In the mid 1990's, interest in nanofibres increased and electrospinning was seen as one of the primary techniques used to explore novel nanofibres. Today, more than 100 polymers and copolymers have been electrospun to form nanofibres with different morphologies such as hollow nanofibres, core-shell nanofibres, nanorods and highly cross-linked nanofibres (Huanga 2003). Due to its versatility and relatively simple experimental setup electrospinning is being applied to a broad range of products including filtration, textile manufacturing, drug delivery, medical devices, sensors, composites, and catalyst supports (Huanga 2003; Andrady 2008). There are some

companies which have been utilizing electrospinning process and developing electrospun fibres in large scale for a number of applications such as cell-based therapies, drug discovery and filtration. The Electrospinning Company Ltd (Chapman 2010) and SNS LLC (Frazier 2007) are two examples of nanofibre production companies which have launched a range of scaffolding materials for tissue engineering and established industrial collaborations to develop other medical devices from biocompatible electrospun fibre. The *eSpin* company(*eSpin* 2010) has also commercial scale manufacturing capabilities to produce nanofibers (20-200nm in diameter, up to 1 meter wide) which is formed as membranes with very high porosity for air, liquid and molecular filtration. Donaldson Company (Donaldson 1915) in USA has also commercialized nanofiber filter media consisted of 10| μm size cellulose fibers and 250 nm size nanofibers, so called Ultra-Web. The Ultra-Web filter which is made of sub-micron electrospun fibre indicated 92% dust reduction.

1.2 Effects of spinning parameters on fibre morphology

The morphology and diameter of electrospun fibres can be affected by a number of parameters. These parameters are categorized as i) processing parameters, ii) ambient parameters, and iii) polymer solution (fluid) properties (Seeram 2005; Andrady 2008). Processing parameters include voltage, flow rate, needle diameter and distance between the needle tip and collector. The voltage, and resulting external electric field induces the necessary charges on the polymer solution to distort the shape of drop at the tip of the needle, forming the Taylor cone. As the voltage is increased a critical voltage is reached where the electrostatic forces produced on the solution overcome the surface tension of the polymer solution and initiate the fibre jet. Above the critical voltage, the electric field can lead to significant stretching of the polymer solution jet and reduction in the fibre diameter as well as bead density on the fibre (Demir 2002). As the electric field

strength increases a greater columbic force is generated on the electrospun fibre jet, which can affect the physical appearance of the fibre (Zhao 2004). Under very high voltage conditions, the electrostatic field causes the polymer molecules to become more ordered and thereby induces greater crystallinity in the fibre; however, above a certain voltage the crystallinity is reduced as the jet is accelerated, reducing its flight-time and thus time to promote molecular organization (Zhao 2004).

Changing the flow rate also influences the fibre diameter and pore size in the resulting fibre mat (Rutledge 2000). Overall, an increased flow rate increases the fibre diameter and the number of beads on the fibres. Bead formation is the result of incomplete jet drying that also leads to the formation of ribbon-like or flattened fibres (Rutledge 2000; Megelski 2002). By increasing the flow rate, the solvent evaporation process is delayed, allowing solvated fibres to reach the collector which results in thick fibres with beads.

Similarly, an increase in the distance between the droplet and collector can decrease the average fibre diameter, which is again attributed to a longer flight-time for the fibre jets in the instability region. In general, the distance between the capillary tip and collector can influence fibre diameter by 1 – 2 orders of magnitude (Buchko 1999). The internal diameter of the needle also affects fibre diameter: a small internal diameter reduces the diameter, reduces clogging and the amount of beads on the fibre (Mo 2004). The reduction in clogging is attributed to the reduced exposure of the polymer solution to the atmosphere during ejection from the needle.

Ambient parameters, such as humidity and pressure, and their interaction with the polymer solution also affect the jet and resulting fibre morphology. High humidity, for example, has been found to cause the formation of pores on the surface of the fibres (Bognitzki 2001; Megelski

2002). Under enclosed condition, reduction in the pressure surrounding the electrospinning jet does not improve the electrospinning process and also the polymer solution in the syringe will have a greater tendency to flow out of the needle and there causes unstable jet initiation (Ramakrishna Seeram 2005; Seeram 2005; Andrady 2008).

Although processing and ambient parameters influence fibre morphology, they are less significant than the solution parameters; polymer solution properties have the most significant influence on the electrospinning process and the resultant fibre morphology (Fong 1999; Reneker 2000; Jiang 2004). The effects of solution properties such as surface tension and viscosity have been extensively investigated. High surface tension decreases the surface area per unit mass of a fluid and leads to the formation of droplets or beads-on-a-string morphology (Seeram 2005). One can diminish the beads-on-a-string fibre morphology by using an appropriate solvent mixture or increasing polymer concentration. As the formation of fibres results from the interaction of polymers, such as polymer polymer entanglement, basic solution properties like polymer concentration and polymer molecular weight have significant effects on fibre formation (Fong 1999; Reneker 2000). Solutions with higher viscosity promote the formation of bead-free nanofibres. Higher viscosity can be achieved by increasing the polymer molecular weight or polymer concentration. However, the higher viscosity also produces a commensurate increase in fibre diameter. It is, therefore, important to identify the lowest concentration threshold for the onset of fibre formation in order to produce uniform fibres with the smallest diameter.

The minimum concentration at which the polymer can be spun into uniform fibres is determined by the entanglement density as given by critical entanglement concentration (C_e) (McKee 2003; Shenoy 2005). The critical entanglement concentration is the boundary between the semi-dilute

unentangled and the semi-dilute entangled regions. This boundary represents the onset of conditions where significant overlap can occur between the polymer chains and can constrain the chain motion. The presence of entanglements prevents the breakup of the charged fluid into droplets, resulting in the formation of uniform fibres. It was experimentally determined that the C_e is the minimum concentration required to obtain beaded nanofibres and that uniform bead-free fibres can be obtained at 2 – 2.5 times C_e (McKee 2003).

The required polymer concentration for sufficient polymer chain entanglement of linear polymers can be described by the Berry number (Be), which is equal to the intrinsic viscosity, [η], multiplied by polymer concentration; Be=[η]c (Ko 2003; Gupta 2005; Shenoy 2005; Ko 2006). The intrinsic viscosity [η] is obtained by capillary viscometry. Experimental evidence has shown that the molecular entanglement in solution, which is related to the Berry number, influences the diameter of the electrospun fibres in predictable ways: four regions can be observed in a plot of Be vs. fibre diameter as illustrated in **Figure 1.2.** In region (I), in which Be<1, fibre formation is impossible via electrospinning due to lack of chain entanglement or interaction. In region (II), 1<Be<3, the defected fibres (fibre and bead) are generated and fibres diameter are in the range of 100 – 500 nm. In region (III), 3<Be<4, fibre diameters increases rapidly and are usually in the range of 1700 – 2800 nm. In region IV (Be>4), the fibre diameters are less dependent on Be and are more affected by other processing parameters such as electric field strength and needle to collector distance (Gupta 2005; Ko 2006).

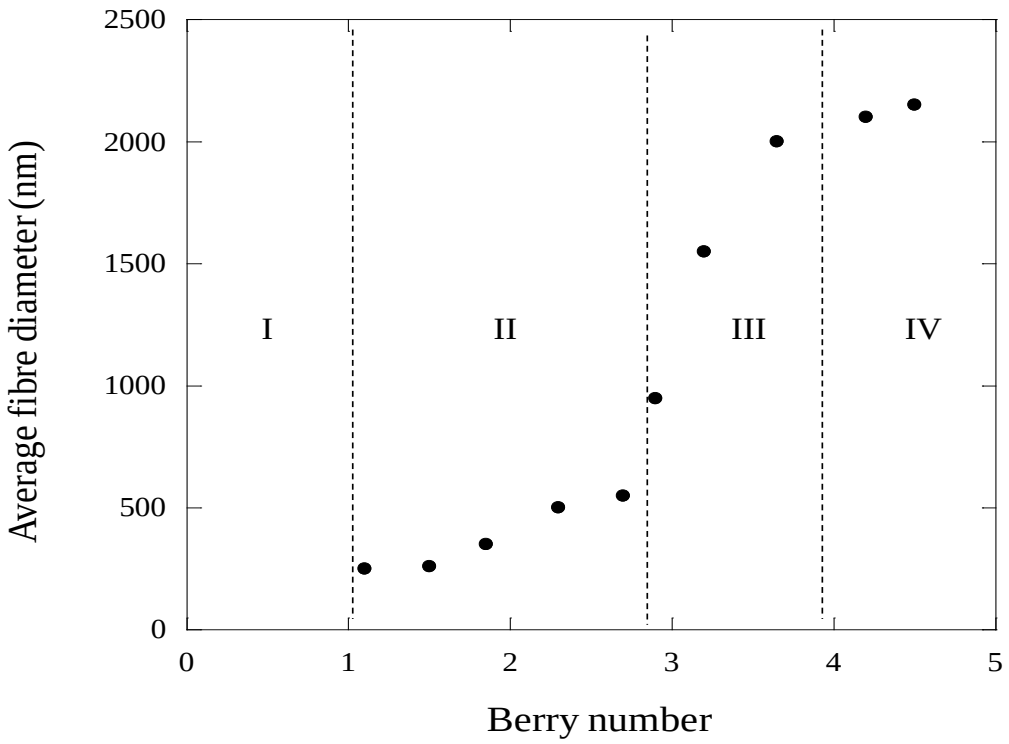

Figure 1-2: Relationship between Berry number and fibre diameter (Gupta 2005; Ko 2006).

1.3 Fibre properties and applications

Nanofibres are solid state, linear nanomaterials characterized by high flexibility and with an aspect ratio greater than 1000:1 (Ko 2006). Diameters of electrospun fibres are typically in the nanometer range, while lengths can be several kilometres. Predominately produced as nonwoven nanofibrous mats, they bridge both the nano- and the macro-scale worlds. As such they are being investigated for a wide variety of applications, including drug delivery and scaffolds for tissue engineering, wires, capacitors, transistors, and diodes for information technology, systems for energy transport, conversion and storage, such as batteries and fuel cells, and structural composites for aviation and aerospace applications (Li 2002b; Yoshimoto 2003; Kim 2005). In particu-

lar electrospun nanofibrous networks have been shown to enhance electronic and mechanical properties as well as improved bio-reactivity. For example, superior electrical conductivity was observed when conductive polymers were electrospun into nanofibres; the high intrinsic fibre conductivity attributed to the high geometric surface and high packing density associated with the significant reduction in fibre diameter (Choi 2004). Similarly, fibre strength increases exponentially with decreasing fibre diameter (Reneker 1996); the high strength of nanofibres is attributed to the increase in strain energy per atom as the diameter of the fibre decreases. Likewise, cell adhesion and proliferation (human mucosal keratinocytes) were observed to be greater on biopolymer (silk) nanofibres ($d \approx 80$ nm) as compared to microfibres ($d \approx 1100$ nm) and films; the three-dimensional nanofibrous scaffolding providing a better environment (surface area and nutrient access) for the cells (Reneker 1996; Price 2003; Min 2004). The same behaviour is being exploited in the delivery of drugs and other bioagents, e.g. electrospun nanosized bioagent-loaded polymeric fibres; the higher surface area of the nanofibrous mats enabling better control and more complete release of loaded bioactive agents (Kenawy 2002).

In many biomedical and bioengineering applications synthetic polymers offer distinct advantages over natural polymers. Materials produced from synthetic polymers typically have uniform chemical composition and consistent quality. As well, synthetic polymers can be readily designed to have mechanical properties that best match a particular biomedical or scaffolding application (Lu 2004). Polyurethanes are among the most widely used synthetic polymers in biomedical applications, especially in those that have contact with blood. Electrospun polyurethane fibres have shown great promise in the area of wound healing due to the inherent non-thrombogenicity (resistance to clotting), high porosity and thus excellent oxygen permeability (Han 2008). Some of the most frequently used synthetic polymers for tissue scaffolds are the bi-

odegradable aliphatic polyesters that are derived from lactide (Jiang 2004), glycolide (You 2005), and caprolactone (Yoshimoto 2003) monomers. While synthetic polymers with good mechanical and chemical properties are particularly good matches for bio-medical scaffolding applications, the synthetic polymers such as those described above are slow to degrade or are non-biodegradable, which limit their applications in bioengineering.

The use of natural polymers has always been of great interest due to their biocompatibility and biodegradability. Characteristics such as low toxicity, low immunogenicity, and enhanced cell adhesion and proliferation have made natural polymer nanofibres top candidates for biomedical applications. Most natural polymers can be degraded by naturally occurring enzymes and thus can be used in temporary implantation (Matthews 2002) or for drug delivery (Sombatmankhong 2007) in biological environments. Most of the biopolymers that have been electrospun are proteins such as gelatin (Zhang 2006), collagen (Matthews 2002), silk (Jin 2002), polysaccharides, such as alginate (Wayne 2005), hyaluronic acid (Yoo 2005), dextran (Jiang 2004), starch (Pavlov 2004) and cellulose (Kim 2005), and DNA (Fang 1997). Electrospun nanofibres with outstanding mechanical properties such as silk and collagen have been used for cell adhesion and proliferation in tissue scaffolding (Ayutsede 2005). Polysaccharides such as hyaluronic acid (HA), cellulose and its derivatives have been used in ophthalmology, medical implants and drug delivery applications (Son 2004; Luong-Van 2006).

1.4 Bioactive loaded electrospun fibres

The electrospinning process can be easily adapted to accommodate encapsulation of different bioactive materials. Bioactive loaded electrospun fibres with large surface area to volume ratios offer efficient mass transport and delivery. Many different bioactive agents such as low molecu-

lar weight drugs, plasmid DNA and large bioactive components such as proteins, enzymes, bacteria, and viruses have been incorporated into electrospun fibres.

A variety of low molecular weight drugs have been incorporated into electrospun fibres, including lipophilic drugs such as ibuprofen (Jiang 2004), rifampin (Zeng 2003), and itraconazole (Verreck 2003), as well as hydrophilic drugs such as cefazolin (Katti 2004), mefoxin (Kim 2004) and tetracycline hydrochloride (Kenawy 2002). The majority of these studies have been carried out with polyester fibres, particularly poly(lactic acid) (PLA), poly(glycolic acid) (PGA) and poly(caprolactone) (PCL) because of their biocompatibility, biodegradability, and FDA-approval status. In general, a burst phase of rapid drug release is often observed when low molecular weight drugs are encapsulated in electrospun fibres (Kenawy 2002; Jiang 2004). As a result, numerous studies have been performed to try to control the drug release kinetics. Such attempts include: conjugation of the drug to the polymer (Jiang 2004), alteration of drug-polymer interactions (Kenawy 2002), use of enzymatically degradable polymer matrixes (Zeng 2003), and alteration of mass transport by coating the electrospun fibre with another polymer to obtain the desired release profile (Verreck 2003).

Electrospun fibres have also been used for gene delivery for transfecting and transforming cells (Luu 2003; Liang 2005). For example, the release of DNA from poly(lactic-co-glycolic acid) (PLGA) fibres was dependent on the location of the DNA within the fibre. Analysis of the release kinetics showed an initial burst release, related to the proportion of DNA located on the surface of the fibres, followed by a slower diffusion mechanism with the release of the remaining encapsulated DNA being dependent on the degradation of the PLGA fibre. Through evaluation of the structural integrity and bioactivity of the released DNA using gel electrophoresis and

transfection, it was demonstrated that the released DNA remained bioactive after the electrospinning process (Luu 2003).

The encapsulation of proteins via electrospinning appears to be a challenging task due to the fact that biomacromolecules are quite labile and denature easily. This is especially the case when they are subjected to harsh processing conditions such as high electrical potential and exposure to organic solvents. In one study, protein encapsulation was performed by electrospinning a heterogeneous protein-polymer solution (Chew 2005). The electrospinning solution was comprised of an aqueous solution of human nerve growth factor (NGF) stabilized with bovine serum albumin (BSA) as a carrier protein and incorporated into PCL electrospun fibres. Incubation of the protein-encapsulated fibre in an aqueous medium exhibited a diffusion controlled sustained release, with the bioactivity of the electrospun NGF being partially retained throughout the period of sustained release. This study demonstrated the feasibility of encapsulating proteins *via* electrospinning to produce biofunctional tissue scaffolds (Chew 2005).

The encapsulation of large bioactive agents such as bacteria and viruses in a dry form (e.g., electrospun fibre), while preserving activity; can be useful in many applications. Bacterial cultures are used to produce cheese and yogurt, to vaccinate animals and humans, and also as expression hosts for biotechnology applications (Salalha 2006; Yongsheng 2008; Klein 2009). Similarly, viruses such as bacteriophage, which are a class of bacteria specific viruses have been used as an alternative to antibiotics, i.e. bacteriophage therapy (Soothill J. 2004). In one research study, several bacteria and viruses were encapsulated in electrospun polymer fibres (Salalha 2006). The bacteria and viruses were suspended in a solution of poly(vinyl alcohol) (PVA) in water and subjected to an electrostatic field. This work showed that a range of organisms could be efficiently

encapsulated in electrospun fibres; however, only a limited portion of the bacteriophages tested remained viable after electrospinning, although less sensitive bacteria, such as *Escherichia coli* B strain (*E. coli* B), with thick cell walls, managed to survive the electrospinning process with up to 100% viability (Salalha 2006).

Electrospinning may represent an excellent alternative to lyophilization for the preservation of organisms for strain collections, maintaining genetically modified bacterial strains of industrial importance, and for applications such as biosensing. Moreover, bioactive electrospun nanofibre mats can be used to conveniently cover three-dimensional surfaces (e.g. tissues and organs) and release their contents for the potential treatment of wounds and cutaneous fungal infections, and possibly for gene and bacteriophage therapy (Sun 2003; Venugopal 2005; Salalha 2006).

1.5 Morphology of bioactive loaded electrospun fibres

There are several well established methods for the entrapment of bioactive agents in polymeric materials, such as solvent evaporation (Park 1994), spray drying methods (Freitas 2005) and electrospinning (Verreck 2003; Andrady 2008). In electrospun nanofibres the combination of varying fibre morphology and high surface area can offer sustained release rates and efficient delivery of biocomponents. There are many factors that can affect the release profile and the rate of release of bioactive agents from electrospun fibres. One is the distribution of bioactive agents within the electrospun fibres. Currently, four different fibre morphologies have been investigated for the delivery of various types of bioactive components (Andrady 2008). These different morphological structures can be achieved via different sample preparation and processing conditions. The different morphologies of bioactive-loaded nanofibres are as follows:

A. Dissolution of bioagents in the fibre matrix at the molecular level (**Figure 1.3a**).

B. Dispersion of bioagent particles in the electropsun polymer matrix (**Figure 1.3b**).

C. Incorporation of bioagents in the core of fibres, core/shell structure (**Figure 1.3c**).

D. Dispersion of pre-encapsulated bioagent reservoirs in electrospun fibres (**Figure 1.3d**).

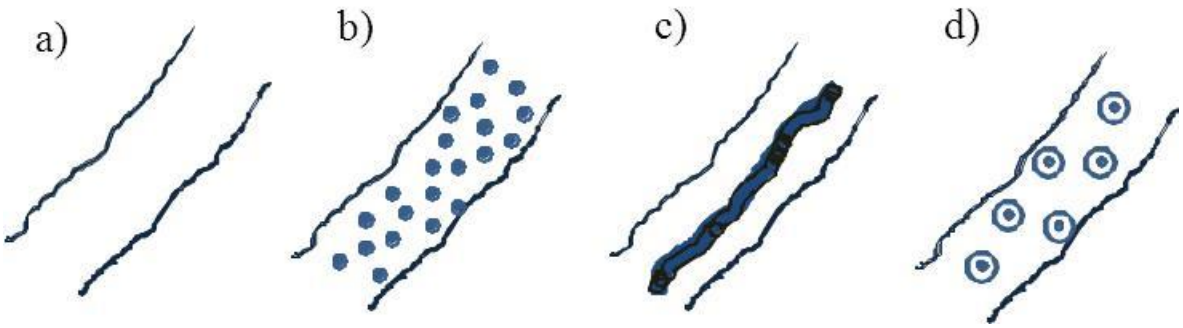

Figure 1-3: Illustration of the four morphological models of bioagent loaded electrospun fibres (Andrady 2008).

The complete dissolution of bioactive components in a polymer solution results in the simplest fibre morphology: Type A (**Figure 1.3a**). In this type of morphology, the bioactive components need to be fully dissolved in the polymer/solvent system and are therefore fully distributed in the electrospun fibre matrix at the molecular level. However, there is little interest in Type A morphology for the encapsulation of biological active components such as proteins and enzymes as they easily lose their bioactivity after dissolution in harsh and toxic organic solvent systems. This type of morphology is more applicable for small molecule drugs, which are not as sensitive to the organic solvent system. Hydrophobic drugs such as rifampicin and paclitaxel have been en-

capsulated directly into hydrophobic electrospun poly(l-lactic acid) (PLLA) nanofibres by first dissolving the drugs in the PLLA/chloroform solution (Zeng 2003). Transmission electron microscopy (TEM) examination of the drug–loaded nanofibres (average d ≈ 700 nm) revealed fully transparent fibre morphology with no crystalline inclusion, suggesting the drug was completely dissolved/dispersed in the polymer matrix. In this case, the release of rifampin into a buffer was shown to be very slow with virtually no release observed for more than ten hours.

In the case of hydrophilic biomolecules, such as doxorubicin hydrochloride (Dox), its poor solubility in hydrophobic polymer solutions leads to poor incorporation into the corresponding hydrophobic nanofibres; the drug is allocated to the surface of the electrospun fibres (Xu 2006). Although water-soluble drugs can be electrospun into water-soluble polymers, such fibres quickly dissolve and rapidly release the encapsulated the drug when exposed to aqueous environments such as tissue fluids, thereby limiting their effective use as a delivery systems. Successful incorporation and sustained release of hydrophilic biomolecules in hydrophobic biopolymers has, therefore, been investigated through other processes such as suspension and emulsion electrospinning.

Suspending biomolecules in a spinning "dope" of a polymer solution (i.e., particles of hydrophilic bioactive agents in hydrophobic polymer solutions) results in an electrospun morphology of Type B (**Figure 1.3b**). Bioactive particles such as biocides silver (Son 2004), chlorhexidine (Liang Chen 2008), bacteria and viruses (Salalha 2006) have been incorporated in electrospun nanofibres using this method. Depending on the nature of the polymer and solvent system, the resulting electrospun fibres reveal the presence of bioactive components, on the surface of the electrospun fibres. This highlights one of the disadvantages of the suspension electrospinning

process which is the formation of beaded nanofibres and the non-uniformity of dispersed material throughout the fibre (Zhang 2005). In the suspension electrospinning process, the bioactive particles are randomly oriented and dispersed non-uniformly throughout the electrospun fibre matrix from the core to surface. Due to nanoscale surface effects, the suspended particles in the electrospun nanofibres tend to accumulate on the fibre surface. Thus, a burst release can be expected unless the bioactive components are incorporated in the core of the nanofibre (Zeng 2003). As such emulsion or coaxial electrospinning have shown to be promising methods for incorporating the bioactive components in the core of the nanofibres as core/shell structures.

Coaxial electrospinning has been used as an effective method to encapsulate bioactive components such as DNA, proteins, viruses, and enzymes (Sun 2003; Dror 2008; Klein 2009). Coaxial electrospinning forms a core-shell fibre structure, as shown in morphology Type C, (**Figure 1.3c**). In coaxial electrospinning, two immiscible components can be conveniently electrospun into bi-component composites fibres with a core layer encapsulated inside a polymer shell layer by means of a spinneret with twin capillaries (Sun 2003). In particular, bioactive components or drugs can be enclosed within the polymer shell to form a reservoir-type delivery device. Therefore, the polymer shell provides protection for the bioactive molecules and avoids the denaturation or deformation of their structures. The coaxial electrospining process has been shown to be an easy and reliable process for controlling the release rate of bioactive components (Huang 2003; Pham 2006; Dror 2008; Klein 2009). This morphology is particularly well suited for protein or DNA delivery as it minimizes burst release, avoids denaturation, and provides greater control of the release rates (Zeng 2005).

Emulsion electrospinning has also been used as a novel process to prepare core-shell fibres, like coaxial spinning and as depicted in morphology Type C (**Figure 1.3c**). In the case of water in oil (w/o) emulsion systems, the core of the electrospun fibre is made of a dispersed aqueous phase and the shell is composed of a polymer organic solution. In such a system, the emulsion flows through a long capillary and forms rapidly expanding jets, the dispersed phase has a tendency to accumulate in the center of the liquid phase along the direction of the fluid. This helps the dispersed phase settle into the center of the fibres rather than at the surface and results in a core-shell structure (Hongxu 2006). Emulsion electrospinning has been used to encapsulate hydrophilic doxorubicin hydrochloride (Dox) in hydrophobic PLLA electrospun fibres (Xu 2006). Similar to coaxial electrospun fibres, the emulsion electrospun fibres avoid the burst release of the biomolecules as they are incorporated in the core of the fibres.

The incorporation of pre-encapsulated bioactive molecules is another effective strategy for avoiding denaturation and increasing the stability of bioactive components. Morphology Type D (**Figure 1.3d**) shows the pre-encapsulated bioactive agents distributed randomly throughout an electrospun fibre. Until now only a few studies have investigated the incorporation of pre-encapsulated bioactive components in electrospun nanofibres. One such study was the incorporation of pre–encapsulated DNA in an amphiphillic triblock copolymer of polylactide-poly(ethylene glycol)-polylactide, PLA-PEG-PLA within electrospun poly(lactic-co-glycolic acid) PLGA scaffolds (Liang 2005). Here, the pre-encapsulated DNA nanoparticles were prepared by solvent-induced condensation of plasmid DNA in a solvent mixture (N,N-dimethylformamide (DMF)/TE buffer, 94:6%) and subsequently encapsulated in a triblock PLA-PEG-PLA copolymer. The mixture was then electrospun to form non-woven nanofibrous and nanocomposite scaf-

folds; the solvent mixture rapidly removed by evaporation from the jet stream during fibre formation. In this system the DNA was fully preserved in the nanofibrous scaffolds (Liang 2005).

In another study, bovine serum albumin (BSA) was used as a model protein and pre-encapsulated in microspheres of calcium alginate (Hongxu 2006). The pre-encapsulation of BSA was performed using a w/o emulsification system where a mixture of an aqueous alginate/BSA solution was emulsified in a chloroform/surfactant solution. The pre-encapsulation was completed by the crosslinking the alginate through the addition of calcium chloride. PLLA was then dissolved in the external phase of the emulsion system (chloroform) and the electrospinning process was carried out to immobilize the BSA/calcium alginate capsules in the PLLA electrospun fibres. A bead-in-string fibre structure was generated, where the beads were reported to contain the BSA loaded calcium–alginate microspheres. While it was reported that a sustained release behaviour was observed as compared to the naked alginate microbeads, the amount of successfully loaded protein into the calcium-alginate capsules and the biological activity of the BSA after electrospinning was not reported (Hongxu 2006).

1.6 Release of bioactive components from electrospun biodegradable polymers

The delivery of bioactive components (e.g. drugs) with regard to prolonged release and localization of release is a potentially powerful tool in biomedical sciences. Prolonged controlled release of drugs using polymeric materials is now well established. In controlled drug release, polymeric materials can be design in such a way to deliver drugs at a predetermined rate for a defined period of time. Designing polymers for drug delivery systems requires the understanding of two key characteristics. The first characteristic is related to the process of release and the second characteristic is related to the physicochemical properties of polymers (Langer 2003).

The process of release of incorporated compounds (eg. Drugs) from polymer carriers is referred to as the release mechanism. The release profile and mechanism of drugs is highly affected by the amount of incorporated components and their distribution pattern. In the case of a single polymer, three possible release configurations exist (**Figure 1.4**):

1. Diffusional control
    a. Reservoir
    b. Matrices
2. Chemical control
    a. Polymer degradation (surface and bulk erosion)
    b. Chemical cleavage of drug from polymer
3. Solvent activation
    a. Polymer swelling
    b. Osmotic effect

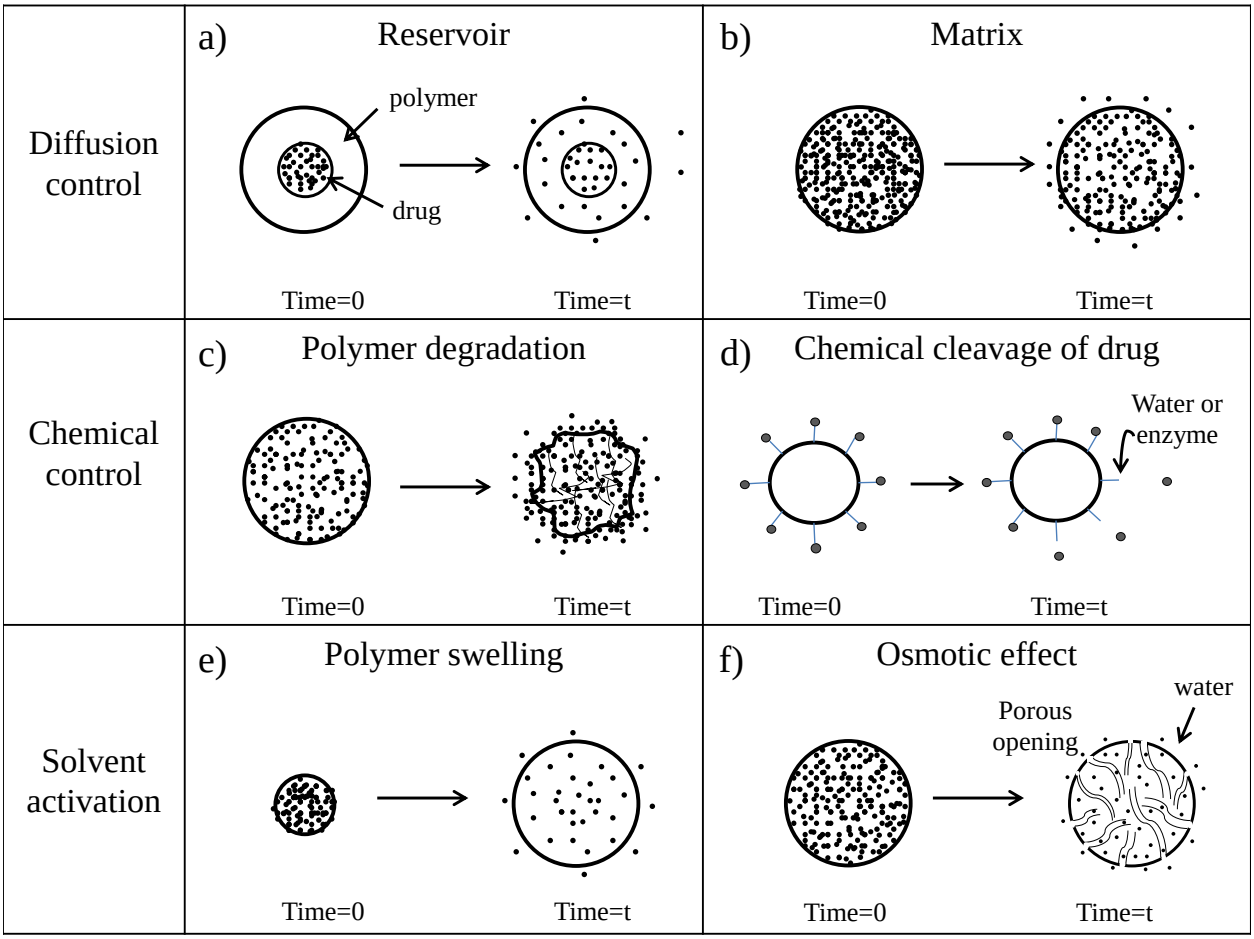

Figure 1-4: The most common release mechanisms from polymeric materials: (a) diffusion through the reservoir where the drug migrates from the core to the outer surface of the polymer; (b) diffusion from the polymer matrix where the drug is uniformly distributed in the polymer matrix; (c) release of the drug via degradation of the polymer matrix; (d) cleavage of the drug from the polymer backbone where the drug is chemically attached to the polymer matrix; (e) release of the drug via solvent activation where the polymer matrix is swollen; and (f) release of the drug via osmotic forces where pores are created in the polymer matrix.

Diffusion control is a major release mechanism in polymeric materials whereby the drug migrates from its initial position in the polymeric system to the polymer's outer layer and then to the surrounding environment (Verreck 2003). Diffusion may occur from a reservoir in which the drug is incorporated into the core of polymeric material and is surrounded by a polymer matrix

(**Figure 1.4a**) or where the drug is uniformly distributed throughout the polymer matrices (**Figure 1.4b**). As expected the diffusion controlled release from electrospun fibres with reservoir-type morphology is slower than that from electrospun fibres with the drugs uniformly distributed throughout the polymer matrix (Andrady 2008; Srikar R. 2008). For example the release of BSA and lysozyme restricted to the core of PCL electropsun nanofibres was shown to be much slower as compared to electrospun nanofibres with a randomly dispersed morphology (Jiang 2005; Zhang 2006). Although, other factors such as electrospun polymer shell thickness and variation in feeding rate of the core (inner) and shell (outer) solutions dramatically affected the release rate profiles. A higher flow rate or faster loading of components in the core resulted in fibres with an accelerated release; similarly, increasing the thickness of polymer shell layer resulted in a slower release (Zhang 2006).

In the case of such polymeric devices loaded with chemical components, the difference in concentration of the component inside and outside the polymer matrix is the primary driving force for diffusive transfer. Expressions for the diffusion kinetics of solutes through polymers are derived primarily by employing Fick's Law (Crank 1980). Experimentally, the fraction of components released in time *t* can be quantitatively measured when a drug-laden polymer sample is placed in a known volume of buffer media over a period of time (M_t/M_∞) (Crank 1980). The anticipated fraction of the released components by the polymer matrix or relationships between (M_t/M_∞) at time *t* can be calculated as follows:

$$(M_t/M_\infty)= 4(Dt/\pi r^2)^{1/2} - (Dt/r^2) \qquad (1)$$

where r is the thickness or diameter of polymer matrix, D is the diffusion coefficient of encapsulated components, M_t is the amount of drug released at time t, and M_∞ is the total amount released at infinite time (Crank 1980; Comyn 1985).

The simple kinetics predicted by Fick's law for the diffusive release of small chemicals from polymer film geometries appears to be applicable to electrospun nanofibre geometries as well (Luong-Van 2006). The controlled delivery of heparin from electrospun PCL nanofibres displays Fickian diffusion, and the fraction of heparin released increased with the square root of time as suggested by equation 1. In this study the calculated diffusion coefficient for heparin was shown to be the same for both film and fibre mat systems (Luong-Van 2006).

Besides the diffusion mechanism, degradation of the polymer matrix also influences the release rate and mechanism of the incorporated drug (i.e chemical control). In general, two main mechanisms of chemical erosion can be considered; heterogeneous and homogenous. Heterogeneous erosion occurs only at the polymer surface and is often referred to as surface erosion, while homogenous erosion, or bulk erosion, causes degradation throughout the polymer matrix (**Figure 1.5**). The biodegradation of polymers can also occurred using either biological components such as enzymes, (i.e. enzymatic hyrolysis) to breakdown the polymeric materials or through simple hydrolytic breakdown of the ester linkages in the polyesters, polylactones and related polymer series.

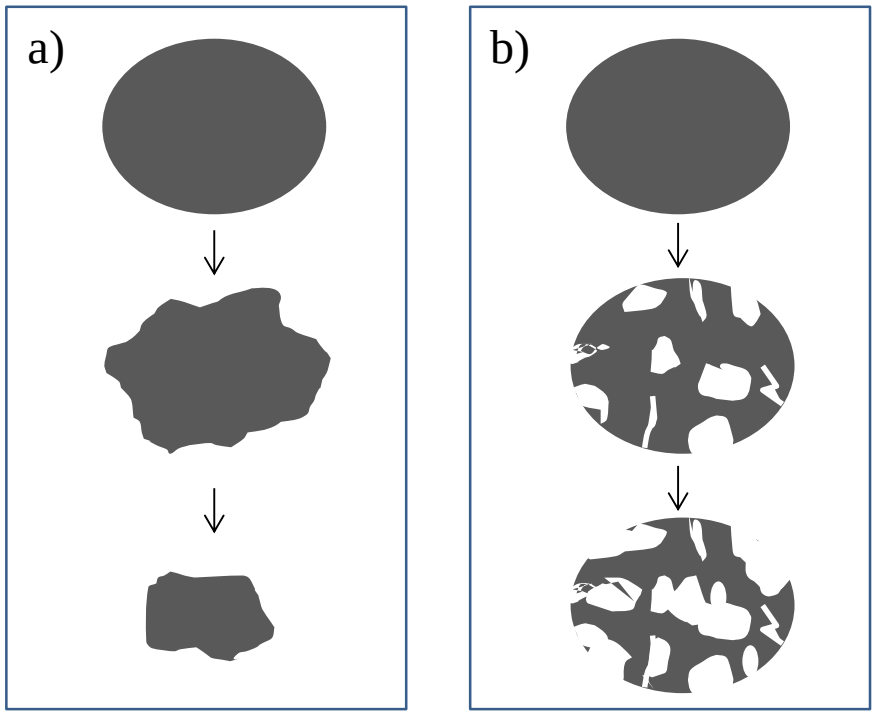

Figure 1-5: Diagram of polymer degradation with time in water, displaying (a) surface erosion and (b) bulk erosion.

In the surface eroding release mechanism of polymeric systems, the drug release rate is proportional to the erosion rate at the polymer surface. To achieve surface erosion, the degradation rate at the polymer surface should be faster than water penetration into the polymer bulk matrix. In fact, for surface erosion, it is desired to have a hydrophobic polymer with water-labile inter-monomer linkages. In the case of bulk erosion, there are various steps that must be taken into account. For example in the degradation of polyesters, the diffusion of water into the polymer matrix results in random chain scission through the hydrolytic cleavage of ester linkages. This results in the formation of polymeric segments or oligomers with smaller molecular weight that

solubilized in the surrounding water. The removal of these solubilized oligomers and/or low molecular weight polymers creates pores throughout the polymer matrix, which ultimately leads to further breakdown of the polymeric matrix and results in substantial mass loss.

For example, the release of evenly distributed BSA in hydrophobic PLLA fibres exhibited different rates in the absence and presence of an enzyme (proteinase K) (Zeng 2005). PLLA has low porosity and is a poorly soluble/swollen polymer in aqueous media; thus surface erosion of the fibre is the primary release mechanism. In the absence of the enzyme, almost no or only a minimal diffusive release of BSA was observed; the hydrophobic PLLA has a high resistance to bulk erosion. However, upon introducing proteinase K, a slow and sustained release of BSA was obtained. In this case, the presence of proteinase K results in the surface erosion of the PLLA polymer fibre and a sustained release of BSA (Zeng 2005).

Drugs can also be attached to or interact with the polymer matrices via specific interactions and/or degradable linkages. Using this process, different distribution and pharmacokinetics release mechanisms can be obtained. Usually, the release of drugs that strongly interact with the electrospun fibre matrix can be very slow and prolonged. For example, when ibuprofen was randomly dispersed in a poly(lactic-glycolic acid) (PLGA) fibre, a rapid release profile was observed (Jiang 2004). However, a blend of PEG-g-chitosan polymer with PLGA significantly reduced the release rate of ibuprofen due to hydrogen bonding interactions between the NH_2 groups on chitosan and the acid moieties of ibuprofen. Covalently bonding the ibuprofen to chitosan via the amine groups further prolonged and significantly reduced the release rate.

Finally, release mechanisms as result of solvent activation involve either solvent induced swelling of the polymer or osmotic effects. In both cases, exposure of the polymer matrix to a solvent

or environmental fluid activates drug release. In the swelling process, the drug is locked inside the polymer matrix, "trapped" within the network of polymer chains. Typically glassy polymers are used in swelling controlled release systems. Thus upon exposure to an environmental fluid, the fluid penetrates into the polymer matrix and swells the polymer. Swelling is typically accompanied by a glass-to-rubber transition, which facilitates the liberation of the drug, which can diffuse through the "softened" fibre matrix. Similarly in the case of the osmotic effect, the fluid or water penetrates the semipermeable polymer matrix due to the difference in drug (osmolyte) concentration between the surrounding medium and the loaded fibre. The influx of fluid dissolves the drug, which results in a gradient in drug concentration across the fibre, which leads to more fluid entering the fibre, and displacing the dissolved drug into the surrounding medium. Increasing the permeability of the polymer matrix further facilitates drug delivery. For example, drugs incorporated in electrospun poly caprolactone (PCL) fibres showed almost no release over a prolonged period of time. However, the addition of poly(ethylene glycol) (PEG), a water-soluble polymer to the hydrophobic PCL system produced fibres which exhibited a sustained release of the encapsulated components. This was attributed to the dissolution of PEG upon exposure to fluid, which resulted in PCL fibres with an interconnected porous network that along with the osmotic driving force sustained release (Jiang 2005; Dror 2008; Klein 2009).

Along with the discussed release processes, there are a number of polymer properties (physico-chemical properties) that can influence release characteristics. These properties are polymer molecular weight, degree of crystallinity, glass transition temperature, and geometry of polymeric devices (Langer 1980). As well environmental factors such as pH, ionic strength, and temperature also affect release characteristics (Langer 1978; Langer 1980). It is well established that the degradation process starts with a decrease in the polymer molecular weight by random hydrolytic

cleavage of the polymer backbone (e.g., ester linkages). Polymers with smaller molecular weights usually degrade faster than those with higher molecular weights. Therefore the molecular weight of the polymer has influence on the degradation and release rate of drugs (Langer 1978; Langer 1980; Langer 2003). The morphology of the polymer is also an important factor in release characteristics. Crystalline regions of polymers typically degrade slower than amorphous or noncrystalline regions due to the more intensive degree of bonding. Usually, water penetration in the amorphous/noncrystalline regions is easier and faster compared to the crystalline regions and therefore, hydrolytic degradation occurs there first. As a consequence, highly amorphous/noncrystalline polymers degrade faster and have faster release rates (Rathbone 2003). Polymers with low glass transition temperatures (T_g) are ideal for fast-acting drug delivery; polymers with T_g's lower than body temperature (37^oC) are rubbery under *in vivo* conditions and a rubbery state degrades faster than a glassy state (Park 2000; Rathbone 2003). In the rubbery state there is greater polymer chain flexibility and easier water penetration.

Geometrical factors such as shape, size, and surface to volume ratio also influence degradation. Usually, a more sustained release can be observed from a cylinder sector or fibre morphological polymer matrix (Langer 1978; Langer 1980; Rathbone 2003; Andrady 2008). In fact, by adjusting the fibre diameter, a desired release profile can be easily obtained (Zhang 2006). However, the release kinetics is still highly dependent on the previously discussed release processes and polymer properties.

1.7 Cellulose acetate electrospun polymers as delivery materials

Cellulose acetate (CA) is the acetate ester of cellulose, wherein the hydroxyl groups at the C2, 3 and/or 6 positions of the anhydroglucopyranose unit (AGU) of cellulose are substituted with ace-

tyl groups (Heinze 2004). Cellulose acetates can be fully acetylated with all three hydroxyl groups of the AGU being derivatized, or only a portion thereof in a regioselective or statistically distributed manner (**Figure1.6)**. Depending on the degree of acetylation, CA has a wide range of properties and applications. Of the various acetates, the so-called secondary acetate or cellulose diacetate (CDA) is of commercial significance. Despite its name, cellulose diacetate has an average degree of substitution (DS) of 2.5 acetate groups per anhydroglucopyranose unit. Likewise, commercial cellulose triacetate (CTA) refers to cellulose acetates with a DS above 2.7 (Pintaric 2000; Gomez 2004; Heinze 2004).

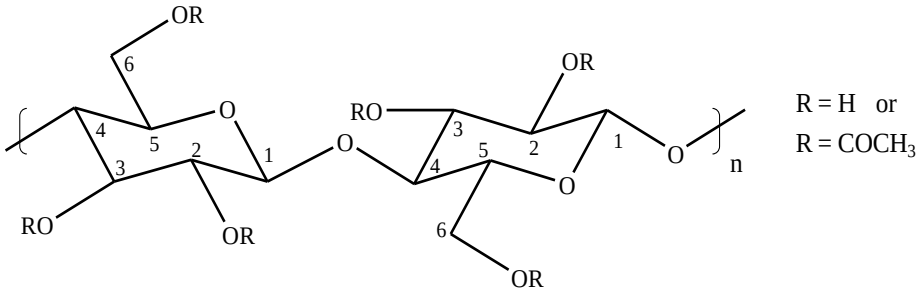

Figure 1-6: Structural representation of cellulose acetate.

The solution properties of cellulose acetates are strongly influenced by the average degree of substitution and distribution of acetate groups along the cellulose chain. For example, CA with a degree of substitution between 0.5 - 1 is soluble in aqueous solutions, while those with DS >1 tend to be insoluble in aqueous medium, but soluble in many organic solvent systems (Gomez 2004). The solubility of CA in different solvents at different degrees of substitution is summarized in **Table 1.1**. This phenomenon is attributed to both the disruption of intra- and intermo-

lecular hydrogen bonding within the CA chains and the formation of specific interactions between functional groups on the CA and the solvent molecule. For example, basic solvents like acetone interact primarily with the hydroxyl groups on the CA chain, while acidic solvents such as formic acid primarily solvate the acetyl groups (Gomez 2004; Heinze 2004). Therefore, the use of specific solvents can induce structural changes in solutions depending on the amount of acetyl and hydroxyl groups along the partially substituted CA chains.

Table 1-1: Dissolution of CA at different degree of substitution (Heinze 2004).

DS of CA	Solvent
2.92	TFA[1], DMAc[2], DMF[3] DMSO[4] and TCM[5]
2.46	DCM[6], chloroform chloroform/methanol DMAc, acetone, formic acid and ionic liquid
1.75	THF[7], DMF and DMAc
0.49	water, formamide DMAc

[1]Trifluroacetic acid; [2]N,N-dimethylacetamide; [3]N,N-dimethylformamide; [4]dimethylsulfoxide; [5]trichloromethane; [6]dichloromethane; [7]tetrahydrofurane.

Cellulose acetates are polymers with a high melting temperature and low melting entropy. Thermal data for cellulose triacetate (CTA) shows that the polymer has a glass transition temperature (T_g) around 190 °C, melting temperature (T_m) of 307 °C and decomposition temperature (T_d) of 356 °C (Heinze 2004). In addition to the T_g and T_m, the DSC thermogram of CTA has an endothermic peak between 50 and 80°C related to the evaporation of water, and a small exothermic peak at 190 to 206 °C which has been assigned to the crystallization temperature (T_c). For secondary CA, the DSC thermograms show a drop in melting and crystallization temperature, due in part to the smaller and less perfect crystallite structure. As expected the T_g, which is related to segmental chain motion, is affected by the degree of acetylation, varying between 190 and 220 °C for CA samples with 61 - 52.6% (DS of 2.9 to 2.5, respectively) acetyl content (Tang 1996). An extensive investigation of the thermal properties of cellulose acetates of various DS (0.49, 1.75, 2.46, 2.92) has been reported (Kamide 1985; Pizzoli 1985). The effect of the average DS on the T_g, T_m and T_d is shown in **Figure 1.7**.

For this plot the T_g and T_m were determined by DSC and T_d was determined by thermogravimetric analysis (TGA) as function of DS. The T_g of CA increases almost linearly with a decrease in DS suggesting that intra- and intermolecular hydrogen bonding between the OH groups are stronger than between the *O*-acetyl groups. T_g of cellulose (DS = 0) was calculated by extrapolating T_g curve and it was found to be 523 k. The T_m and T_d of CA became minimum at DS of 2.2 and 1.0, respectively. Fully acetylated cellulose acetate (DS $\geq$ 2.92) has high crystallinity and melting temperature. Decreasing the DS decreases the crystallinity and lower the melting temperature. The CA with DS $\leq$ 1.8 does not have melting since the T_d is far below melting temperature. DS dependence of T_d suggests that molecular interaction and degradation temperature of CA solids is influenced by amount of acetyl group. As the DS decreases the degradation tem-

perature of CA decreases. In case of DS = 0 or neat cellulose the degradation temperature again increases which is attributed to the presence of strong intra- intermolecular hydrogen bonding between the hydroxyl group (Kamide 1985; Heinze 2004).

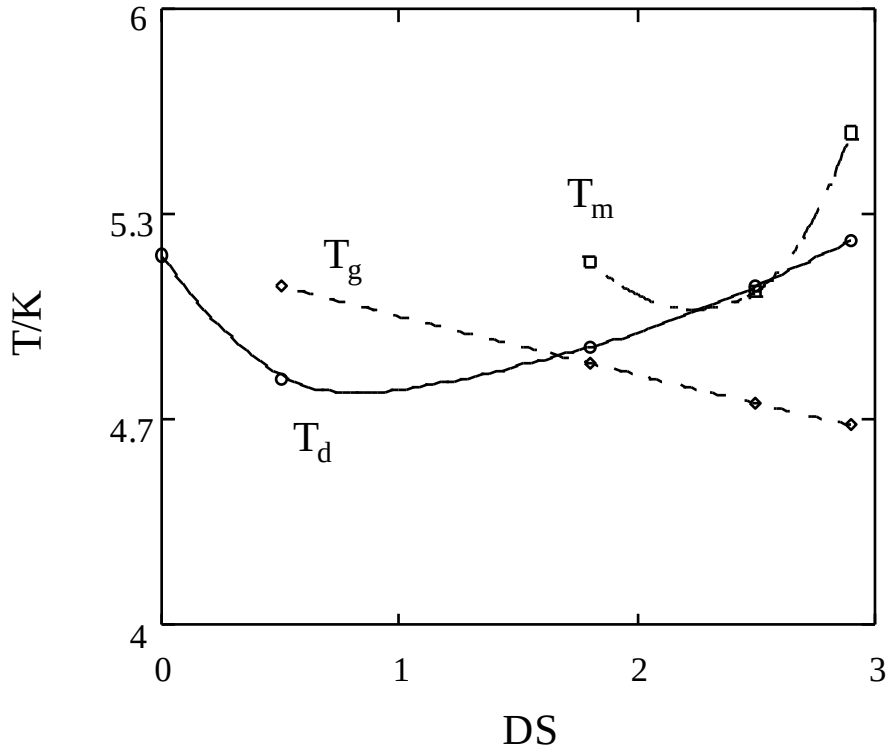

Figure 1-7: Dependence of T_g, T_m and T_d on the average degree of substitution (Kamide 1985).

The properties of CA, including high toughness, high dimensional stability, low toxicity, and good biocompatibility have led to its use in a variety of industrial applications including biomedical fields (Heinze 2004; Rustemeyer 2004). Cellulose acetate is one of the most commonly used materials for preparation of semipermeable membranes applicable to dialysis, ultrafiltration and

reverse osmosis (Rustemeyer 2004). CA membranes have very low adsorption characteristic (high-throughput) and thermal stability with high flow rate (Son 2004). Research is still underway to determine the effectiveness and applicability of CA nanofibre membranes as carriers for bioactive components.

Cellulose acetate has the advantages of being soluble in many solvents suitable for electrospinning. However, uniform electrospun fibres cannot be achieved using a single solvent. Electrospinning of cellulose acetate from acetone results in very short discontinuous fibres with diameters above 2 μm being formed (Liu 2002). The high volatility of acetone causes clogging at the nozzle tip and prevents continuous electrospinning. Similarly, the high surface tension and high boiling temperature of solvents like dimethylacetamide (DMAc) lead to instability of the electrospinning jet, which rupture and retract into spherical form. Therefore, mixed solvent systems are typically used for producing uniform electrospun CA nanofibres. A list of some of the solvents used for electrospinning of CA is presented in **Table 1.2**.

Table 1-2: Typical mixed solvent systems used to form electrospun cellulose acetate fibres.

Solvent	Fibre diameter	Reference
Acetone/DMAc (75:25)	100-1000nm	(Liu 2002)
Acetone/water (85:15)	500nm	(Son 2004)
Acetone/DMSO (80:20)	500-1000nm	(Haas 2010)
Chloroform/Methanol (90:10)	200-500nm	(Tungprapa 2007)
Acetone/DMF/Trifluoroethylene	200-1000nm	(Zuwei 2005)

Liu and Hsieh (2002) have reported the preparation of ultra-fine CA electrospun fibre mats using an acetone/DMAc solvent system, 2:1 v/v (Liu 2002). CA fibres were formed with average diameters between 100 nm - 1 μm. By changing the concentration of the cellulose acetate solution as well as the ratio of the mixed solvent system (acetone/DMAc) the CA electrospun fibre morphology can be altered. Fifteen percent CA in acetone:DMAc mixtures (2:1 ratio) resulted in continuous electrospinning process and formed uniform beaded free fibre. Increasing CA concentration to 25 %wt resulted in thick fibrous membrane (Liu 2002). There is a range of other binary solvent mixtures for CA electrospinning. These include acetone/DMSO, which has been used to produce highly connected fibrous network structures with potential applications for scaffolding and tissue engineering (Haas 2010). Similarly, ultrafine electrospun CA fibre (1 μm) at 10 %wt concentration has been also prepared from 8:2 w/w acetone/water solvent (Son 2004). The CA electrospun fibre had been also produced from chloroform-methanol mixture (Tungprapa 2007). Addition of CA polymer to this solvent mixture (chloroform-methanol with extracted bioactive components from plants and herb) followed by electrospinning process resulted in the bioactivated electrospun CA fibre material (Tungprapa 2007). The CA fibrous mat has also be prepared using three components solvent such as acetone/dimethylformamide (DMF)/trifluoroethylene (TFE), 3:1:1 v/v/v CA solutions (Zuwei 2005). The CA fibre from this solvent system was notably fluffy like cotton batting.

The resulted electrospun CA fibre mats have been applied to further processing reaction to obtain the new materials. Several researchers have proceeded with the deacetylation of nonwoven electrospun cellulose acetate fabrics (treated in a NaOH solution) to produce regenerated cellulose membranes (Liu 2002; Wang 2004; Haas 2010). Overall, the deacetylation process formed smooth cellulose membrane or in some cases cellulose with a thermoplastic cellulose acetate

core (Zuwei 2005). Surface modification of CA electrospun fibre has been also performed by addition of methacrylate functional groups on the fibre surface to transform the electrospun fabric from hydrophilic to hydrophobic material (Lu 2003). Analysis confirmed that methacrylation of the fibres had occurred only at the fibre surface. Functionality of the CA electrospun has also been influenced by including functional compounds in the spinning dope. Silver particles were incorporated on cellulose acetate fibres by including silver nitrate ($AgNO_3$) in the electrospinning dope (Son 2004). Subsequent UV light photo-reducing irradiation of the fibres resulted in silver nanoparticles on fibre surfaces and produce strong antimicrobial CA elecrospun fibre material (Son 2004).

There have been only a few studies exploring CA electrospun fibrous mats as drug carriers or delivery devices. One study investigated vitamin-loaded electrospun cellulose acetate (DS=2.5) fibrous mats produced from CA/acetone/DMAc solutions (Pattama 2007). Vitamin loading was achieved by their dissolution in the polymer solution followed by electrospining process. Submerging the fibrous mats in acetate buffer showed that the vitamin A and E release from the CA fibres followed a basic Fickian diffusion mechanism; The vitamin-loaded electrospun CA fibre mats exhibited a gradual increase in the release of the vitamins. This was in stark contrast to the corresponding as-cast CA films, which exhibited a burst release. The same group of researchers have incorporated anti-tumor / antioxidant drugs (curcumin) (extracted from the plant longa) into electrospun CA nanofibres (Tungprapa 2007). The curcumin-loaded CA fibre mats showed the same release characteristics as the vitamin loaded fibres. The integrity of the loaded curcumin in CA fibre mats was characterized after release using ^1H nuclear magnetic resonance (NMR) spectroscopy and appeared to be intact. (Tungprapa 2007).

Bactericidal CA (DS=2.5) fibres have also been successfully produced by electrospinning CA/PEO polymer blends containing the biocide, chlorhexidine (CHX). The presence of CHX within the fibres was confirmed by infrared (FTIR), Raman and XPS measurements, and the bactericidal properties of CHX was determined by placing CA fibre mats on top of an agar plate containing *E. coli* and *S. epidermidis* bacteria. The CA-CHX fibres demonstrated bactericidal capability through a gradual release of encapsulated CHX from inside the fibres. The authors mentioned that this strategy is not limited to incorporation of only CHX, but could also enable the incorporation of a wide range of antibacterial agents in CA fibres (Chen 2008).

Although small or low molecular weight bioactive molecules can be slowly released from commercial CA (DS=2.5) fibres through a diffusion mechanism, the release of large bioactive components such as protein, bacteria and viruses is more challenging. Despite this, several researchers have designed electrospun nanofibres to encapsulate and deliver large bioactive components, particularly large cells such as bacteria and viruses (Lee 2004; Salalha 2006; Klein 2009). However, most of these studies have only confirmed the localization of the bacteria and viruses inside of electrospun fibres, few have provided detailed investigations on the release mechanism(s). As such cell immobilization in fibres has been investigated for numerous applications including biomedical, agricultural, and the bioremediation of pollutants in soils and water. In particular, bacterial viruses (bacteriophages) are being tested as an alternative to bacterial antibiotics (bacteriophage therapy) and as vectors for gene delivery (viral and non-viral vectors) (Soothill 2004). In the next section bacteriophages and biomedical application of encapsulated bacteriophages in electrospun polymeric fibres is briefly described.

1.8 Bacteriophages and bacteriophage activated electrospun fibre

1.8.1 Bacteriophage structures, therapy and applications

Tailed bacteriophages, or "phages," are viruses that consist of a polyhedral head and a tubular tail. According to the tail morphology and structure, bacteriophages are classified into three families (Ackermann 1987): *Podoviridae* with short noncontractile tails; *Siphoviridae* with long, noncontractile tails; and *Myoviridae* with long, contractile tails (**Figure 1.8**).

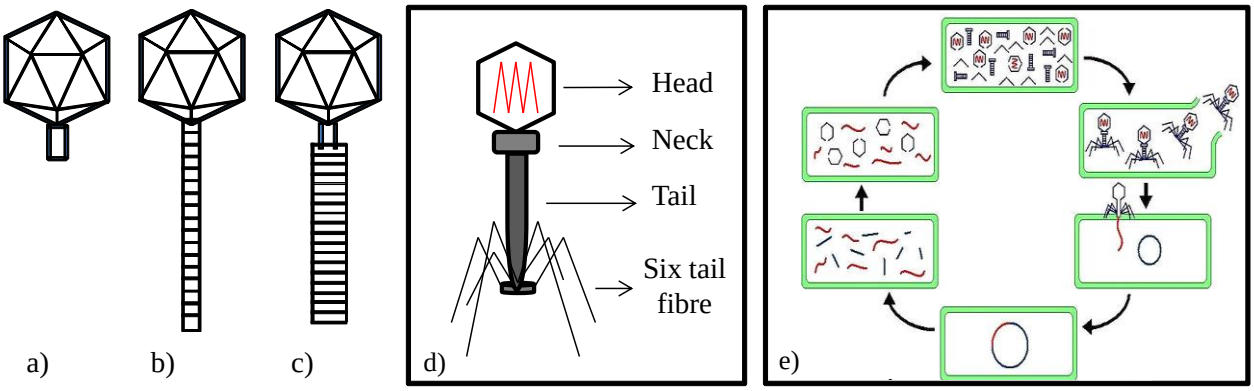

Figure 1-8: Tailed phages families: (a) *Podovirida*; (b) *Siphovirida*; (c) *Myovirida* and (d) T4 Bacteriophage from *Myovirida*; (e) lytic life cycle of T4 bacteriophage(Ackermann 1987).

The T4 bacteriophage is an example of a *Myoviridae* bacteriophage (**Figure 1.8d**). It is a virus that can target and kill harmful pathogens such as *E. coli* B that can exist in food products, drinking water, and air. The T4 bacteriophage has an icosahedral head (capsid) with a length and width of 110 and 85 nm, respectively, and a 130 nm long tail (Matthews 1983). It also has six

long fibres at the end of the tail that can bind to receptors on the surface of bacteria. The T4 bacteriophage replicate through a lytic life cycle (**Figure 1.8e**). After binding to the bacterial host the T4 bacteriophage inject its genetic material into the bacteria cell. The injected genetic material is then incorporated into that of the host bacteria, which allows the T4 bacteriophage to propagate inside the host using the host's replication machinery. The replicated bacteriophages eventually cause the cell to lyse, killing the bacterium, releasing newly replicated phages which can infect other bacteria in the same manner (Kutter 2004).

The clinical benefits of bacteriophage therapy have begun to attract the attention of the research community (Yongsheng 2008; Puapermpoonsiri 2009). For example, it has been used for treating ear infections in pet dogs (Soothill 2004), treating *E. coli* infections in calves and lambs (Smith 1983), and also for reducing bacteria colonization of broiler chickens (Atterbury 2007). Other studies include the application of bacteriophage for the control of *Salmonella* and *Campylobacter* bacteria on the surface of meat (Goode 2003). Typically, bacteriophages are either administered by oral gavage, in the case of infected animals, or simple spraying techniques in the case of surface infection treatment. In oral administration, the viability of the bacteriophage can be rapidly reduced due to the acidic conditions of the stomach or by the presence of enzymes and other digestive components. As such, encapsulation in polymeric matrices was also investigated to protect the bacteriophages structure (Sturesson 2000; Yongsheng 2008).

In the surface treatment of bacterial infected meat, the timing of bacteriophage dosing is critical; too early of an inoculation can result in a dramatic reduction in efficiency and bacteriobacteriophage activity and even complete treatment failure (Payne 2003). This is due to different pharmacokinetic principles of bacteriophage as compared to conventional drugs. These living organ-

isms interact, replicate, evolve, and demonstrate different kinetic behavior than the conventional antibiotic drug (Payne 2003; Greer 2005). In the treatment of infection with bacteriophages, there is an increase in bacteriophage numbers via rapid viral self-replication, and in principle a small initial inocula would be needed to set out an active bacteriophage therapy (Ackermann H. W. 1987; Ackermann 1987; Greer 2005). Therefore, instead of a simple spraying technique, there is a strong desire to develop a polymeric matrix delivery device that can encapsulate the bacteriophage in a viable mode and liberate them in a slow controlled fashion.

1.8.2 Encapsulation and incorporation of bacteriophages in electrospun fibre

Electrospinning has been used as a straightforward technique to encapsulate bacteriophages in fibres. Bacteriophage M13 is a rod-like virus (900 nm in length and 10 nm in diameter), which has been used to form anisotropic films (Lee 2004). It is a pliable virus compared to other bacteriophages, and M13-containing fibres can be fabricated using wet spinning and electrospinning processes. When smectic suspensions of M13 in hexafluoro-2-propanol (HFP) were spun into fibres using wet spinning, a dramatic decrease in the virus viability was observed due to the toxicity of HFP (Lee 2004). The electrospinning of bacteriophage M13 suspended in an aqueous solution of polyvinyl pyrolidone (PVP) formed uniform encapsulated fibres. The instant release of bacteriophage M13 showed infectious activity; however the percent viability of encapsulated M13 was not reported (Lee 2004).

Electrospinning has also been used to encapsulate bacteriophages such as T4, T7, and lambda (λ) phages in water-soluble electrospun PVA fibres (Salalha 2006). The exposure of T4 bacteriophage to PVA aqueous solutions showed little or no effect on its viability, but following fibre formation, the released phages demonstrated very low activity (T4:1%, T7:2%, λ: 6%). The mechanical stresses produced during electrospinning are about 5×10^4 g cm^{-1} s^{-2} (Reneker 2000),

which is far below those which bacteriophages can withstand, which for these species are up to ~10^5 times the force of gravity (Salalha 2006). The decrease in viability of these bacteriophages must be the result of other variables or forces during the process. The leading hypothesis is that the loss of bacteriophage activity is attributed to the rapid dehydration or evaporation of water during fibre formation, which ultimately leads to bacteriophage damage (Kohn 1974; Salalha 2006).

As a member of the *Myoviridae* family of phage, T4 bacteriophage has one of the most sensitive and delicate structures amongst the various phages. It is easily dehydrated during the electrospinning process and cannot be readily and actively incorporated into electrospun fibres (Salalha 2006). Thus the use of *Myoviridae* bacteriophage requires a new electrospinning process. The leading approach is one of pre-encapsulation, where the bacteriophages are incorporated in a biopolymer capsule prior to electrospinning. This would prevent dehydration and protect the sensitive structure of the *Myoviridae* bacteriophage during the electrospinning process. Biopolymers such as spermine-alginate (Moser 1998), chitosan-alginate (Yongsheng 2008), poly(DL-lactide-co-glycolide) (Sturesson 2000; Puapermpoonsiri 2009), and chitosan-bile salt microspheres (Lameiro 2006) have been used to encapsulate bacteriophages. These encapsulation methodologies have some limitations such as the involvement of organic solvents, conformational changes to bacteriophage DNA and proteins, low encapsulation efficiency, and poor protective effects upon exposure to acidic conditions or strong mechanical forces. Another reliable method is dependent on the core-sheath morphology from coaxial electrospinning, where phages are incorporated in the core of the fibre and protected by a polymer shell layer. Coaxial electrospinning has been used to encapsulate sensitive biological components such as enzymes, proteins and DNA (Huang 2003; Pham 2006; Dror 2008; Klein 2009).

1.9 Hypothesis and objectives

The utility of antimicrobial components such as bacteriophages as bactericidal agents for food surfaces, and/or in food packaging materials, would be a significant benefit for food preservation and food storage. Traditionally, antimicrobial polymeric film coated materials are used as packaging to inhibit spoilage and kill pathogenic microorganism in contaminated foods (Ahvenainen 2003). One drawback is low available surface area of polymeric film coating materials which reduces their bioactivity. The fibrous material, specifically electrospun fibre mat with submicron fibre diameter and high available surface area could readily overcome this problem. Electrospinning process can produce 3D nonwoven fibre mat and it is recognized as easy process for encapsulation of a broad range of bioactive components. The 3D structure of electrospun fibre mat acts as a passive barrier in food packaging and it can also exhibit higher antimicrobial activity. Therefore, electrospun fibres with incorporated bacteriophages (as antimicrobial agent) could be ideal as food packaging materials where they can act as killing agent and/or inhibit bacteria growth on surface of foods; however, maintaining the viability of the bacteriophages in the electrospun fibres is still a major challenge.

Previous work has shown that single nozzle electrospinning of suspended T4 bacteriophage in water-soluble polymer solutions (PVA and PVP) is not a reliable encapsulation method (Lee 2004; Salalha 2006). The rapid solvent evaporation during fibre formation leads to dehydration and deactivation of the bacteriophages that are close to the surface of the fibre. Therefore, we propose to use two different electrospinning techniques to incapsulate T4 bacteriophage in electrospun fibres, while maintaining bacteriophage viability. In the first method, the T4 bacteriophage will be pre-encapsulated in an alginate shell and then incorporated into electrospun fibres through emulsion electrospinning. Here, we hypothesize that the bioactivity of the T4 bacterio-

phage can be maintained using protective alginate capsules within the electrospun fibre. In the second method, coaxial-electrospinning will be used to encapsulate the T4 bacteriophages in the core of the electrospun fibre. In this process the core of the fibre contains the T4 bacteriophage buffer where it is protected by a polymer shell fibre. Here, it is hypothesized that the core/shell structure can minimize/alleviate the dehydration and destruction of the T4 bactriophages during the electrospinning process. To evaluate the effectiveness of each process, the bioactivity of the T4 bacteriophage is a key measure. To tailor/control the release rate of the T4 bacteriophages from the electropsun fibres, various blend ratios of hydrophilic/hydrophobic polymers (poly(ethylene oxide) (PEO), cellulose diacetate (CDA)) are used for the electrospun polymer shell layer. The effect of blending ratio and polymer molecular weight on electrospun fibre morphology and T4 bacteriophage release are investigated.

Objective 1*: To incorporate pre-encapsulated T4 bacteriophage-alginate nanocapsules into electrospun fibres through water/oil (w/o) emulsion electrospinning.*

Specific aims*:*

A. Study the effect of the emulsification process and emulsion electrospinning on T4 bacteriophage activity.

B. *Study the release profile of T4 bacteriophage from the capsules and electrospun fibres.*

In this approach, calcium alginate capsules were used to pre-encapsulate the T4 bacteriophage. The pre-encapsulated T4 bacteriophagewas then incorporated into electrospun fibres via emulsion electrospinning. Here, the water/oil emulsion system was made of a dispersed phase of aqueous sodium alginate-bacteriophageT4 in a continuous phase of chloroform and in the pres-

ence of a surfactant. The slow addition of calcium chloride to this emulsion system forms cross-linked alginate capsules in which a mild gelation of the alginate retains the biological activity of the T4 bacteriophages. The matrix polymer was then dissolved in the external phase of the emulsion and formed into fibres by electrospinning. Although this system contains a multiphase composition, the polymer emulsion was readily electrospun into fibres. The single stream electrospinning of this system forms encapsulated electrospun fibres in which the T4 bacteriophage/alginate capsules are allocated deep in the fibre; thus, the structural integrity of the T4 bacteriophages are maintained. The bioactivity of the T4 bacteriophage was measured after emulsification as well as after *in vitro* release tests from the electrospun fibres. The T4 bacteriophage activity, or bacteriophage titer, was tested before and after each process and is expressed in plaque forming unit (PFU) per mL. Initially, PEO, a water-soluble polymer (soluble in chloroform too) was used to evaluate the feasibility of T4 bacteriophages immediately after emulsion electrospinning.

Objective 2*: To investigate coaxial electrospinning for encapsulating the T4 bacteriophages in water-soluble PEO electrospun fibres.*

Specific aims*:*

A. Study the effect of coaxial electrospinning (PEO) on T4 bacteriophage viability.

B. *Study the effect of PEO molecular weight on fibre morphology & release profile of T4 bacteriophage.*

In this method, a novel approach is presented whereby the T4 bacteriophages are encapsulated in electrospun fibres using coaxial electrospinning. Coaxial electrospinning is capable of forming electrospun fibres with a core/shell structure in which the core contains an aqueous T4 bacterio-

phage solution and the shell is an organic polymer solution. In this experiment, the T4 bacteriophages (dispersed in aqueous buffer) are incorporated into the core of the fibres, while the shell is composed of a water-soluble polymer (PEO). Using this method, the biopolymer serves as an external protective layer around the T4 bacteriophages. This process prevents dehydration of the T4 bacteriophageand minimizes the exposure to harmful organic solvents. The core/shell structure electrospun fibre morphology was characterized using transmission (TEM) and scanning (SEM) electron microscopy. The viability and activity of the entrapped bacteriophage was assayed by dissolving the electrospun fibre mats in buffer and plated against *E. coli B* as previously described in objective 1. The effect of PEO molecular weight (100, 300, 600k M_n) on the electrospun fibre morphology, fibre diameter, and release profile of the T4 bacteriophage was evaluated. Increasing the PEO molecular weight was expected to increase in the electrospun fibre diameter and enhance the viscosity of the releasing medium upon immersion of electrospun fibre in buffer medium, which would result in a relatively slower release profile of T4 bacteriophage.

Objective 3: *To control the release rate of T4 bacteriophage by preparing coaxial electrospun fibres using water-soluble and insoluble polymer blends*

Specific aims*:*

1. *Study the effect of various blend ratios on fibre morphology before and after release.*
2. *Study the effect of the blend ratios on release profile of T4 bacteriophage.*

The rapid and immediate leaching of T4 bacteriophage from water-soluble electrospun fibres limits their practical application in long-term uses (e.g., food packaging material). To overcome this problem, a blend of hydrophilic/hydrophobic polymers, poly(ethylene oxide)

(PEO)/cellulose diacetate (CDA) was used as the shell layer for coaxial electrospun fibres. It is expected that the addition of CDA to the PEO spinning dope will produce electrospun fibres with a significantly decreased release rate of T4 bacteriophage. Depending on the PEO/CDA ratio, the degree of swelling of the electrospun fibres will vary and impact the rate of T4 bacteriophage release. The miscibility of PEO/CDA polymer in form of electrospun fibre will be investigated using DSC analysis. Previous studies showed miscibility of these two polymers and therefore fine electrospun fibre morphology and uniformly distributed copolymers throughout fibre matrix is expected. The immersion of the blend PEO/CDA polymer fibre would lead to fibre swelling and formation of interconnected channels in the shell of the electrospun fibres. As a result, the transfer of T4 bacteriophageout of the electrospun fibres is expected to be through diffusion, controlled by the PEO/CDA blend ratio. In this study, a full spectrum of polymer blend ratios will be studied and the effect on the release characteristics and electrospun fibre morphologies investigated.

Chapter 2: Materials and Methods

2.1 Materials

Sodium alginate (Alginic acid sodium salt from brown algae), bovine serum albumin (BSA) (fraction V), sodium bis(2-ethylhexyl) sulfosuccinate (AOT), fluorescein isothiocyanate (FITC), calcium chloride, poly(ethylene oxide) (PEO) with average molecular weight (M_n) of 100k, 300k, and 600k, and cellulose diacetate (CDA) with an average molecular weight (M_n) of 30,000 and degree of substitution of 2.5 were all purchased from Sigma-Aldrich and stored and used as specified. *Escherichia coli* bacteria (*E. coli* B) strains and wild type T4 bacteriophage were kindly provided by the laboratory of Professor Mansel Griffiths, University of Guelph, Canada.

Tryptic soy agar (TSA – solid media) and Tryptic soy broth (TSB – liquid media) were each prepared by dissolving 30 g of respective powder in 1 L of distilled water. Tryptic soy broth semi-solid (TSB_{SS}) was made by dissolving TSB (30 g) and agarose (4 g) in 1 L of distilled water. Storage media buffer (SM) for T4 bacteriophage storage was made by dissolving NaCl (5.8 g), $MgSO_4 \cdot 7H2O$ (2 g), 1M Tris–hydrochloride (pH 7.5, 50 mL) and 1 mL of 10% (w/v) gelatine in 1 L of distilled water. All the above reagents and media were purchased from Sigma–Aldrich and were autoclaved prior to use.

2.2 T4 bacteriophage propagation and plaque assay test

The bacteria host for T4 bacteriophage propagation was grown by dispersing 100 μL of *E. coli* B in 5 mL of TSB media and shaking at 120 rpm and 37°C overnight. 100 μL of this culture was then mixed with 100 μL of T4 bacteriophage stock solution. This mixture was incubated at 37°C for 20 min and was mixed with 4 mL of partially cooled TSB_{SS}. This was then poured onto a cooled TSA plate and incubated at 37ºC overnight. The resulting T4 bacteriophage lawn was

identified as a clear transparent plate in comparison to the cloudy control plate (100 μL of *E. coli*). Subsequently, 4 mL of SM buffer was used to flood the plates and chilled at 4°C for 1 hr. The Storage medium containing T4 bacteriophage and TSB_{SS} was then centrifuged for 20 min at 6800 rpm and 4°C. The supernatant was then passed through a 0.45 μm sterile filter and the lytic activity of the T4 bacteriophage was determined by plaque assay test.

In the plaque assay testing, serial dilutions (ten times dilution up to eight fold) of the above-propagated T4 bacteriophage was first prepared. Aliquots (100 μL) for each dilution were added to an equal volume of *E. coli* bacteria. Each mixture was then added to 4 mL of partially cooled TSB_{SS}, poured onto a TSA plate, and stored at 37°C overnight. A negative control, bacterial culture without T4 bacteriophage was prepared in the same manner. Following incubation overnight, the number of plaques was counted for each dilution and used to calculate the number of plaque forming units (PFU/mL). The T4 bacteriophage titer was calculated using the following the formula:

$$\text{Bacteriophage titre (PFU/mL)} = (\#\ \text{plaques})/\ (\text{dilution plated} \times \text{volume plated}).$$

Bacteriophage activity was determined to be 10^8 PFU/mL under the above condition.

2.3 Fluorescence labeling

For T4 bacteriophage labeling, a 10 mg (2.5×10^{-5} mol) excess of fluorescein isothiocyanate (FITC) was added to 10 mL of freshly propagated filtered T4 bacteriophage equilibrated in storage media buffer at pH = 7.5, and agitated continuously for 2 h at room temperature. Following agitation, the resulting suspension of T4 bacteriophage was dialyzed in SM buffer, pH 7.5, in a

dialysis bag with a molecular weight cut-off of 500 Da (Spectra/Por FloatA-Lyzer, G2). The dialysis buffer was exchanged every 6 h for 24 h to remove unreacted FITC.

For BSA-FITC conjugation, 67 µl of FITC/dimethylformamide dissolution (1.0 %wt; 2.5×10^{-5} mol FITC) was added to 1 mL BSA/buffer solution (0.5 %wt; 7.5×10^{-8} mol BSA) at a ratio of about 35 µg FITC per mg of BSA in a 2 mL round bottom flask. The flask was wrapped in aluminum foil and rotated at 100 rpm for 1 hour at room temperature. Then, the solution was passed through a desalting column (Dextran, 5K MwCO) to remove any unreacted FITC and exchange the BSA into storage buffer. The BSA-FITC conjugate was identified using UV-Vis spectroscopy at 280 nm (extension coefficient of 68,000 M^{-1} cm^{-1}).

2.4 Emulsification process

The aqueous phase of the emulsion system was prepared by suspending the freeze-dried T4 bacteriophage (obtained from 2 mL of an aqueous bacteriophage solution with 10^8 PFU/mL bacteriophage concentrations) in 1 mL of 2 %wt sodium alginate aqueous solution. This solution was allowed to sit for 10 min at room temperature and then added drop-wise to an AOT (0.166 g; 3.7×10^{-4} mol) chloroform (5.0 g) solution while mechanically stirring at 12000 rpm. Immediately after this process, 0.33 mL of $CaCl_2$ solution (5%wt; 4.5×10^{-4} mol) was added to cross-link the alginate and the emulsion was allowed to sit for 10 min at room temperature. This emulsion was found to be stable up to 30 minutes. To entrap the bovine serum albumin (BSA) in the calcium alginate particles, the procedure was the same as the one just described above, except that weight ratio of sodium alginate to BSA was set to 9 to1.

2.5 Emulsion electrospinning

Prior to electrospinning, the polymer (PEO or CDA) was dissolved in chloroform and the above prepared emulsion system was added to the polymer solution to obtain the optimized final polymer concentration for electrospinning (PEO 1.0-3.0 %wt and CDA 5.0-10.0 %wt). The optimal conditions will be discussed in the results section. The emulsion electrospinning process was carried out at 25°C using a vertical spinning apparatus and a 0.9mm flat needle. The spinning voltage was set at 1kV/cm, and the distance between the spinneret and collector plate was set to be 20cm. The flow rate was set at 0.2 mL/min using a 1mL syringe with a 5mm internal diameter. The fibres were collected on a sterilized aluminum plate. These parameters were obtained from optimization of the spinning process and are discussed in the following Results and Discussion section.

2.6 Coaxial electrospinning

Coaxial electrospinning was performed using PEO and PEO/CDA blend solutions (in chloroform: methanol 98:2 %wt) as the shell stream and a T4 bacteriophage/buffer suspension as the core stream. Two separate syringe pumps controlled the flow rates of the core and shell solutions: 0.01 mL/min for the shell and 0.001 mL/min for the core. The 10:1 dilution ratio between the core and the shell streams was based on those reported in the literature (Dror 2008; Klein 2009). The electrostatic field used was 1 kV/cm, and the distance between the spinneret and collector plate was 20 cm. The fibres were collected on a sterilized aluminum plate, which was then freeze dried overnight to avoid fibre dissolution due to presence of buffer in the core.

2.7 In-Vitro release

The bioactivity of the T4 bacteriophage after alginate pre-encapsulation was determined prior to electrospinning by removing the chloroform using rotary evaporation (25°C), followed by freeze drying to remove the remaining water. Then, the freeze-dried alginate/bacteriophage capsule was suspended and dissolved in 2 mL SM buffer under constant shaking (120 rpm) at room temperature. In the case of the fibre mats from emulsion electrospinning, 0.5 g of the fibre mat was dissolved in 2 mL SM buffer at pH= 7.5 while shaking at 120 rpm at room temperature (By using the same 2 mL volume as that from which the original T4 bacteriophage suspension was freeze-dried from a direct comparison of T4 bacteriophage activity can be made). For the fibre mats prepared from coaxial electrospinning, 1.0 g of the fibre mat was submerged in 10 mL SM buffer (pH = 7.5) in a test tube and it was shaken at 120 rpm at room temperature. In all of the release experiments, a 50 µL aliquot of the released T4 bacteriophage was removed from medium at predetermined time intervals and its activity was determined by the plaque assay test. The T4 bacteriophage activity was expressed as PFU/mL and to report activity percentage, the PFU/mL values were converted to log value (Matthews 1983).

2.8 Microscope analysis

The morphology of the electrospun fibres was examined by a Hitachi S-2600N Scanning Electron Microscopy (SEM). SEM samples were prepared by directly electrospinning fibres onto an aluminum SEM stub and subsequently imaged using an operating voltage of 25 kV and a working distance of 10mm. Images were taken over a magnification range of 250× to 4000× from duplicate samples. Prior to imaging, the samples were quickly frozen, lyophilized, and sputter coated using a Cressington high resolution sputter coater under vacuum between 0.04 to 0.03 torr for 3 minutes until the fibre samples were covered with a thin layer of Au (5nm).

For transmission electron microscopy (TEM) analysis the specimens were prepared by direct deposition of the electrospun fibre onto a carbon film coated copper grid. Images were collected using a Hitachi H-800 TEM at 120 kV without any sample staining.

The encapsulated fluorescein-labeled components (T4 bacteriophage and BSA) were viewed with a Leica SP5X white light laser confocal microscope (CSLM). The fluorescein conjugates were excited with an Argon laser set to 488 nm with an emission bandwidth of 521 – 616 nm. Leica (SP5X) 20 X dry objectives were used and the pinhole was automatically adjusted for optimal performance.

2.9 Thermal analysis

Dynamic weight loss tests were conducted using a TA instrument thermogravimetric analyzer (TGA Q 500). All tests were conducted in a N_2 purge (25 mL/min) using sample weights of ~10 mg over a temperature range of 20–600 °C at a scan rate of 10 °C/min. TGA analysis was performed to determine the degradation temperature of each compound prior to DSC analysis.

Thermal characteristics of all components were studied in a differential scanning calorimeter (TA Instruments Q 1000 DSC). In a typical experiment ~5.0 mg samples were accurately weighed, placed in aluminum pans and heated under a nitrogen atmosphere from -90 to 220 °C at 10 °C/min. A heat-cool-heat program cycle was used and the glass-transition temperature (T_g) and melting temperature (T_m) were recorded as the midpoint temperature of the heat capacity transition and the peak temperature, respectively from the second heating run. Samples were run in duplicate and they were within experimental error of each other (1.0 °C).

2.10 Antibacterial activity using optical density measurement

The optical density (OD) measurements of aliquots from all samples were measured using a UV-Vis spectrophotometer (Varian Cary Bio 50) at 600nm. A 20 mL *E. coli* culture was grown overnight in a test tube (16 hr. 120 rpm, 37 ^{o}C) in tryptic soy broth. Then 50 µL of the cultured *E. coli* was used for the serial dilution test to determine the bacterial cell counts (CFU/mL). Another 1 mL of the overnight cultured *E. coli* was diluted in TSB medium up to a 6 fold dilution (with a dilution factor of 0.5), and then OD measurements were performed for each sample to ensure that the optical density of each dilution remained within the dynamic OD range of the spectrophotometer (0.9 to 0.2). To obtain the standard curve, the CFU/mL of each dilution was determined and it was plotted against the OD600.

2.11 Infectivity measurement (*E. coli*) using T4 bacteriophage activated fibres

The effect of T4 bacteriophage activated fibre mats on *E. coli* infectivity was determined by submerging a 1.0 g core/shell electrospun fibre mat in 20 mL of cultured *E. coli* in a test tube and shaking it at 120 rpm at room temperature. At predetermined time intervals (every 60 minutes) a 1mL aliquot was removed from the medium and placed in a 1 cm UV cuvette (already sterilized) and the OD600 was determined. Although the PEO readily dissolved in the TSB medium, the insoluble CDA did not, rather it settled to the bottom of the test tube and care was taken not to disrupt it during sampling. For all fibre systems blank runs were performed using fibres without phage.

2.12 Zone of inhibition measurements using T4 bacteriophage activated fibres

The bactericidal capacity of encapsulated T4 bacteriophages or zone of inhibition tests were determined by the disk diffusion test method (Chen 2008). A mixture of 100 µL cultured *E. coli* and 4 mL TSB_{ss} was poured onto a TSA agar plate and it was allowed to solidify. Then a 25mm

diameter disk (prepared using a glass cover slide) of an electrospun fibre mat (known weight, containing 100 µL of T4 bacteriophage) was gently placed over the solidified agar gel. The agar plates were incubated at 37 ^{o}C for 20 h. Duplicate experiments were conducted for the zone inhibition measurements. Control experiments were performed in the same manner using the same size of electrospun fibre mats with no T4 bacteriophage.

2.13 Steady shear viscosity measurement

Rheological characterization and/or steady shear viscosity measurements were performed using an AR2000 Rheometer (TA Instruments). In a typical experiment, electrospun nanofibre mats were submerged in SM buffer for 10 min at which a 1mL aliquot (non-dissolved material remained settled at the bottom of the test tube) was removed and placed between the cone and plate geometries. Then samples were subjected to a steady shear at a constant shear rate ($\dot{\gamma}$), resulting in the generation of a shear stress (τ). The corresponding shear stress (τ) on the sample was measured using a torque transducer. The viscosity (η) was measured as a function of the steady shear rate (γ). In a typical experiment 1 mL of polymer solution was loaded onto the center of the bottom plate and the upper geometry (40 mm cone with 2^{0} angle) was lowered to the adjusted zero gap and the excess solution around geometry was removed. The solutions were then relaxed for 1 minute to reach an equilibrium state prior to viscosity measurement. Shear rates ranged from 0.05 s^{-1} to 500 s^{-1}. All viscosity measurements were conducted at 25 ^{o}C.

2.14 Data analysis

Experimental error was determined by running multiple samples (minimum of 2 samples) for all different electrospinning conditions and release measurements. For those experiments with duplicate measurements the average of the absolute deviations of data points from their mean

(AVEDEV) were reported. And for the experiments with triplicate measurement and above, standard deviation (STDEV) were reported. In this thesis, all of the raw data presented is the average of the replicate runs and the difference between the highest and lowest values was less than 5%. This was consistently the case for all of the experimental measurements.

In the SEM and CSLM experiments, image analysis was done using Image J software (NIST, version 1.46). The average fibre diameter was obtained from a minimum of one hundred measurements taken from multiple fibres on at least two different SEM scanned images. The brightness and contrast of the confocal images was also adjusted using Image J software with all samples being treated the same.

Chapter 3: Results and Discussion

3.1 PEO fibre formation and encapsulation of T4 bacteriophage via suspension electrospinning

Previous studies showed that the incorporation of tailed bacteriophage such as T4 in electrospun fibres using phage/polymer suspensions was not viable (Lee 2004; Salalha 2006). However, none of the previous studies had tried using PEO as the polymer support. PEO is a flexible water-soluble polymer that has been utilized to manipulate osmotic pressure and even replace water in various applications (Dubrovskii 2001). As such it may enhance the viability of T4 bacteriophage during suspension electrospinning by reducing the effect of dehydration.

3.2 Suspension electrospinning of PEO/T4 bacteriophage

Simple suspension electrospinning of aqueous PEO solutions was employed as a first attempt to incorporate the T4 bacteriophage (T4 bacteriophage) into electrospun PEO fibres. Such an encapsulation process requires the development of a smooth electrospinning process to ensure that the T4 bacteriophage is properly incorporated into the fibres. Fortunately, PEO is one of the most widely studied polymers in electrospinning (Vega Lugo 2012). It readily forms nanofibres and can be easily manipulated to produce fibres with varying morphology and diameters (Doshi 1995). As such we did not need to devote a lot of time to developing the optimal electrospinning parameters. Electrospinning optimization was performed for using PEO (M_n ~300,000 g/mol) in water, where the PEO polymer concentration was varied from 8 to 12 %wt. At 10 %wt concentration uniform bead-free fibres were formed using a flow rate of 0.02 mL/min and a voltage/distance of 15 kV/cm. The same conditions were then applied to the suspension electrospinning of PEO/T4 bacteriophage.

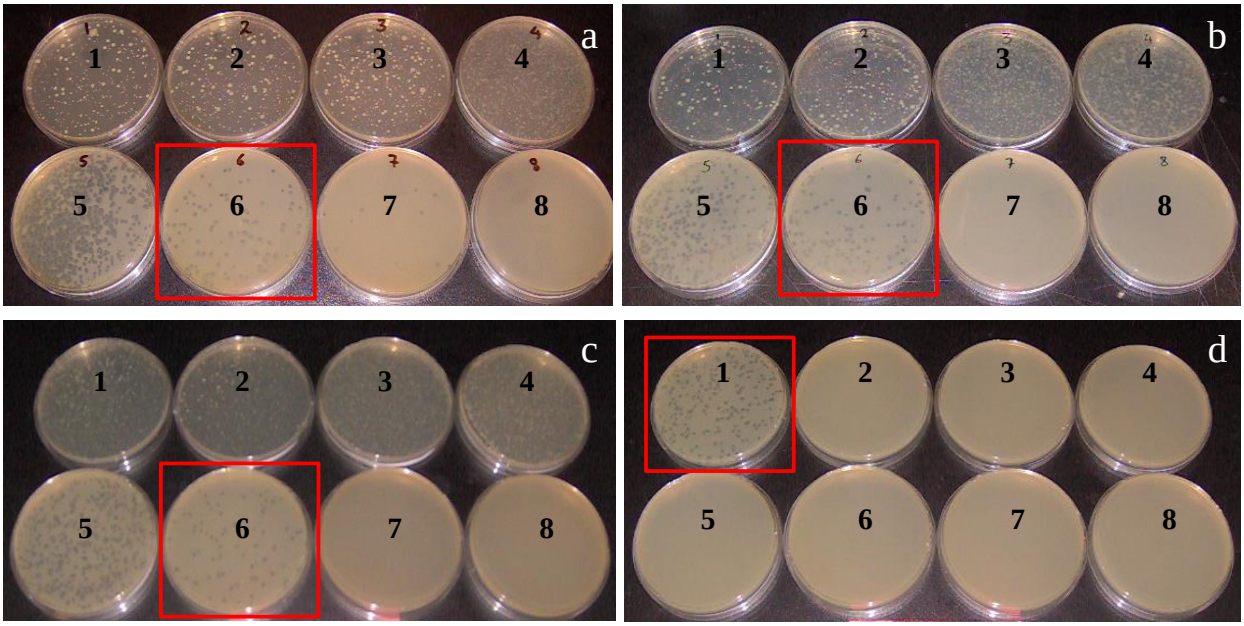

Figure 3-1: Plaque assay testing of T4 bacteriophage activity (performed by 8 fold serial dilution test) of (a) original stock (10^8 PFU/mL), (b) after PEO polymer dissolution (10^8 PFU/mL), (c) after dialysis (10^8 PFU/mL) and (d) after suspension electrospinning (10^3 PFU/mL). *n*=3 for all experiments.

An aqueous buffer containing T4 bacteriophage and PEO (M_n 300,000 g/mol, at 10 %wt concentration) was suspension electrospun to encapsulate the T4 bacteriophage into PEO fibres. PEO has shown to be biocompatible with low toxicity (Hong Chena 2008); however, it was important to understand the effect of the PEO specifically as it relates to the T4 bacteriophage activity. As such, the bacteriophage activity was calculated using the plaque assay test, which is a standard method to determine virus concentration. Plaques were generally counted manually (between 30 to 300) and the results, in combination with the dilution factor used to prepare the plate, were used to calculate the number of plaque forming units per sample volume (PFU/mL). The activity of the stock suspension of T4 bacteriophage was determined to have an activity of 10^8 PFU/mL

(**Figure 3.1a**). The addition of PEO (at 10 %wt concentration) to the T4 bacteriophage dispersion had no effect on the bacteriophage activity; no reduction in activity (10^8 PFU/mL) was observed over one month of incubation (**Figure 3.2)**.

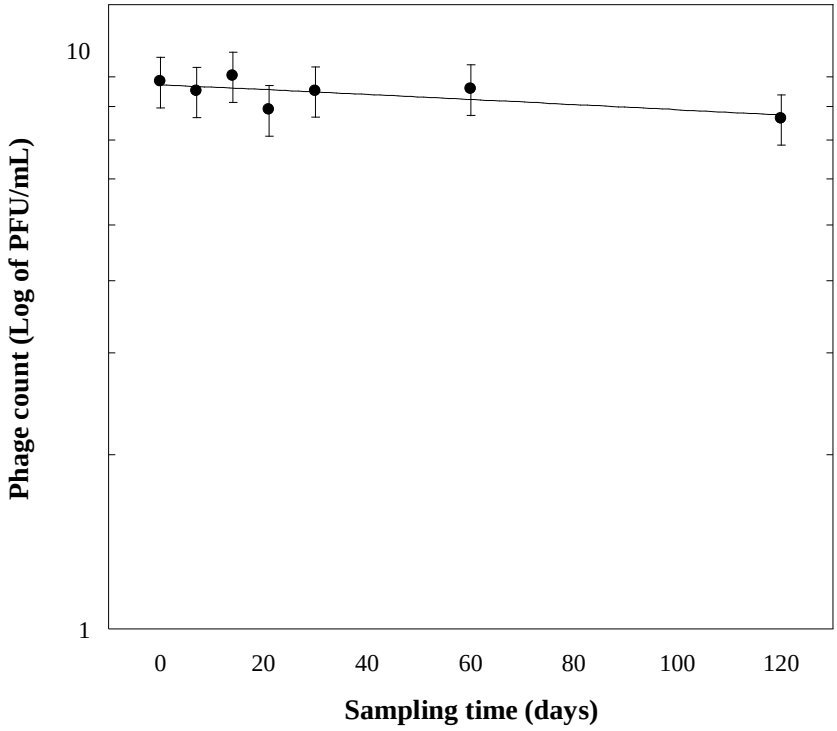

Figure 3-2: Effect of PEO addition on T4 bacteriophage activity. Activity was measured in duplicate by using plaque assay test n=2. Error bar indicate average absolute deviation from the mean of data points.

The PEO (10 %wt)/T4 bacteriophage/SM buffer suspension was then used for electrospinning, however, uniform fibres were difficult to obtain. This was attributed to the presence of salts and

other stabilized components in the T4 bacteriophage buffer. The presence of salt in the buffer suspension increased the net charge density on the fibre jet which negatively influenced the electrospinning process (Xiao and Frey 2007). Therefore, the buffer/T4 bacteriophage solution was dialyzed to remove the ionic components from the buffer. Plaque assay testing was then performed to determine the T4 bacteriophage activity prior to electrospinning, and as shown in **Figure 3.1c** no reduction in the T4 bacteriophage activity was observed after 48 hours of dialysis.

Electrospinning of the dialyzed T4 bacteriophage (2 mL) suspended in an aqueous PEO solution (10 %wt) was then performed using a 5 mm diameter syringe with a flow rate of 0.2 mL/min, a voltage of 1 kV/cm and a gap of 15 cm. The electrospun PEO fibres with T4 bacteriophage were collected on a sterilized aluminum plate and were identified as uniform nanofibres with an average diameter of 500 ± 100 nm (**Figure 3.3a**). The SEM images reveal smooth fibres with no presence of T4 bacteriophage or particles on the surface of the fibres. The encapsulation of T4 bacteriophage was further confirmed by TEM analysis, where the embedded T4 bacteriophage were visible, non-uniformly distributed, near the surface of the fibre matrix (**Figure 3.3d)**.

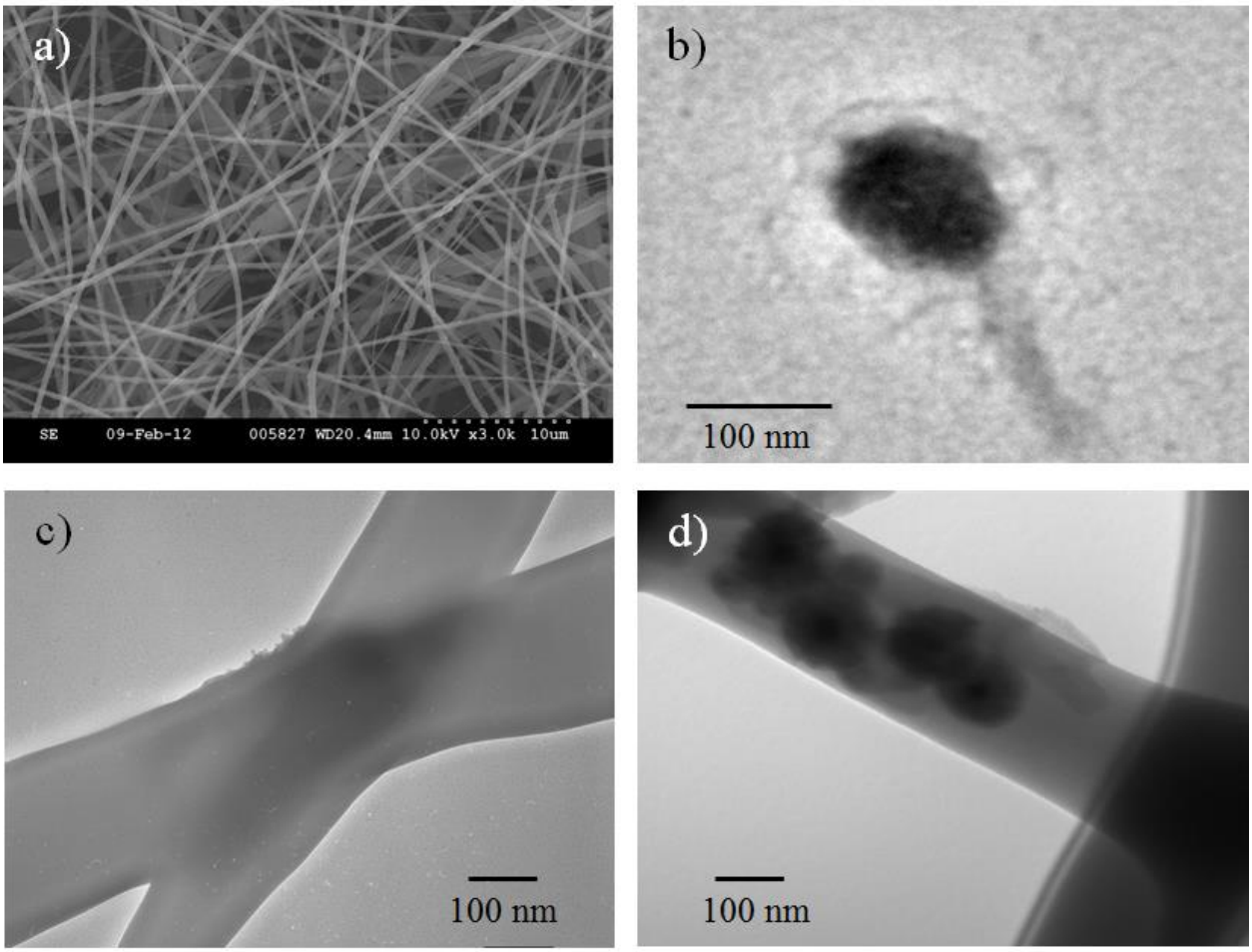

Figure 3-3: a) SEM micrograph of PEO fibres after suspension electrospinning, b) TEM micrograph of the T4 bacteriophage, c) TEM micrograph of plain PEO electrospun fibres, d) TEM micrograph of incorporated T4 bacteriophage in PEO fibres.

The encapsulated T4 bacteriophage nanofibres were then immersed in SM buffer to determine the bacteriophage activity. The fibres immediately dissolved when submerged in SM buffer, instantly releasing the T4 bacteriophage. Usually in blend suspension electrospinning a high initial burst release has been observed, which is attributed to the presence of trapped particles close to the fibre surface (Van de Weert 2000). However, the plaque assay test showed a large drop in T4 bacteriophage activity from 10^8 to 10^3 PFU/mL, which corresponds to near complete loss of ac-

tivity (**Figure 3.1d** and **Table 3.1**). This large drop in activity is likely due to the rapid dehydration of the T4 bacteriophage during the electrospinning process (Lee 2004; Salalha 2006). The non-uniformity of the embedded T4 bacteriophage distributed throughout the fibre matrix (**Figure 3.3d**) was likely caused by solvent evaporation: the embedded phages closer to the surface of the fibre are more vulnerable to the rapid dehydration. To test this and to prevent rapid dehydration of phages, the pre-encapsulation of the T4 bacteriophage in an alginate reservoir and their incorporation into the core of fibre prior to electrospinning was investigated.

Table 3-1: Lytic activity of T4 bacteriophage after each process of encapsulation,* electrospinning (E-spinning) and electrospraying (E-spraying).

T4 bacteriophage activity	*Original stock*	*After freeze drying*	*After suspension E-spinning*	*Released from Ca-alginate capsule, after emulsification*	*Released from Ca-alginate capsule, after E-spraying*	*Released from fibre, after emulsion E-spinning*	*Released from fibre, after coaxial E-spinning*
PFU/mL	10^8	10^8	10^3	10^7	10^3	10^6	10^8

***** based on results from at least three different batches, $n = 3$.

3.3 PEO/Chloroform solution electrospinning

Critical to developing the emulsion electrospinning process for the encapsulation of bacteriophage is the development of the PEO/chloroform electrospinning system. Therefore, a systematic investigation was first performed to set the critical parameters for electrospinning PEO (300 k M_n)/chloroform solutions and assess the morphology of the resultant fibres. The parameters investigated include: polymer concentration, solution volumetric flow rate, electric voltage, and distance between spinneret and collector. The first step was to vary polymer concentration while keeping the initial voltage (15 kV), collector to spinneret distance (15 cm) and flow rate (0.03 mL/min) constant; the initial values were selected based on those reported in the literature (Seeram 2005). A range of polymer concentrations from 0.5 to 3.0 %wt were used and prepared by dissolving PEO in chloroform and allowing the solution to equilibrate for 24 hrs prior to electrospinning. At 0.5 %wt, the PEO/chloroform solution was disrupted considerably at the spinneret tip and formed large and heterogeneous droplets at the target (SEM image not obtained). This observation suggests that the solution had been electrically charged, but did not acquire enough polymer molecular entanglements to form a fibre jet (Seeram 2005). At 1.0 %wt PEO, electrospinning led to the observation of beads with the formation of some thin fibres within the beads **(Figure 3.4a)**. The failure to generate uniform fibres could be due to the low viscosity and surface tension of the solution, causing the jet to break and retract into spherical form (Shenoy 2005). Further increasing the PEO concentration to 1.5 %wt improved fibre formation, however some very large and elongated beads were still observed in the SEM images (**Figure 3.4b**). Increasing the PEO concentration to 2.0 %wt resulted in a continuous electrospinning process and uniform fibre formation with an average fibre diameter of 2.0 μm. At this concentration, there was a sufficient amount of polymer chain entanglement in the solution to enable good fibre for-

mation. At this concentration and with the spinning parameters used the charge present allowed the jet to fully stretch the solution and form uniform fibres without breakup (**Figure 3.4c**). Further increasing the polymer concentration to 2.5 %wt increased the viscosity of the solution and resulted in the formation of a long single jet during the electrospinning process and the expected increase in fibre diameters. Further increasing the PEO concentration to 3.0 %wt significantly increased resulting fibre diameters (**Figure 3.4d)**. Increasing concentration leads to higher polymer entanglement and greater resistance of the solution to be stretched by the charges acting on the jet (Reneker 1996). In the case of 3.0 %wt polymer concentration, a single thick filament of PEO fibre was collected.

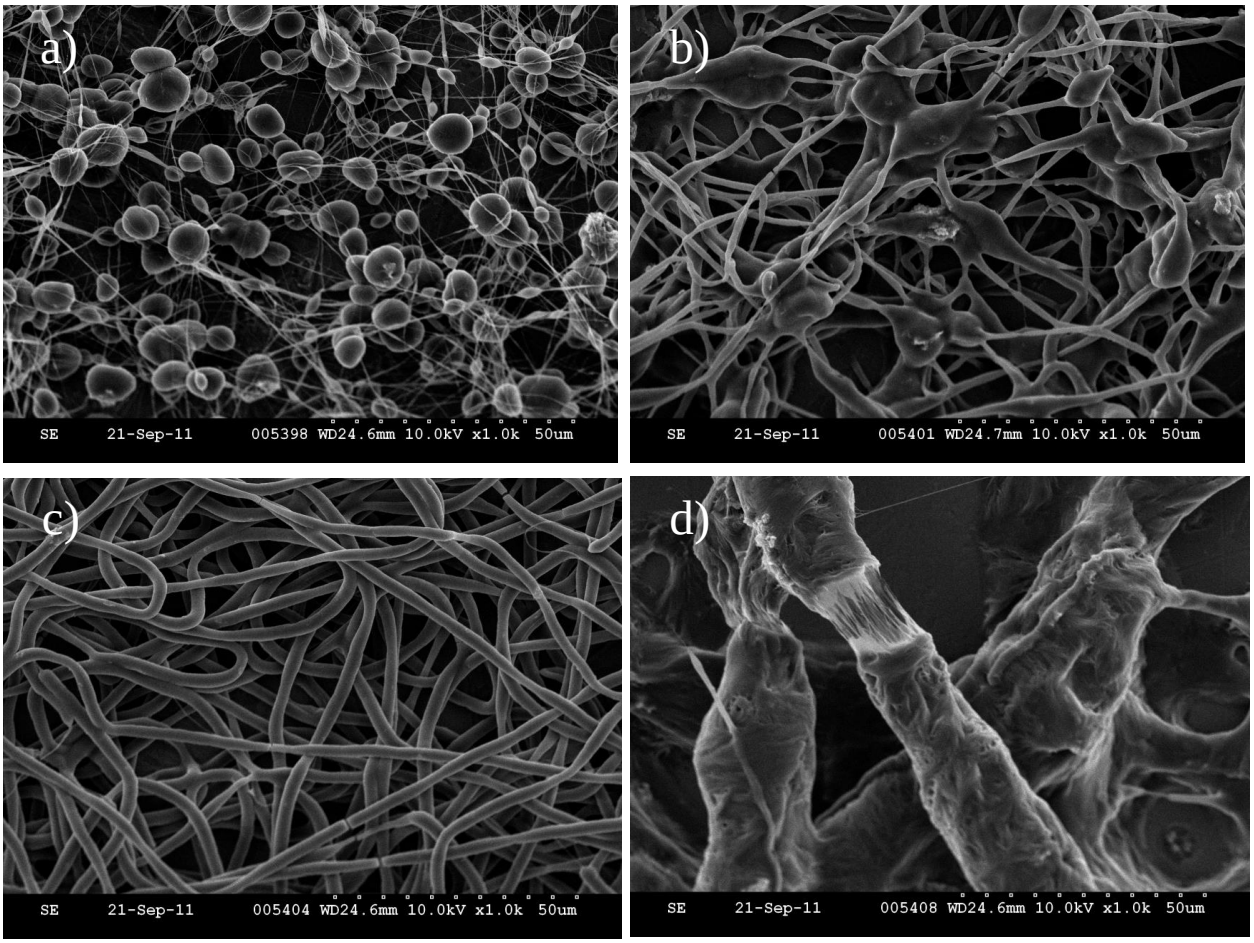

Figure 3-4: SEM images of electrospun PEO fibres using PEO/chloroform solutions of (a) 0.5 %wt, (b) 1.5 %wt, (c) 2.0 %wt, and (d) 3.0 %wt PEO concentration. Electrospinning conditions: flow rate = 0.03 mL/min, voltage = 15 kV and distance = 15 cm. Electrospun fibres were directly collected on SEM stubs and gold coated (5 nm) prior to SEM analysis.

Another important parameter is feed rate. Ideally, the feed rate must match the rate of removal of solution from the tip to maintain a continuous Taylor cone. At a very low feed rate (0.003 mL/min), electrospinning (applied voltage was 15 kV and collector distance was 15 cm) of a 2.0 %wt PEO solution was an intermittent process where the Taylor cone was depleted, causing the

emerging solution to block the needle and preclude fibre formation. By contrast, at very high flow rates (> 0.3 mL/min) using the same conditions (15 kV; 15 cm), a greater volume of solution is drawn from the needle tip, resulting in a rate that did not allow for the solvent to evaporate before hitting the collector. The residual solvent caused the fibres to fuse together and form a continuous web (**Figure 3.5b**). However, when the flow rate was adjusted to 0.03 mL/min uniform fibres could be obtained under the electrospinning conditions used (applied voltage was 15 kV and collector distance was 15 cm) (**Figure 3.5a**).

Next the effect of applied voltage was investigated. **Figure 3.5c** and **3.5d** illustrate the effect of increasing acceleration voltage from 5 to 25 kV respectively on the fibres obtained from the electrospinning of 2.0 %wt PEO solutions; a flow rate of 0.03 mL/min was chosen and the collector distance was maintained at 15 cm. A crucial element in electrospinning is the application of high voltage to the polymer solution. As the applied voltage is increased it reaches a critical value, which together with external electric field induce the necessary charge on the polymer solution to distort the solution droplet at the tip of needle into the shape of a Taylor cone (Seeram 2005; Andrady 2008). If the electrostatic forces can overcome the surface tension of the solution then the initial jet can be initiated from the Taylor cone to start forming fibres. In the case of a low electric voltage (<5 kV), the 2.0 %wt PEO/chloroform solution did not form a stable Taylor, which resulted in electrospraying **(Figure 3.5c)**. By contrast at very high electric voltage (>25 kV) less uniform and thick fibres were produced **(Figure 3.5d)**. This can be attributed to the increase in the instability of the jet and/or formation of high density beads that eventually join together to form a thicker fibre (Deitzel 2001).

The effect of applied voltage needs to be considered together with other parameters, particularly the gap or distance between the tip and the collector. Gap distance determines the time of travel (and the rate of drying) for the jet and influences the fibre morphology. When the distance between the tip and the collector is short, the jet will have a shorter distance to travel before it reaches the collector plate. As a result, there may not have enough time for the solvents to evaporate prior to arriving at the collector. The result is similar to that of using too fast a feed rate were excess solvent may cause the fibres to merge where they contact to form junctions resulting in inter and intra layer bonding. In fact, at a distance of 5 cm, and the same applied voltage (15 kV) and flow rate (0.03mL/min) resulted in fused fibres as observed in **Figure 3.5e**. Increasing the gap to 10 cm maintained some fibre integrity; however the collected fibres were very nonuniform. Again, the short gap prevented the development of fibre jets in the whipping instability region, resulting in poor quality electrospun fibres (Buchko 1999). Further increasing the distance to 15 cm improved fibre morphology, with the formation of uniform electrospun PEO fibres on the collector (**Figure 3.5a**). Further increasing the collector distance to 25 cm had little effect of fibre morphology (**Figure 3.5f**). Basically, when a very high voltage is applied to a polymer solution, a large distance between the tip and collector is required to form a fine fibre (Megelski 2002). The larger gap increases the flight time of the jet and reduces the fibre diameter, which ultimately results in uniform and smooth fibres. For our system it was found that a voltage/collector distance ratio of 1 kV/cm resulted in continuous electrospinning of uniform fibres.

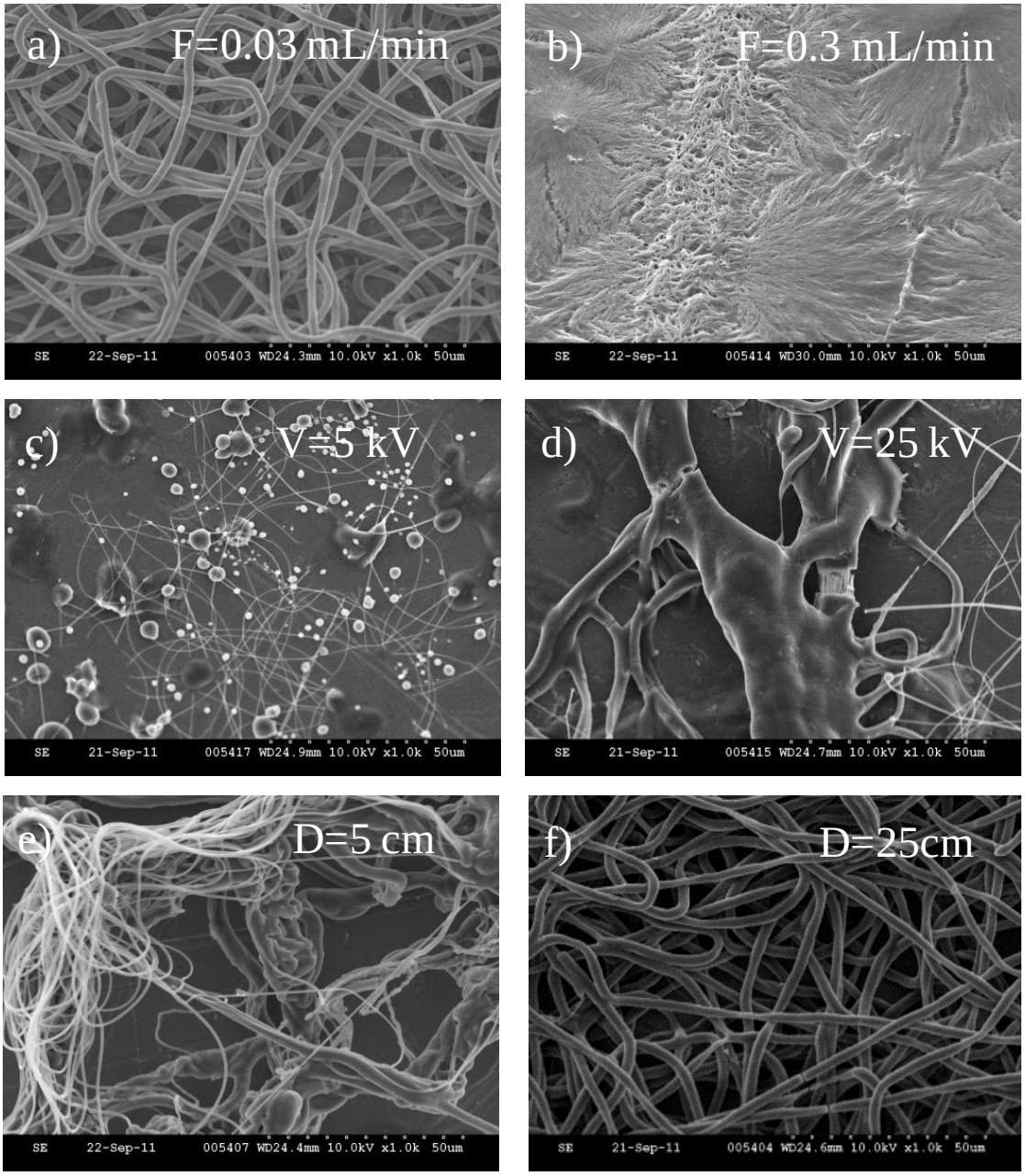

Figure 3-5: Effect of governing parameters on the electrospinning of PEO/chloroform solutions and resulting fibre structure: a) 15kV, 0.03 mL/min, 15 cm; b) 15kV, 0.3 mL/min, 15 cm; c) 5kV, 0.03 mL/min, 15 cm; d) 25kV, 0.03 mL/min, 15 cm; e) 15kV, 0.03 mL/min, 5 cm; f) 15kV, 0.03 mL/min, 25 cm.(applied voltage, flow rate, collector distance).

3.4 Incorporating phage/alginate capsules into fibres using emulsion electrospinning

To improve the viability of T4 bacteriophage during electrospinning, a pre-encapsulation technique was developed. Specifically T4 bacteriophage were pre-encapsulated in a cross-linked alginate reservoir, emulsified and incorporated into fibres via an emulsion electrospinning process. Alginate polymer has been extensively used to encapsulate a range of small to large bioactive components (Jiang 2007). Bacteriophages are also pre-encapsulated in alginate reservoir, but there is no available literature in their further incorporation into electrospun fibre (Yongsheng Ma 2008). Previously report has demonstrated the pre-encapsulation of bovine serum albumin (BSA) in alginate followed by further incoporation into electrospun PLA fibres (Hongxu 2006). Although no specifics were given as to the effectiveness of pre-encapsulation, or even if the BSA was truly encapsulated within the alginate "reservoirs". Therefore, we first set out to investigate the pre-encapsulation process using BSA to optimize and investigate encapsulation efficiency. Then the same methodology of BSA encapsulation was subsequently used to incorporate T4 bacteriophage into an emulsion electrospun fibre and the effect of T4 bacteriophage viability determined.

Pre-encapsulation using a cross-linked alginate "reservoir" was employed to protect the structural integrity of the T4 bacteriophage and avoid dehydration during the electrospinning process. The emulsion system was water in oil (w/o) emulsion where the aqueous phase contained the alginate and bioactive agent and the oil phase (chloroform) contained the PEO and a surfactant. After dissolution of the polymer in external phase (chloroform), the emulsion system was then put through the electrospinning process. The resultant electrospun fibres were shown to incorporate the bioactive agent/alginate capsules inside the fibre. Here, the bioactive agent was trapped in the alginate capsules and protected from the organic external phase and dehydration during

electrospinning. The ability to incorporate alginate capsules in both hydrophilic and hydrophobic polymers using emulsification electrospinning was investigated with both poly (ethylene oxide) (PEO) and cellulose diacetate (CDA), respectively. Both polymers were dissolved in the external phase of the emulsion system and electropsun in to fibre. The morphology of these fibres was characterized using SEM, TEM, and LCSM. In addition, the bioactivity of the T4 bacteriophage was measured using plaque assay tests throughout the emulsification process and after fibre formation.

3.4.1 Emulsion electrospinning – evidence supporting the encapsulation of BSA in alginate capsules and electrospun fibres

The use of alginate as a protecting layer or reservoir has been used extensively for encapsulating low molecular weight drugs (Crcarevska 2008), proteins (Benoy 2006), enzymes (Jiang 2007) and to some extent, bacteria (Hammad 1998) and viruses (Yongsheng 2008). In these applications, techniques such as spray-drying (Crcarevska 2008; Yongsheng 2008), solvent evaporation (Freitas 2005), emulsification follow by evaporation of external phase (Benoy 2006) and electrospinning process (Hongxu 2006) have been employed. Unfortunately, not all are suitable for the encapsulation of bioactive agents. For example, the spray drying technique is not applicable for the majority of bioactive agents as they are typically sensitive to high temperatures. In the solvent evaporation technique, the application of a second aqueous phase can result in leakage of hydrophilic bioactive agents from the microcapsules, reducing loading efficiency. As well controlling the capsule size is always a challenge. Furthermore, since the capsules are hardened from droplets and form spherical structures, the products from both techniques cannot serve as tissue engineering scaffolds directly. Among those methods for encapsulation, the emulsion electro-

spinning technique was found to be an easy process to encapsulate bioactive/alginate capsules in electrospun fibre.

Figure 3.6 outlines the major steps involved in the emulsion electrospinning method; emulsification of the core materials, dissolution of the fibre-forming polymers in the continuous phase, and electrospinning of the resultant system. The emulsion system was composed of an aqueous phase, consisting of a biomolecule/alginate solution that was dispersed in a chloroform/surfactant organic phase. This system formed a water in oil emulsion (w/o) in which the alginate polymer acts as a shielding layer around the biomolecule protecting it from the harsh organic solvent environment (Hongxu 2006; Qi Hongxu 2006; Qi 2006; Yongsheng 2008).

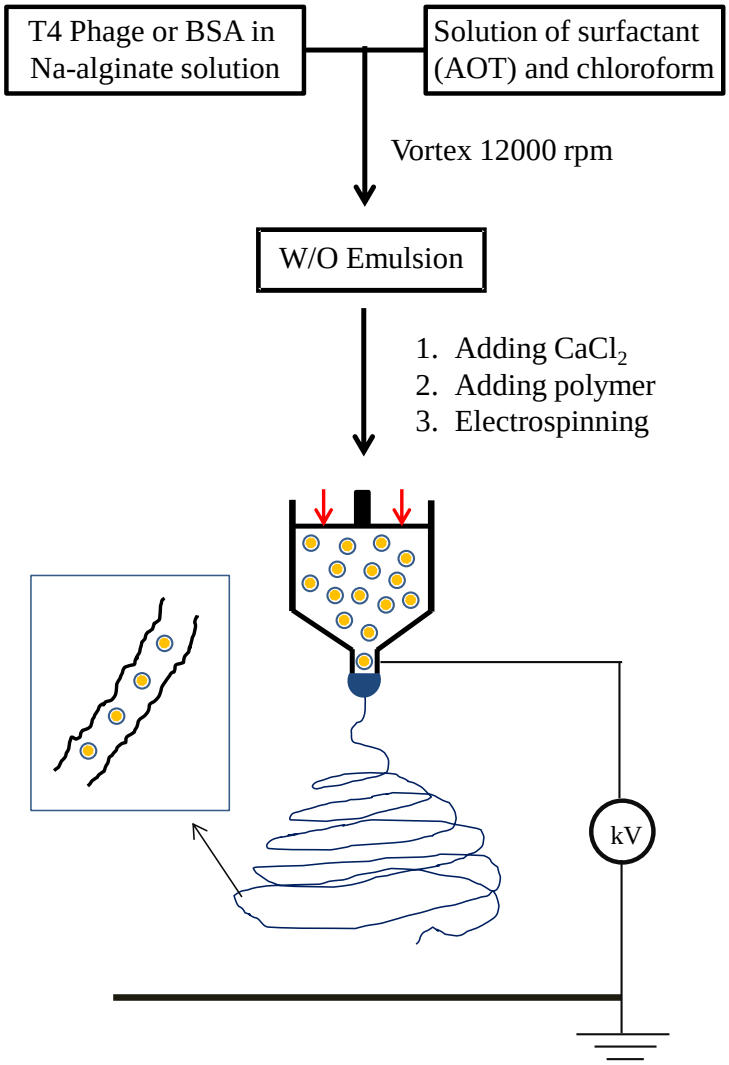

Figure 3-6: Schematic representation of the emulsion electrospinning process used in this thesis.

The pre-encapsulation process was investigated through TEM analysis of the alginate capsules loaded with labeled BSA (BSA-FITC) to enhance image contrast. Accordingly, the emulsion system was prepared by mixing aqueous sodium alginate (2 %wt) with BSA-FITC at a ratio of 9 to 1 (Coppi G. 2002) then dispersing the mixture in chloroform in the presence of a surfactant

(AOT). The sodium-alginate capsules were then *in situ* cross-linked by cationic exchange with calcium chloride. **Figure 3.7** shows the two-dimensional TEM images (2D) of three-dimensional (3D) AOT/alginate and AOT/alginate/BSA-FITC nanocapsules. The TEM images of the AOT/alginate capsules reveal a spherical structure with a dense core (**Figure 3.7a** and **b**); however, the images of the BSA-FITC (fluorescently labeled BSA) loaded capsules clearly show a much darker and denser core (**Figure 3.7c and d**), which supports the encapsulation of the labeled BSA in the AOT/alginate capsules (Benoy 2006). The average AOT/alginate/BSA capsule diameter was found to be ~200 nm, averaged from 6 observation plates. Such capsule sizes could easily pass through a small capillary without clogging and therefore they could readily be incorporated into electrospun fibres.

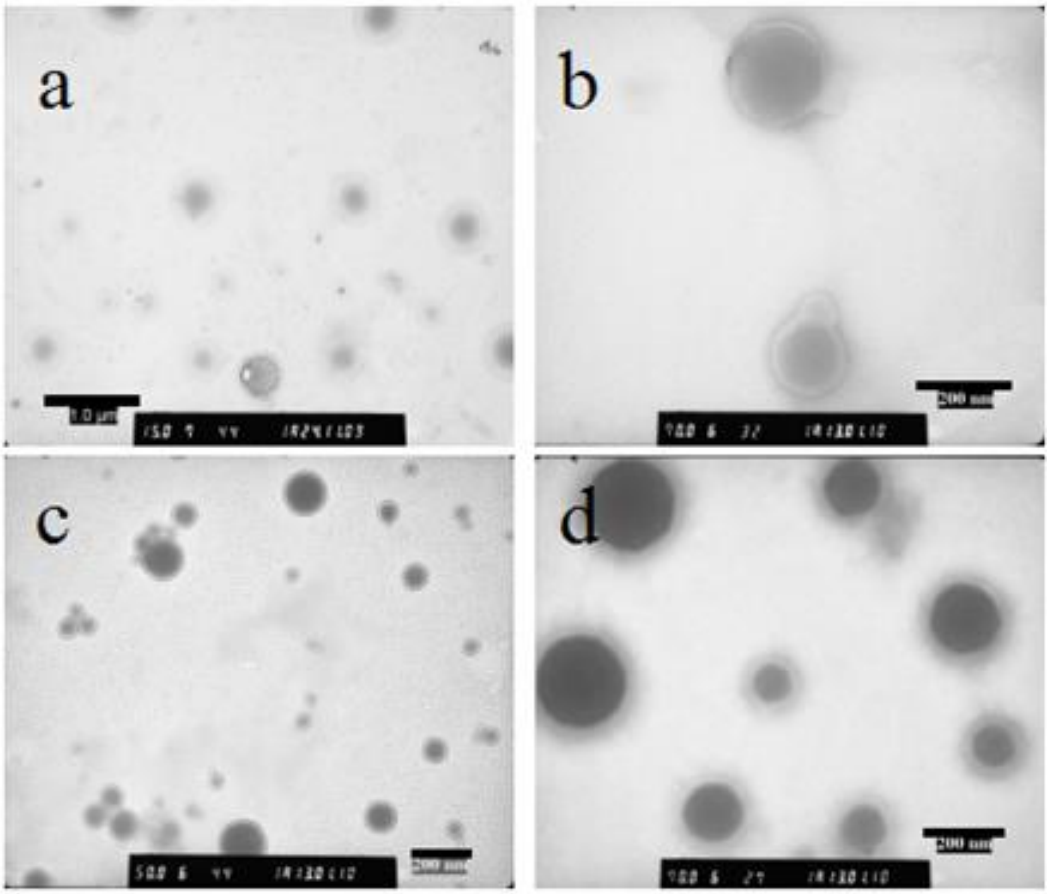

Figure 3-7: TEM micrographs of AOT/calcium-alginate capsules (**a** and **b**) and BSA-FITC encapsulated in AOT/calcium-alginate capsules (**c** and **d**) formed from the emulsification process.

Further support for the incorporation of the BSA within the alginate capsules was made using DSC. **Figure 3.8** shows the second heating run traces for all of the components used in the formulation of the BSA encapsulation process. It can be seen that the DSC trace of the Na-alginate exhibited a glass transition temperature (T_g) at ~159 °C followed by a degradation peak initiating at just before 200 °C (**Figure 3.8)**. By contrast, the thermogram of the cross-linked calcium-alginate had no discernible transitions, which is attributed to the gelation of the alginate biopol-

ymer (Soares 2004). The thermal response of AOT was found to be highly dependent on its molecular conformation. For instance, commercial AOT exhibited a sharp endothermic peak at 184°C (data not shown) whereas AOT micelles showed a broad and blunt peak at 174°C. The pure BSA revealed an endothermic transition at ~159°C followed by a fast and significant degradation starting at about 200°C. However, the BSA/AOT/calcium alginate capsules only exhibited a single broad transition at 173°C. Interestingly, the BSA/alginate/AOT system did not show the aforementioned degradation of the BSA. Although the absence of this peak may be simply due to dilution of the BSA (AOT:BSA 9:1), based on the size of the BSA decomposition peak it is reasonable to expect that some change in the thermogram would be expected if it was just a mixture of the two compounds. In fact DSC analysis of a 9:1 mixture of BSA and Ca-alginate showed degradation peak at about 200°C. The fact that the BSA degradation endotherm (BSA/AOT/calcium alginate) is not present could be associated with the incorporation of this component within the alginate capsules, which may have shifted the degradation peak to higher temperature. A similar finding was also observed and reported in the encapsulation of testosterone in alginate capsules (Benoy 2006). In this system the testosterone melting endotherm disappeared in the alginate formulation indicating it was encapsulated in its amorphous form. Thus the observed DSC results appear consistent with the observed TEM images where the BSA appears to be allocated into the alginate capsules (**Figure 3.7**).

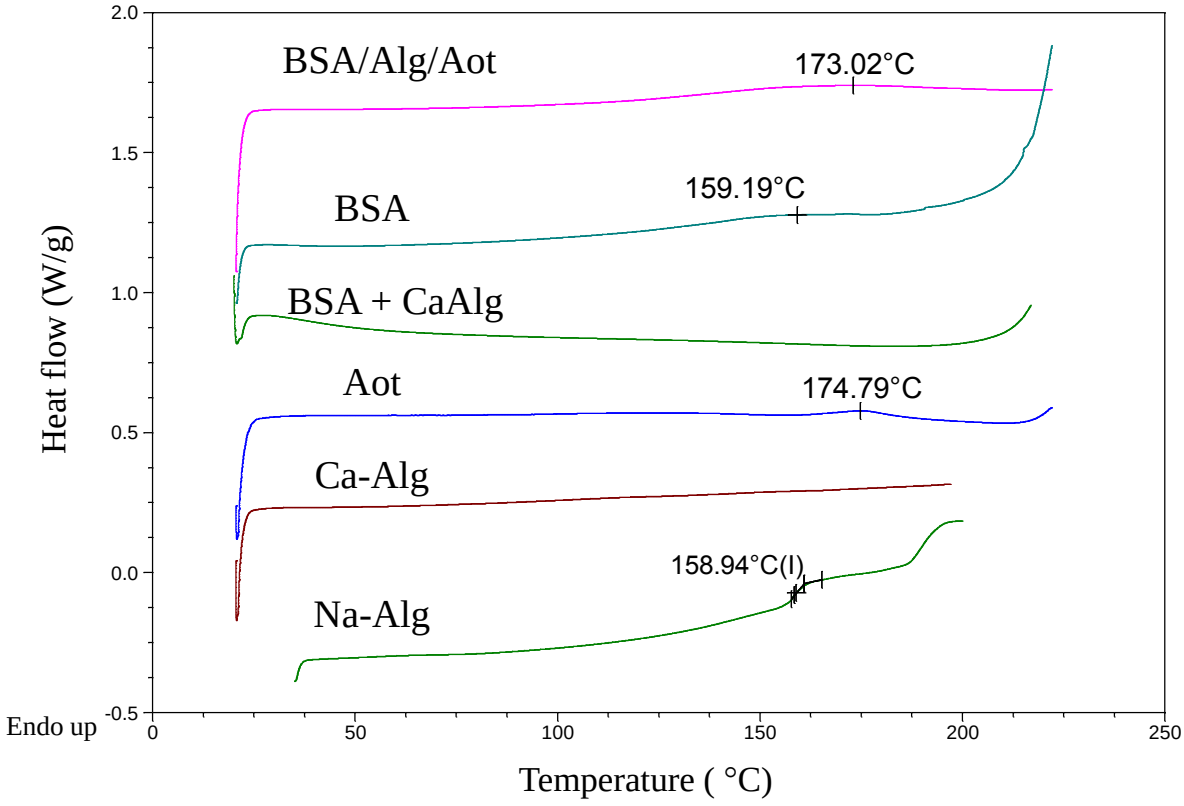

Figure 3-8: DSC analysis of the different components used in the emulsification process. Na-Alg is the commercial sodium alginate powder, Ca-Alg is the calcium chloride cross-linked alginate, AOT is the dried micelles (above the critical micelle concentration) from emulsion system, BSA is the commercial bovine serum albumin powder, and BSA/Alg/AOT is alginate nanocapsules with entrapped BSA collected from emulsion system (dry).

Electrospinning of the prepared emulsion system was performed after dissolving the polymer in the external phase of the emulsion system. The electrospinning of the multiple phase solution resulted in composite electrospun fibres where the BSA/alginate capsules from the dispersed phase were incorporated in the polymer fibre matrix. The solubility and concentration of the polymers in the external phase of the emulsion system was found to be a determining factor for fibre

formation (Xiuling 2005; Xu 2006). The effect of three different PEO concentrations on the emulsion electropsun fibre morphology is illustrated in **Figure 3.9**. The optimal PEO concentration for emulsion electrospinning was found to be ~2.0 %wt, as per that observed in the PEO/chloroform solution spinning. However, in the case of cellulose diacetate (CDA) continuous electrospinning required a higher CDA concentration of 7.5 %wt.

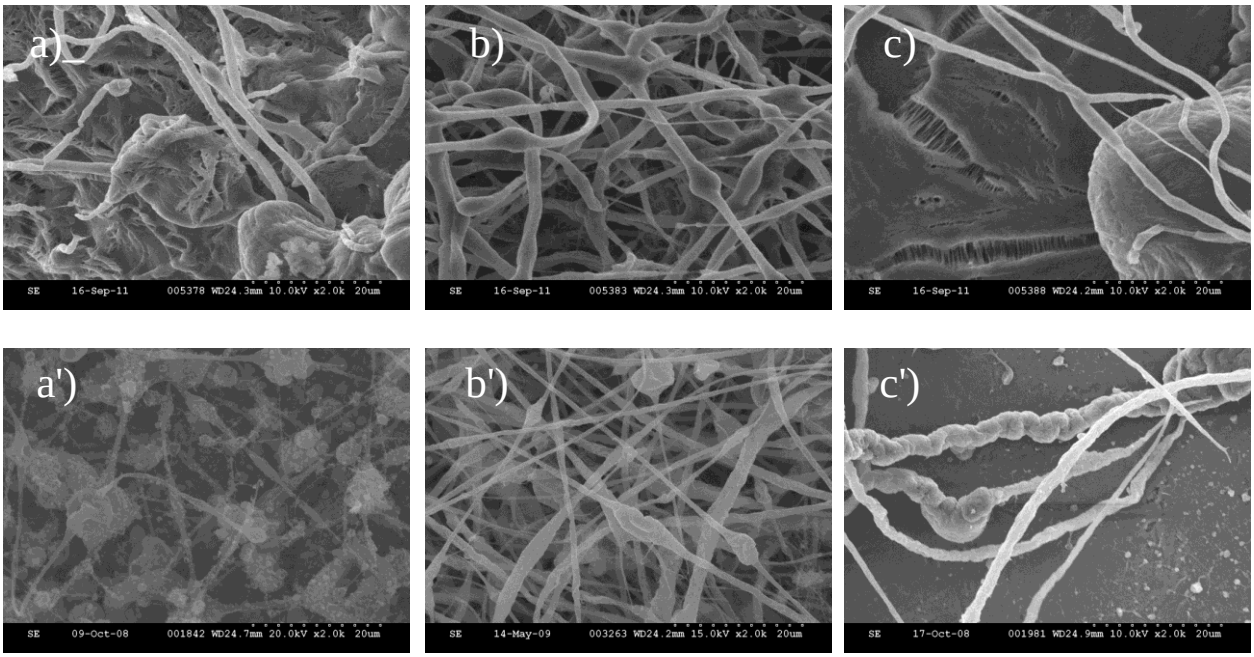

Figure 3-9: SEM images showing the effect of PEO (300k M_n) concentration; a) 1.5 %wt, b) 2.0 %wt; c) 2.5 %wt and CDA (30k M_n) concentration; a') 6.5 %wt, b') 7.5 %wt ; c') 8.5 %wt. on the corresponding emulsion electrospun fibre morphology

Both CDA and PEO chloroform solutions easily produced smooth fibres with an average fibre diameter of 1.0±0.5 μm (applied voltage of 12 kV; 0.02 mL/min flow rate). SEM and TEM images showed fibrous mats as bead-free, transparent, and randomly arrayed fibres (**Figure 3.10**). However, with the emulsion system, a higher voltage (20 kV) was required to form fibres. Moreover, the single nozzle emulsion electrospinning produced non-uniform and beaded fibres; **Figure 3.10** and **Figure 3.11** show fibres produced using CDA and PEO, respectively. The SEM images showed no sign of any particles on the surface of the fibres, indicating the dispersed phase was incorporated in the fibres. In fact TEM images of the emulsion electrospun fibres showed the presence of darker areas within the fibres (**Figure 3.10 and 3.11**), which were not observed in the fibres produced without alginate capsules. Although detailed structural information cannot be observed in the TEM imaged, the darker, bulging areas most likely represent the AOT/calcium alginate encapsulated BSA.

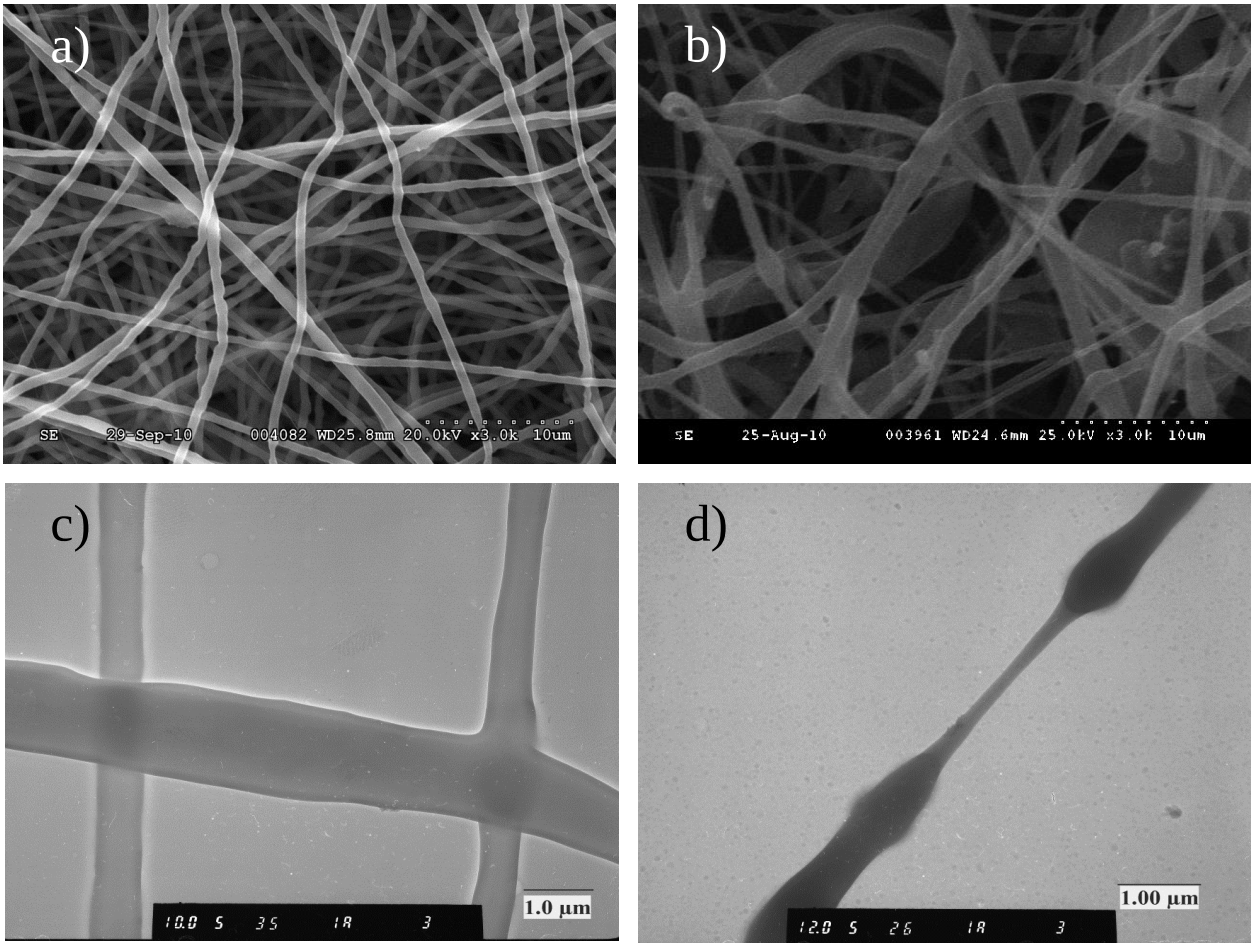

Figure 3-10: SEM images of a) PEO solution electrospun fibres, b) PEO emulsion electrospun fibres, and the corresponding TEM images of c) PEO solution electrospun fibres and d) PEO/AOT/alginate/BSA emulsion electrospun fibres.

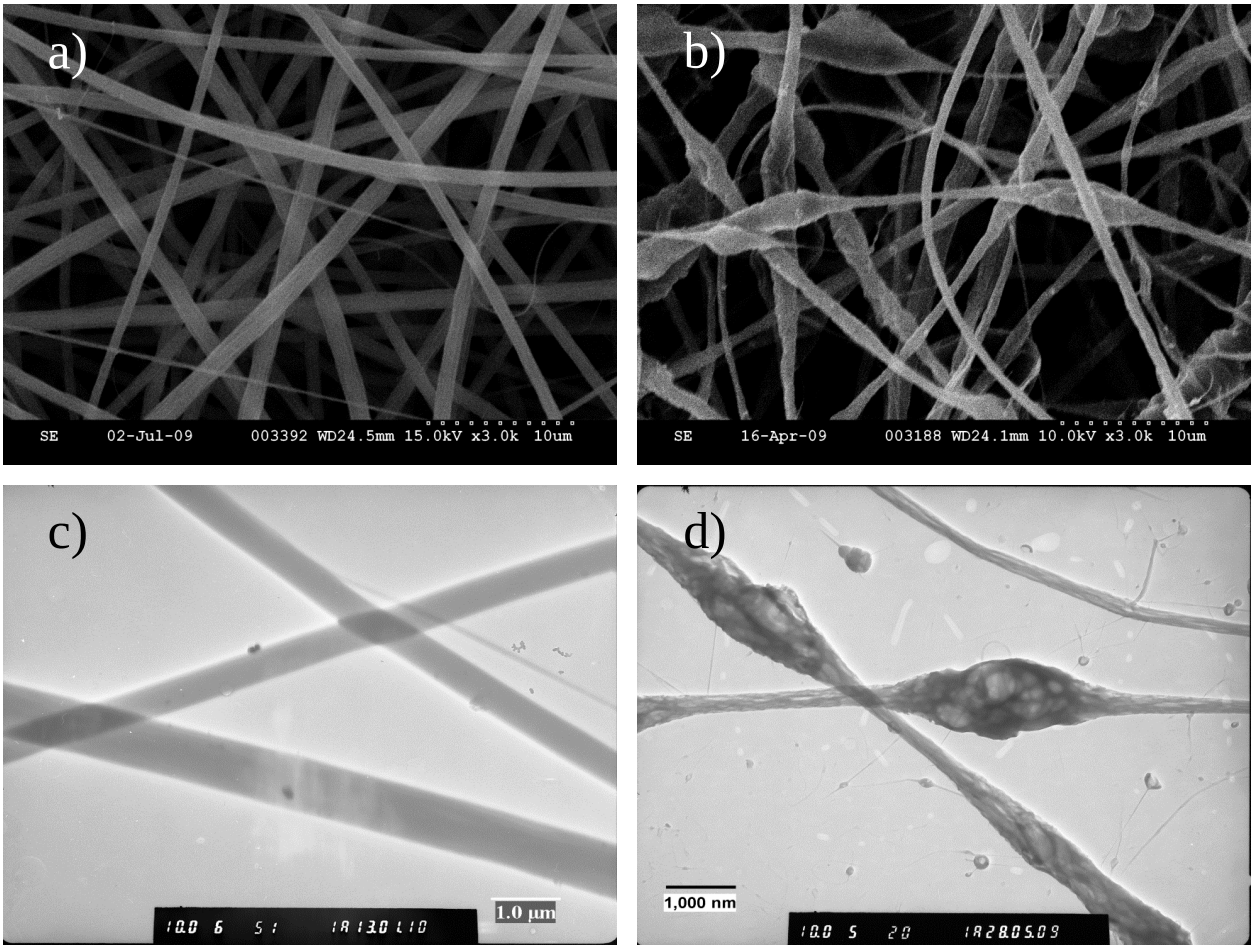

Figure 3-11: SEM images of a) CDA electrospun fibres, b) CDA emulsion electrospun fibres, and the corresponding TEM images of c) CDA solution electrospun fibres and d) CDA/AOT/alginate/BSA emulsion electrospun fibres.

Further support for the encapsulation of the BSA within the electrospun fibres can be seen from the LCSM image (**Figure 3.12**). The confocal images clearly exhibited the green fluorescence of the labeled BSA-FITC along the fibre.

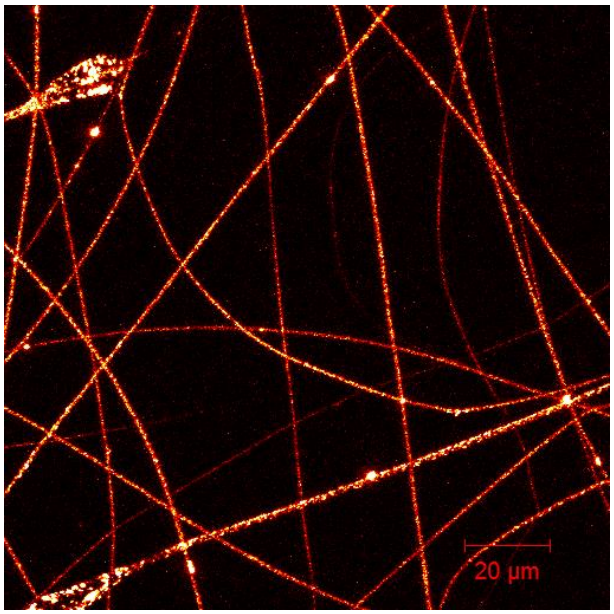

Figure 3-12: Laser confocal scanning microscope image of the emulsion electrospun cellulose acetate fibres loaded with AOT/alginate/BSA-FITC.

The observed morphology wherein the BSA is located inside the polymer electrospun fibre is to be expected due to viscosity differences between the aqueous and polymer organic solvent phases in the emulsion system (Xiuling 2005; Hongxu 2006). In such an emulsion system, the dispersed droplet phase will move perpendicularly from the surface to the center so as to achieve their enrichment in the axial region, which stretches into an elliptical shape in the direction of the fibre trajectory during electrospinning. This inward movement of the emulsion droplets is caused by the rapid elongation and evaporation of the solvents during electrospinning. As the chloroform phase evaporates faster than the water phase, the viscosity of the outer layer of the fibre increases more rapidly than that of the inner layer. As result, the alginate beads settle into the fibres rather than on the fibre surface (Xiuling 2005; Hongxu 2006).

Depending on the volume of the aqueous phase in the w/o emulsion system, the enrichment and rapid accumulation of these droplets in the core of the fibre would also induce a coalescence effect. This could explain the deformation of the spherical shape of the alginate capsules after their incorporation into the electrospun fibres as illustrated by the TEM images. This would also likely affect the distribution of the aqueous dispersed phases within the fibres, the release profiles, and likely the structural stability and bioactivity of the encapsulated components. In the next section, the incorporation and activity of T4 bacteriophage in emulsion electrospun fibres is examined.

3.4.2 Incorporation of T4 bacteriophage/alginate capsules in PEO emulsion electrospun fibres

From the BSA experiments it was clearly shown that small to medium sizes biomolecules could be pre-encapsulated into alginate capsules and successfully incorporated into electrospun fibres. Large size bioactive agens such as bacteria and viruses have been also pre-encapsulated in alginate capsules (Yongsheng Ma 2008); however, further incorporation of these larger size alginate capsules in electrospun fibre has never been reported in the literature. Therefore, the established emulsification and emulsion electrospinning procedure of the BSA (**Figure 3.6)** was employed to incorporate T4 bacteriophage/alginate capsules in electrospun fibre. Again, the encapsulation process involved *in situ* alginate crosslinking using calcium chloride to form a three-dimensional gel network of alginate capsules (Qi Hongxu 2006; Qi 2006). This relatively mild gelation process yielded stable alginate beads, which were obtained as dried alginate capsules loaded with T4 bacteriophage by evaporating the external phase of the emulsion system followed by lyophilisation. The morphological structure of the alginate capsules was characterized using SEM (**Figure 3.13**). SEM images showed relatively uniform alginate beads with no exposure of T4 bacterio-

phage at the surface of the capsules. The average size of the alginate capsules was ~ 800±150 nm, significantly larger than the BSA/alginate capsules (200 nm). The greater size of the T4 bacteriophage/alginate beads is likely due to the larger size of the encapsulated T4 bacteriophage which is ~200×300 nm in size (Ackermann 1987).

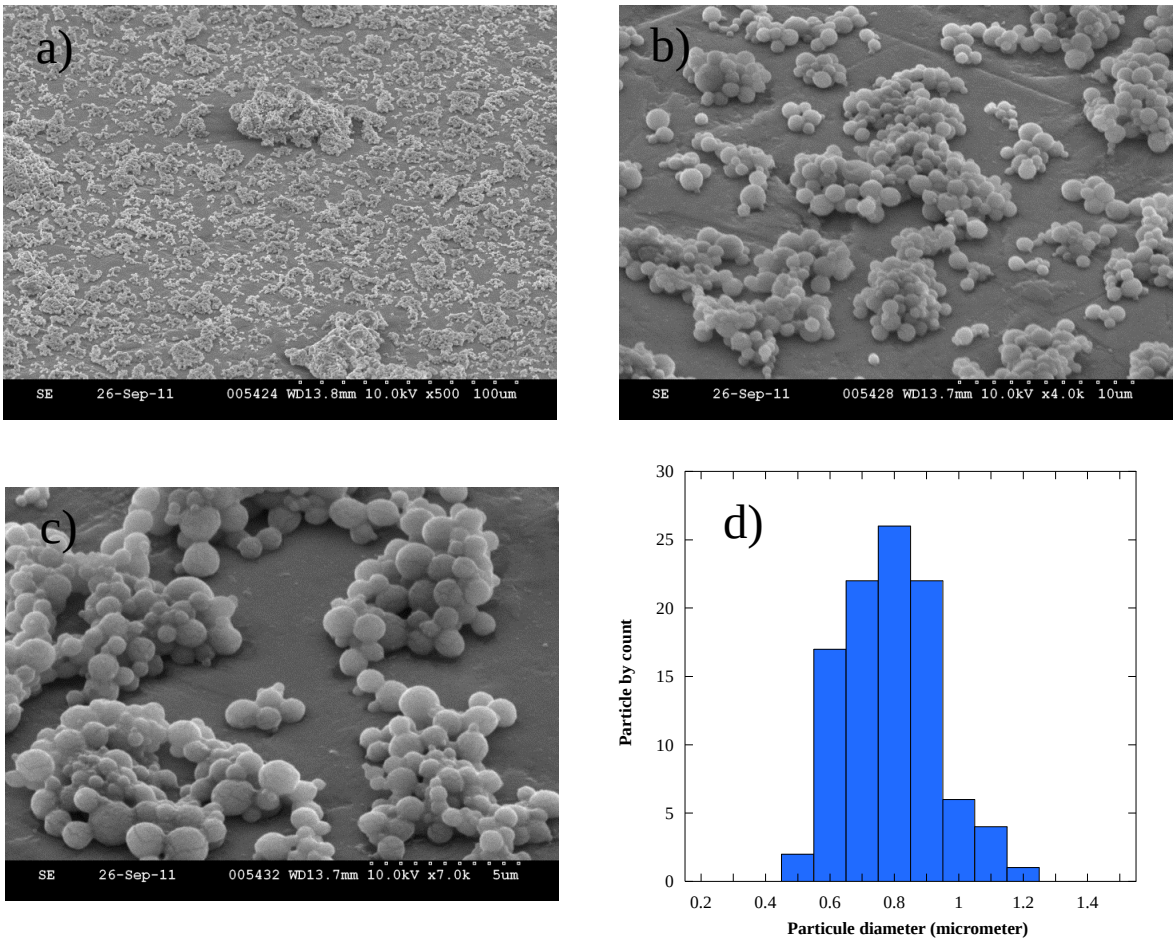

Figure 3-13: Scanning electron micrographs of dried T4 bacteriophage/calcium-alginate capsules prepared by emulsification; a) 500, b) 4.0 k, c) 7.0 k, magnification, and d) T4 bacteriophage/alginate capsule size distribution histogram plot.

Bacteriophages are sensitive microorganisms that are usually damaged upon exposure to organic solvents, acidic or basic conditions, dehydration and/or high temperature (Joerger 2003). As our approach is to protect the T4 bacteriophage through pre-encapsulation prior to electrospinning, it is important to understand the impact of the emulsification process on the stability and activity of the T4 bacteriophage. The lytic activity of T4 bacteriophage after emulsification is illustrated in **Figure 3.14** and listed in **Table 3.1**. T4 bacteriophage activity was not affected by exposure to surfactant, nor to mechanical stirring (10k rpm) or freeze-drying, as measured using a plaque assay test. After the emulsification process, and prior to electrospinning, the bacteriophage activity was maintained to some degree, dropping only one order of magnitude from 10^8 to 10^7 PFU/mL (activity reduced from plate 6 to plate 5. **Figure 3.14a** and **b**). This drop in T4 bacteriophage activity could be due to a deficiency in T4 bacteriophage loading in the alginate capsules and/or leaching of T4 bacteriophage from the capsules prior to cross-linking. Although previous studies have looked at the encapsulation of T4 bacteriophage in suitable aqueous media (Moser 1998; Yongsheng 2008; Puapermpoonsiri 2009), our emulsification process involves the encapsulation in the presence of an organic solvent, chloroform. It is well known that the chloroform-water interface can strongly denature proteins and therefore it can easily destroy T4 bacteriophage structure (Van de Weert 2000). Therefore, the alginate biopolymer as a pre-encapsulating material is needed to protect the T4 bacteriophage structure from such a biologically harsh solvent system.

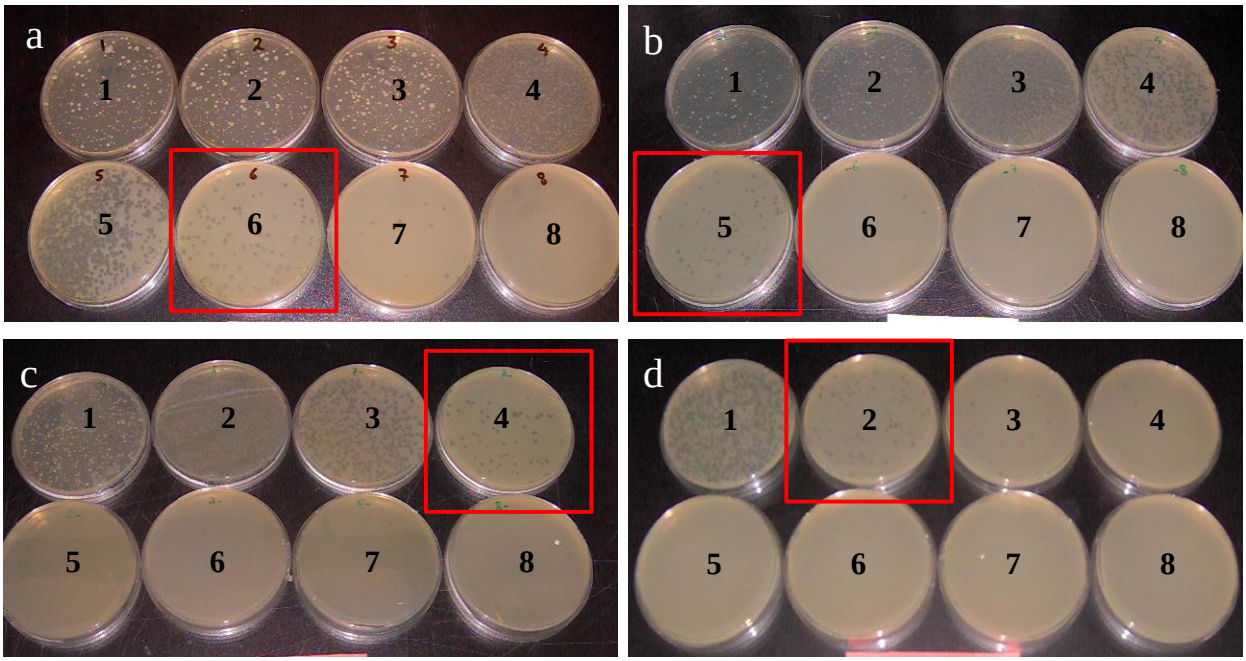

Figure 3-14: Plaque assay tests of T4 bacteriophage (performed by 8 fold serial dilution test); a) original stock, b) after emulsification, c) after emulsion electrospinning, and d) after emulsion electrospraying.

An important aspect in our electrospinning process is the physical stability of the alginate beads as they pass through such an electro-hydrodynamic process. Therefore, electrospraying of the emulsion system without polymer was performed to evaluate the physical stability of the cross-linked alginate capsules. SEM analysis showed that most of the capsules did not survive the electrospraying process; their morphological structures were mostly deformed (**Figure 3.15**). As expected the T4 bacteriophage activity after emulsion electrospraying exhibited a large drop in activity from 10^8 to 10^3 PFU/mL or dropped from plate 6 to plate 4 (**Table 3.1** and **Figure 3.14d**). This could be attributed to the relatively low mechanical strength of alginate capsules (Klein 2009; Ang 2012) and/or the rapid drying that occurs during the electrospraying process. The

electro-hydrodynamics favour rapid desiccation, which results in the deformed morphological structures and the lower T4 bacteriophage activity.

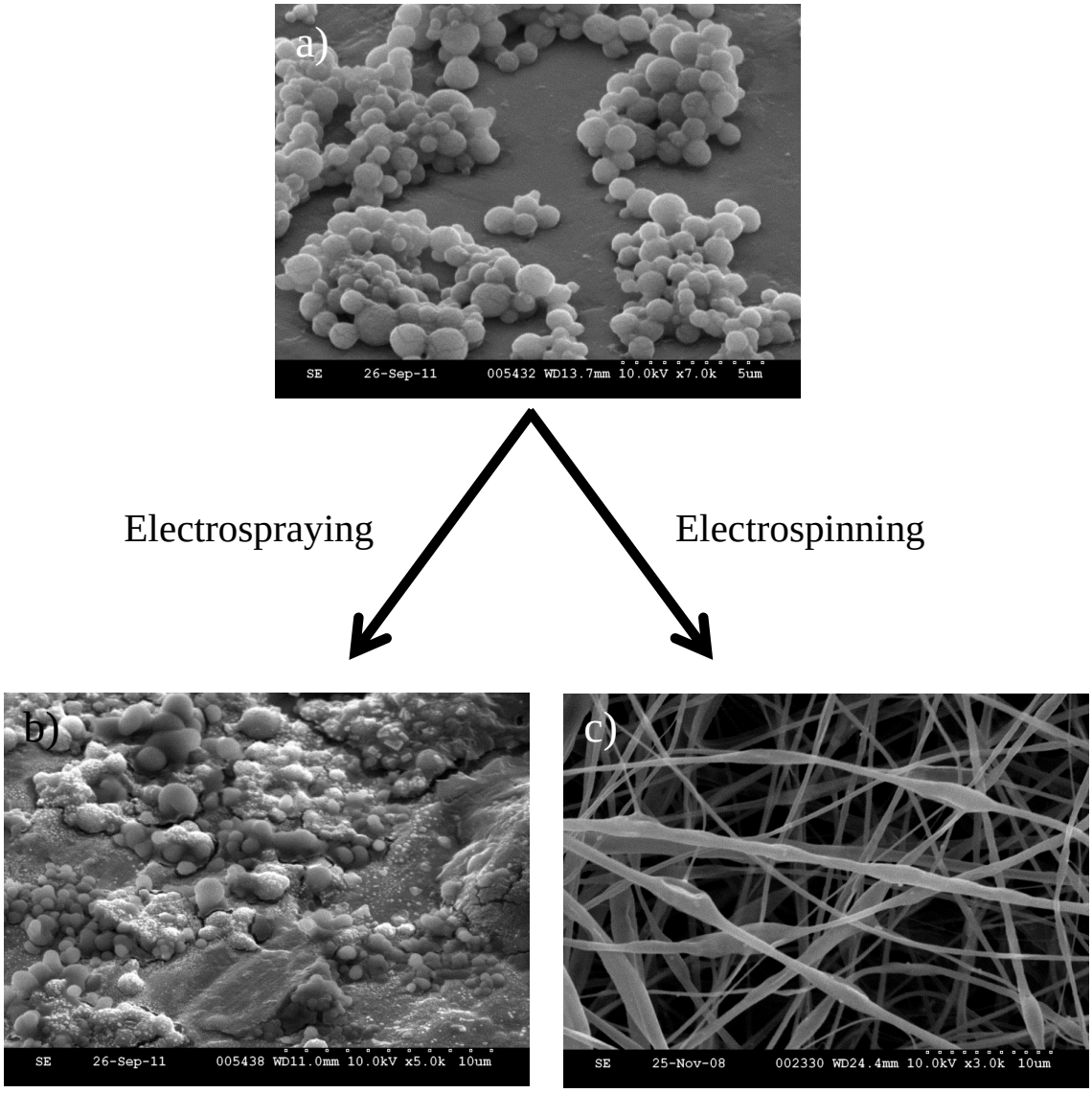

Figure 3-15: Scanning electron micrographs of (a) calcium-alginate capsules prepared using emulsification process, at magnification of 7.0 k, (b) after emulsion electrospraying (no polymer added), and (c) after emulsion electrospinning (with the addition of PEO polymer).

However, through the addition of a fibre-forming polymer the alginate capsules can be protected via the electrospun polymer shell layer, enhancing the mechanical strength of the alginate and avoiding the leaking and denaturation of the encapsulated T4 bacteriophage. We expect the electrospun polymer fibre to provide a protective shell layer around the alginate capsules during electrospinning and we expected that incorporation of T4 bacteriophage/alginate capsules to maintain activity.

Poly (ethylene oxide) is an ideal polymer for emulsion electrospinning. PEO is biocompatible and can be dissolved in both organic and aqueous solvents, making it a suitable carrier for encapsulated T4 bacteriophage. SEM images of electrospun fibres produced from a PEO/phage/alginate emulsion are illustrated in **Figure 3.16**. These fibres have an average fibre diameter of 1.00 ± 0.5 μm with a bead-on-string morphology, indicative of the phage-alginate capsule incorporation (**Figure 3.16b**). The corresponding TEM images show the presence of darker areas within the fibre (**Figure 3.16d** and **3.16e**), which were not observed in the fibres produced without phage/alginate capsules (**Figure 3.16c**).

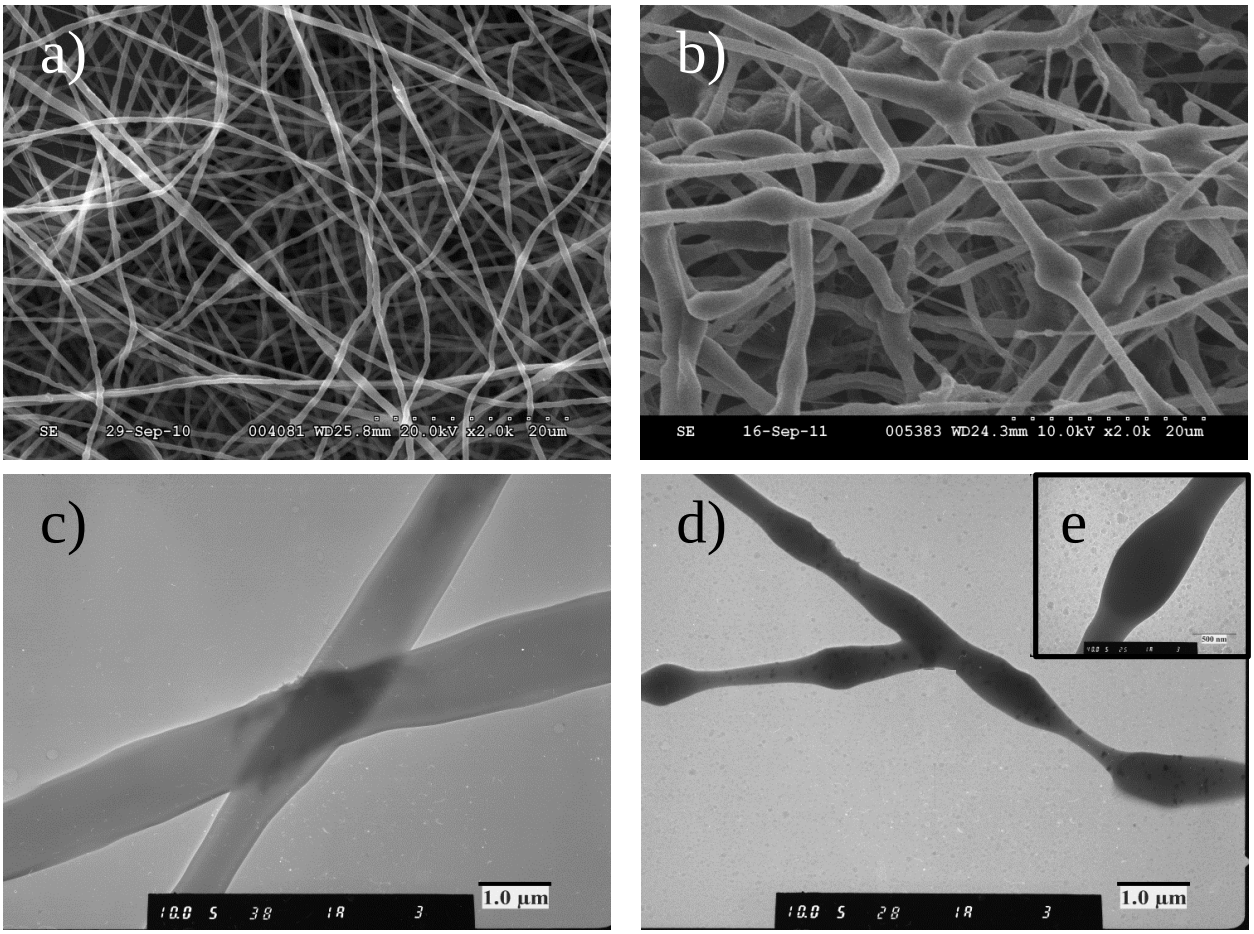

Figure 3-16: SEM images of electrospun fibres from a) PEO solution electrospinning; b) PEO emulsion electrospinning, and TEM images of c) plain PEO fibres from solution electrospinning and d) and e) beaded PEO fibres loaded with T4 bacteriophage/alginate capsules from emulsion electrospinning.

Further support of the successful containment of T4 bacteriophage within the emulsion electrospun fibres was confirmed from the T4 bacteriophage activity measurements. The plaque assay tests revealed a lytic activity of 10^6 PFU/mL, a two orders of magnitude drop from the original stock activity (10^8 PFU/mL or drop from plate 6 to plate 4) or an additional one order of magnitude drop from the emulsification process. The lytic activity of 10^6 PFU/mL corresponds to a

22% drop in T4 bacteriophage activity, as calculated from the log value of PFU/mL (**Table 3.1** and **Figure 3.14c**). (As part of this test the fibres were submerged for 2 hrs in buffer at room temperature to ensure complete T4 bacteriophage release from the calcium alginate capsules and electrospun fibres. As these conditions were used for both the control and electrospun fibre samples, the impact of time and temperature should be the same.) This level of T4 bacteriophage activity is a significant improvement when compared to the activity measured from the suspension electrospun fibres; 10^3 PFU/mL (**Table 3.1**). The decrease in T4 bacteriophage activity in the emulsion electrospun fibres may be attributed to the low mechanical strength of the alginate capsules, where some were likely disrupted during the electrospinning process; emulsion electrospinning of the same alginate system without the addition of calcium chloride (the gelling agent) exhibited no bacteriophage activity (data not presented). This demonstrates the important role of calcium-alginate crosslinking to protect the phages in the alginate capsules during emulsion electrospinning. Moreover, attempts to increase the amount of bacteriophage loaded to see if there was any impact on the amount released did not increase the fibre activity. This implies that there is a "loading" maximum that can be achieved using the alginate capsule technique.

The release profiles of viable bacteriophage from the alginate capsules and from the alginate capsules enmeshed in PEO fibres are compared in **Figure 3.17**. In both systems, a burst release was observed followed by a plateau behaviour after 30 minutes. The burst release in both processes is attributed to the rapid dissolution of the alginate capsules and PEO fibres in the buffer media. The electrospun PEO fibre showed a slightly slower release rate of T4 bacteriophage in comparison to simple alginate capsules. This was expected, as the T4 bacteriophage must diffuse from the alginate capsules prior to its release from the PEO shell electrospun fibre.

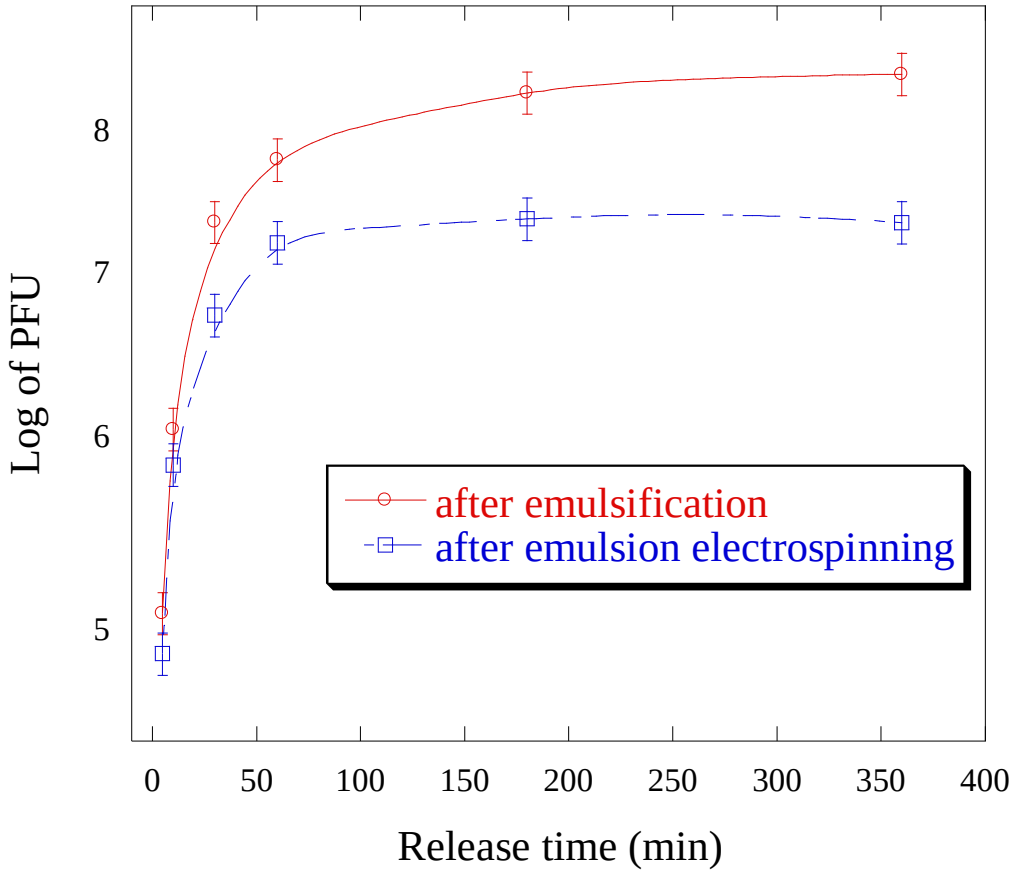

Figure 3-17: T4 bacteriophage release profiles (measured by plaque assaying tests for each point at 37 °C) from alginate capsules (after emulsification) and PEO emulsion electrospun fibres loaded with T4 bacteriophage-alginate capsules (after emulsion electrospinning). Error bars indicate standard deviation; n=3.

SEM analysis of the change in fibre morphology during T4 bacteriophage release is shown in **Figure 3.18.** During the first 2 minutes of soaking in the buffer solution, the PEO fibres begin to swell and rapidly dissolve. Within 5 minutes the PEO fibres are almost completely disintegrated showing very little resemblence to a fibrous nonwoven mat, consistent with measured rapid increase in T4 bacteriophage actvity (**Figure 3.17**).

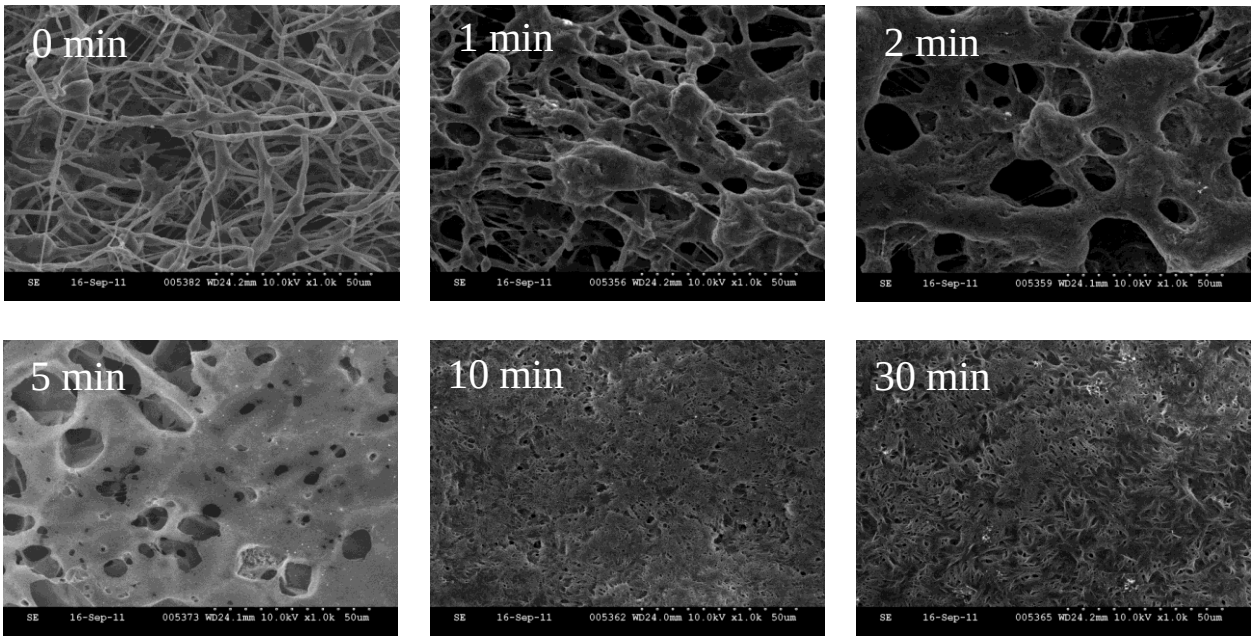

Figure 3-18: SEM images of PEO emulsion electrospun fibres upon exposure to buffer as a function of time. (Samples were freeze-dried prior to SEM analysis).

The decreased bacteriophage activity (2 orders of magnitude, after PEO emulsion electrospinning) and fact that under real-world consumer conditions the release rates would be much different, i.e. less moisture present and thus slower fibre dissolution, make any drop in bacteriophage activity as a result of the loading process (fibre spinning) likely unacceptable. Therefore, coaxial electrospinning was performed in an attempt to improve bacteriophage loading (capacity) and activity and avoid the burst release. In coaxial electrospinning, bacteriophage exposure to harsh organic solvents and rapid water evaporation is minimized and therefore a high viability of encapsulated bacteriophage is expected. Furthermore, by altering the fibre morphology and using a blend of water-soluble and insoluble polymers, a more controlled release profile of the T4 bacteriophage may be obtained.

3.5 Encapsulation of T4 bacteriophage via coaxial electrospinning

In addition to a drop in T4 bacteriophage activity, the drawbacks of alginate-encapsulation and emulsion electrospinning include limitations in bacteriophage loading capacity and low mechanical strength of the alginate capsules. Coaxial electrospinning is a novel method for directly incorporating T4 bacteriophage into the core of the fibre. Using coaxial electrospinning the viability of T4 bacteriophage was fully maintained after encapsulation. The change in morphology and corresponding bacteriophage release profiles of the PEO electrospun fibres were investigated using different microscopic techniques. The effect of PEO molecular weight, and the resultant increase in electrospun fibre diameter, as well as the viscosity of the dissolving medium on the release behaviour of T4 bacteriophage was studied. Encapsulation of T4 bacteriophage within co-axial electrospun fibres affected the long-term storability of T4 bacteriophage, with the observed increased bacteriophage viability representing an excellent alternative to lyophilization for applications such as biosensors and food preservation.

3.6 Coaxial electrospinning and morphology of core/shell electrospun fibre

Core/shell electrospun fibres were produced using a PEO/chloroform solution for the shell and a T4 bacteriophage/buffer suspension for the core (**Figure 3.19**). The idea is to fully incorporate T4 bacteriophage into the core of the fibre and thereby avoid their rapid dehydration during electrospinning. To ensure the complete encapsulation of the T4 bacteriophage in the core of the fibre, the feeding ratio of the core was set to ten times slower than that of the polymer shell solution (**Table 3.2**) (Dror 2008; Klein 2009).

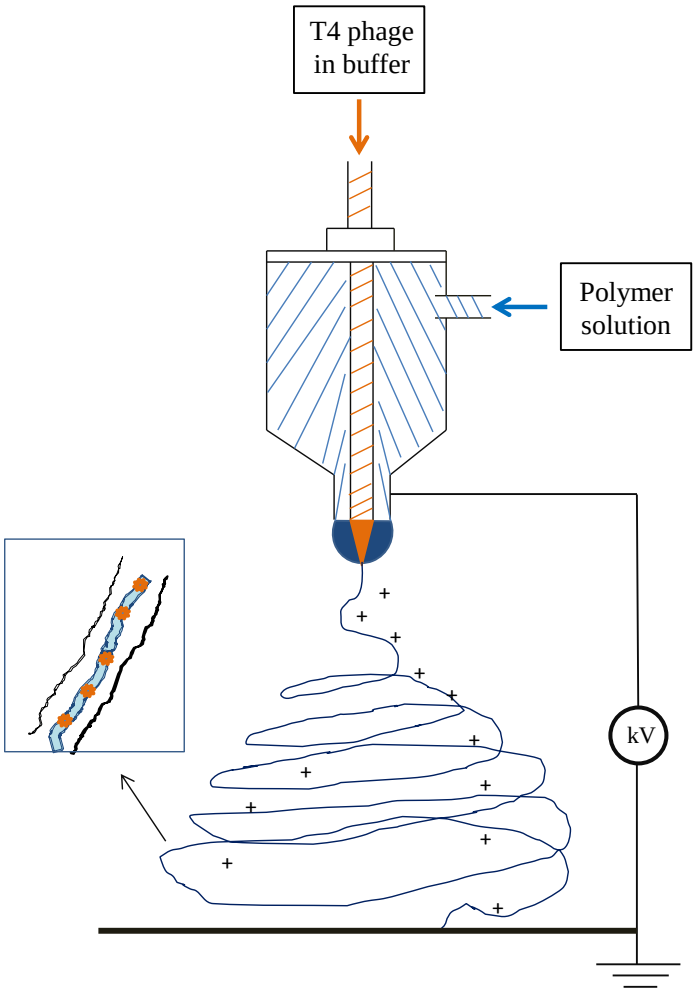

Figure 3-19: Schematic representation of the coaxial electrospinning process.

Table 3-2: Effect of flow rate (shell/core ratio) in coaxial electrospinning on fibre formation. The outer "shell" solution is PEO/chloroform (20 mL syringe) and the inner "core" solution is a T4 bacteriophage dispersion in aqueous SM buffer (1 mL syringe). The inner diameters of the shell and core needles are 1.0 and 0.4 mm, respectively. The applied voltage was 15 kV with a distance of 15 cm.

Flow rate (mL/min) shell:core ratio	**Observation**
1:1	Droplet
5:1	Fibre and droplet
10:1	Uniform fibre

Although the T4 bacteriophage dispersion is not electrospinnable, and it has a tendency to spray, a uniform fibre was obtained via coaxial electrospinning, suggesting the successful formation of a core layer. SEM images of the resulting fibres did not show the presence of any sprayed T4 bacteriophage on the collector or any components on the surfaces of the fibres (**Figure 3.20a).** However, TEM analysis (**Figure 3.20b** and **3.20c)** did confirm the core/shell fibre structure and the presence of T4 bacteriophage in the fibre core. The average diameter of the fibres was determined to be about 1.8 μm (determined from an average of 100 measurements, using duplicate samples). Due to the relatively low contrast between the polymer matrix and the unstained virus particles, the relatively narrow tail could not be seen noticeably although what appears to be the capsid was clearly observed. The lytic activity of the encapsulated T4 bacteriophage was found

to be 10^8 PFU/mL (from three batches); the same as the initial bacteriophage titer before encapsulation 10^8 PFU/mL (**Figure 3.21** and **Table 1**).

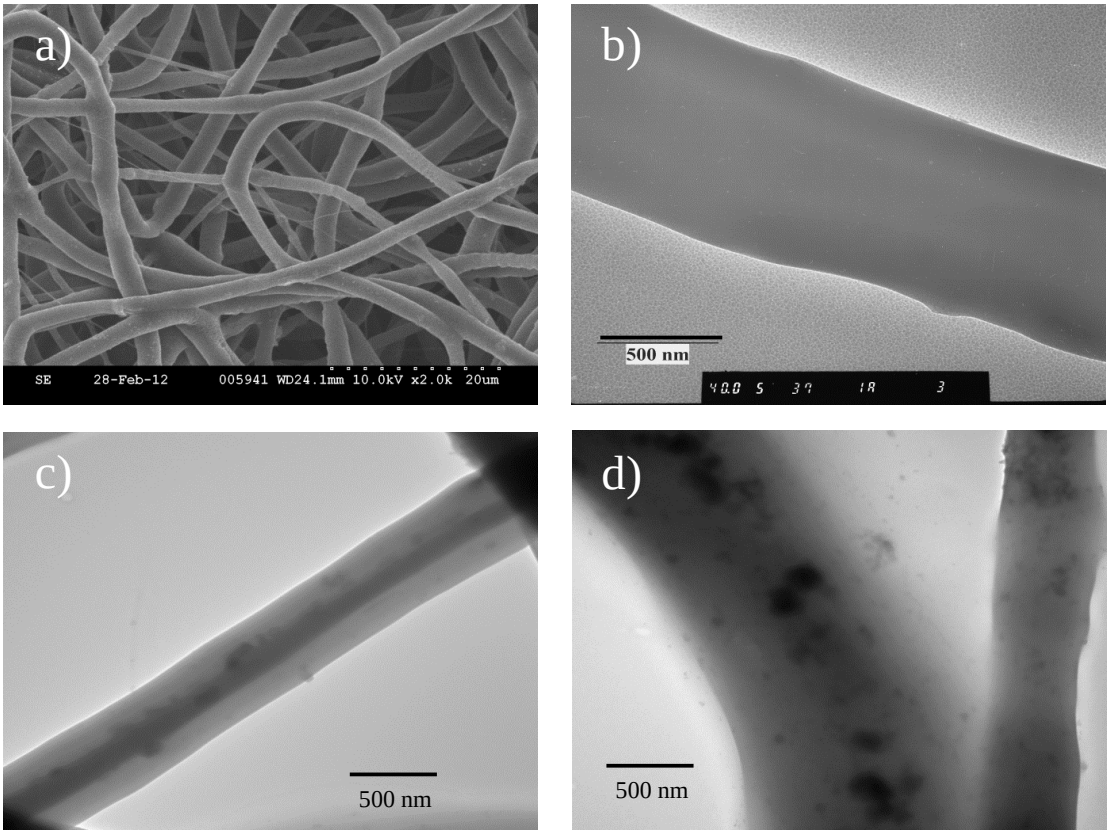

Figure 3-20: a) SEM images of core/shell electrospun PEO fibres, b) TEM image of a plain PEO electrospun fibre, c) TEM image of a core/shell electrospun PEO fibre, and d) TEM image of core/shell electrospun PEO fibres showing T4 bacteriophage incorporated in the core of fibre.

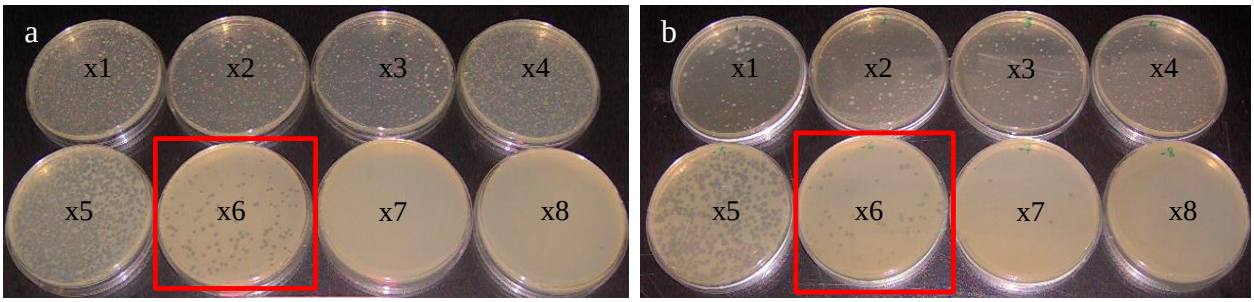

Figure 3-21: Plaque assay tests (performed by 8 fold serial dilution test) of a) original T4 bacteriophage stock, 10^8 PFU/mL, (97 plaques were observed in plate 6), and b), T4 bacteriophage released from coaxial electrospun PEO fibres, 10^8 PFU/mL, (47 plaques were observed in plate 6).

Among the various examined electrospinning processes, coaxial electrospinning appears to be the most reliable process to encapsulate and maintain the viability of T4 bacteriophage. In coaxial electrospinning, the T4 bacteriophage are enclosed in the core of the fibre and shielded by the polymer shell layer, protecting the phages from dehydration during the electrospinning process. In this process solvent evaporation from the core is very slow and, therefore, drastic changes in the osmotic environment of the water-based core is avoided (Klein 2009). Although the PEO fibres with encapsulated T4 bacteriophage maintained complete bacteriophage activity, they were not able to be stored for any prolonged period of time. Fibres stored at 4ºC lost their fibre structure within 24hrs (**Figure 3.22**); the fibres slowly dissolving in the buffer solution remaining in the core of the coaxial electrospun fibres. When the samples were freeze-dried this change in PEO fibre morphology, dissolution was not observed. The presence of the aqueous buffer in the core of the fibre is likely a main reason for the high viability of the T4 bacteriophage during elec-

trospinning. As expected the freeze-dried T4 bacteriophage electrospun fibres did not show any reduction in bacteriophage activity (**Table 3.1**).

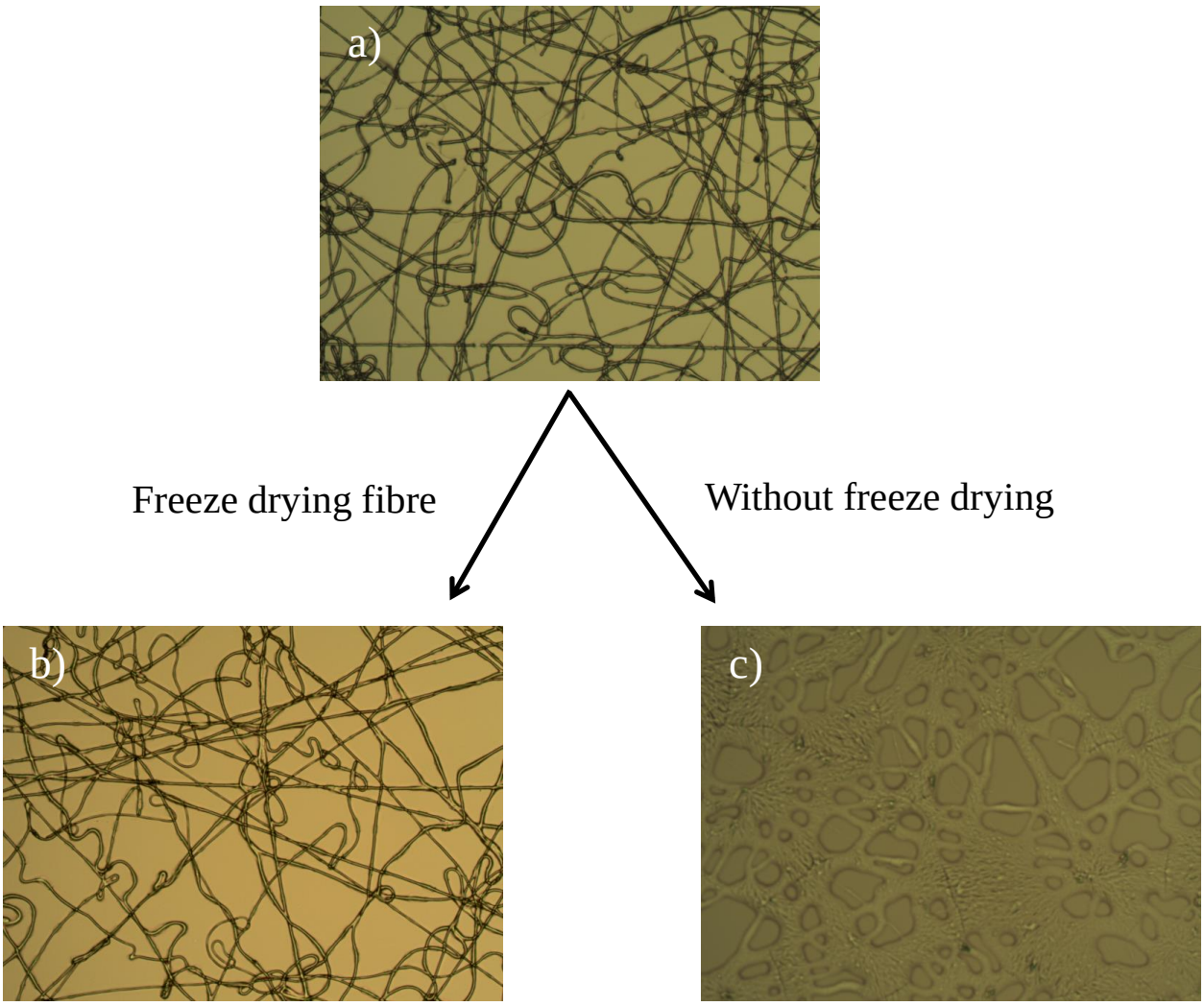

Figure 3-22: Light microscope images of a) core/shell PEO fibres immediately after coaxial electrospinning, b) freeze dried core/shell PEO electrospun fibres, and c) core/shell PEO fibres stored at 4 ºC for 24 hr without freeze drying.

Encapsulated T4 bacteriophage in lyophilized coaxial electrospun fibres may represent an excellent alternative to lyophilized T4 bacteriophage powders for preserving organisms for strain collection, maintaining strains of industrial importance, and for specific applications such as biosensing and food preservation. The loss in activity or storability of T4 bacteriophage in coaxial electrospun fibres were compared to T4 powders over 4 weeks of storage at 20, 4, and −20°C (**Figure 3.23**).

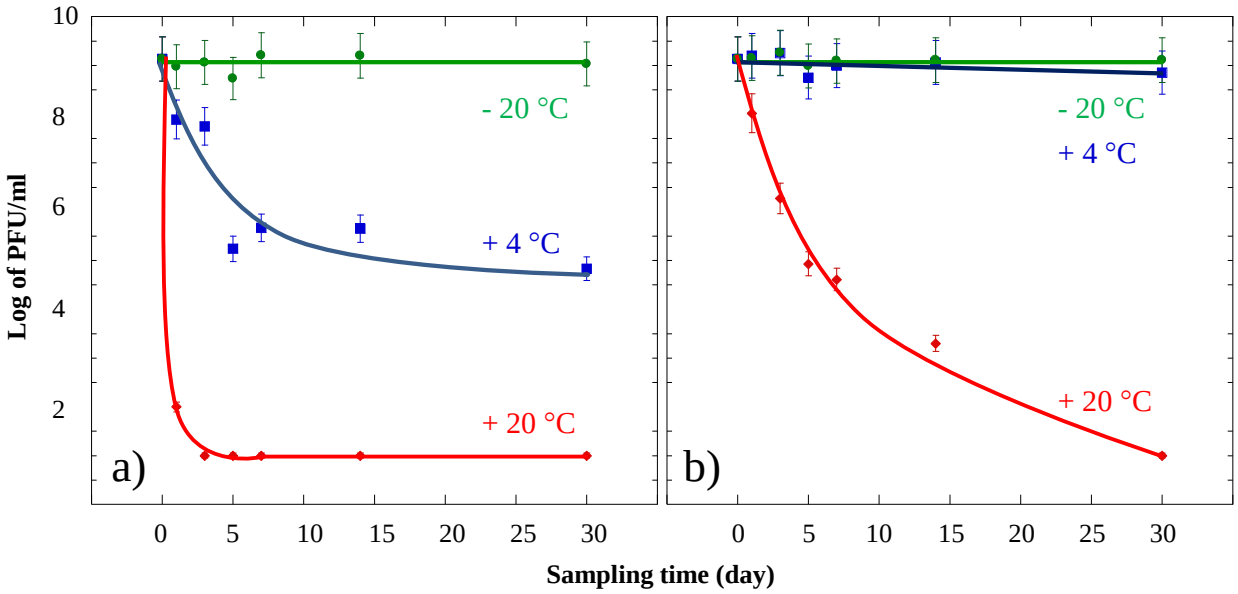

Figure 3-23: Activity-time plots for a) freeze-dried T4 bacteriophage powders and b) encapsulated T4 bacteriophage in freeze-dried core/shell electrospun nanofibres at three temperatures (20, 4, and −20ºC). The titres given represent duplicate plates per point. Error bars indicate average absolute devaition from the mean for each data point; n=2.

Distinct differences in the loss of T4 bacteriophage activity are clearly apparent between the free powders and those incorporated in the electrospun fibres. The activity of the freeze-dried T4 bacteriophage powders (**Figure 3.23a**) decreased rapidly from 10^8 to 10^2 PFU/mL after 1 day of storage at 20°C. At 4°C their activities decreased relatively slower from 10^8 to 10^5 PFU/mL during the one month of storage, with the most significant loss occurring the first week. As expected there was no loss in activity when stored at −20 °C over the 4 weeks of storage. Interestingly, the freeze-dried coaxial electrospun PEO/T4 bacteriophage fibres exhibited significantly different storage behaviour. As shown in **Figure 3.23b**, a significantly slower decrease in viability was observed for the samples stored at room temperature, and those stored at 4 and −20°C were essentially stable for up to one month (longest time tested).

The release profiles of viable bacteriophage from coaxial electrospun PEO fibres, emulsion electrospun PEO fibres and the emulsified calcium-alginate capsules are shown in **Figure 3.24.** In all systems, a burst release was first observed followed by a plateau after about 15 minutes. The burst release in all processes is attributed to the rapid dissolution of the PEO fibre and alginate capsules in the SM buffer. The coaxial electrospun PEO fibres exhibited a faster release than the emulsion electrospun fibres and the emulsified alginate capsules. In the case of the coaxial electrospun fibres, the PEO fibre dissolution is accelerated due to the presence of the aqueous SM buffer in the core of the fibres. The emulsion electrospun PEO fibres exhibited the slightly slower release profile of T4 bacteriophage than that of the emulsified alginate capsules (**Figure 3.24**). In this case, the T4 bacteriophage-alginate capsules are initially liberated from the PEO electrospun fibres, followed by a complete release of the T4 bacteriophage from the alginate capsules.

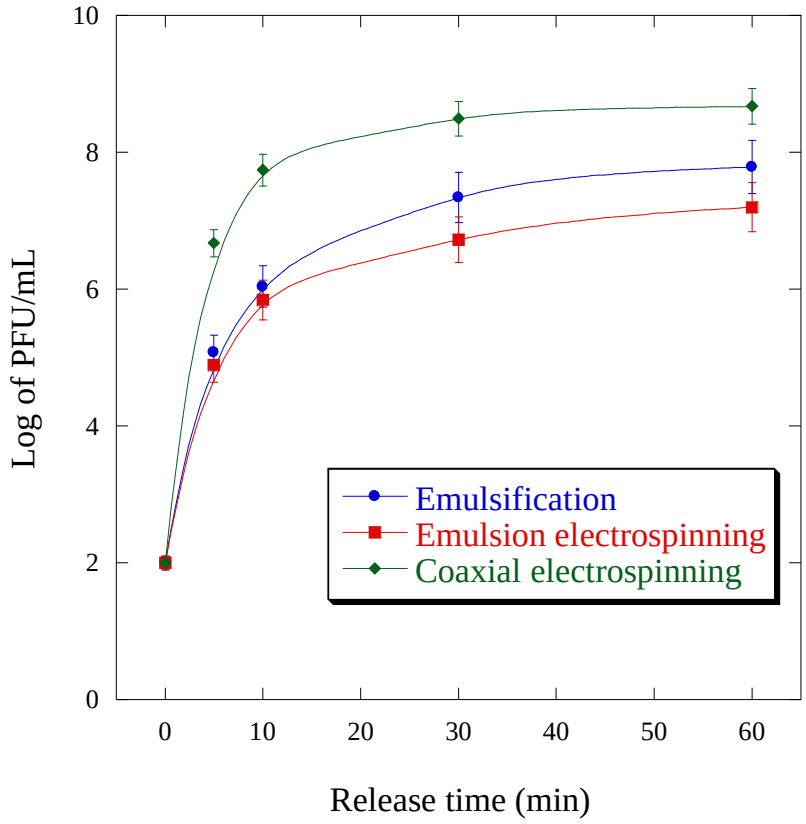

Figure 3-24: T4 Bacteriophage release profiles as measured by plaque assaying testing from emulsified alginate capsules, emulsion electrospun PEO fibres and coaxial electrospun PEO fibres. Error bar indicate standard deviation; *n*=3. Bacteriophage counts of zero were recorded at 100 PFU/mL (or 2 log of PFU/mL), which is the limit of the detection in the assaying test.

The change in morphology of the core/shell electrospun PEO fibres upon exposure to a large excess of aqueous buffer was observed using SEM. Within the first 5 minutes, the PEO electrospun fibre begins to swell followed by complete disintegration within 10 minutes, supporting the rapid release of the T4 bacteriophage observed in a relatively short period of time (**Figure 3.25)**.

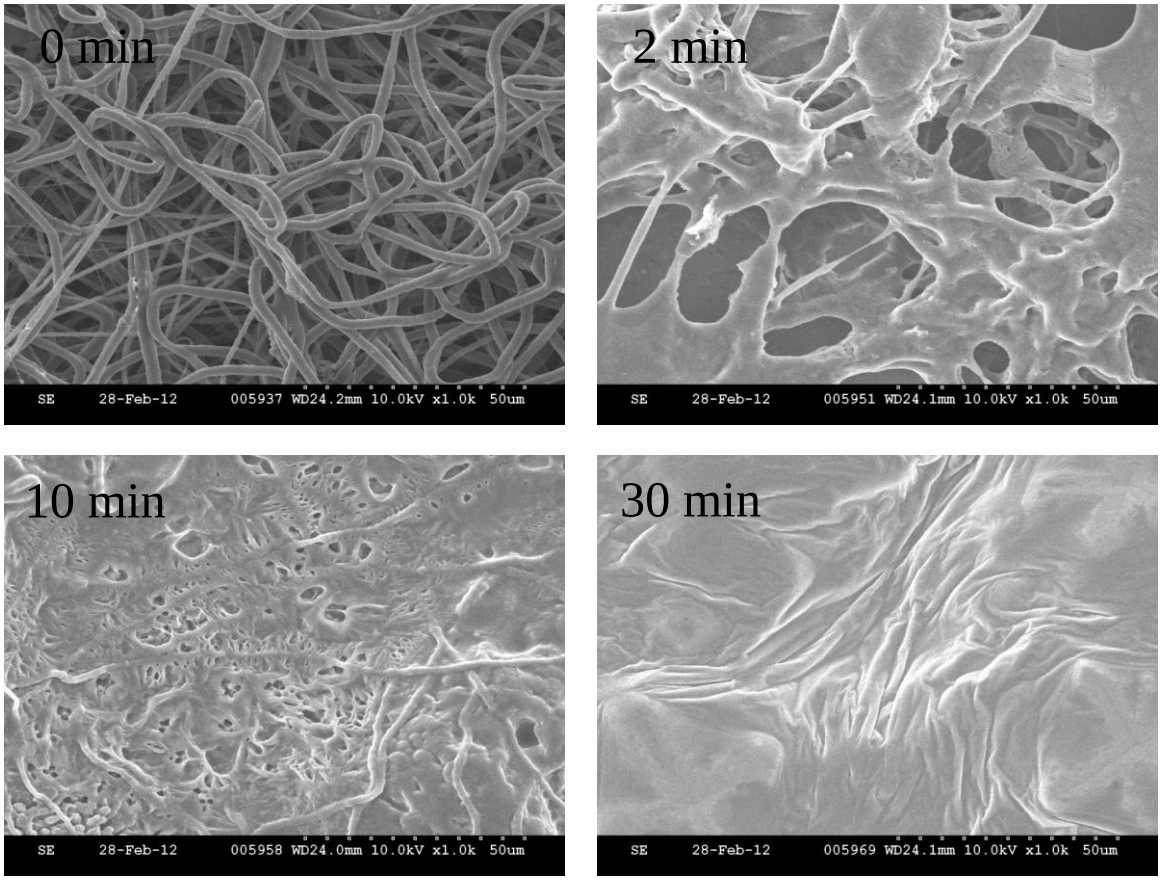

Figure 3-25: SEM images of the changes in morphology of the co-axial electrospun PEO fibres upon exposure to buffer. (Samples were freeze-dried prior to SEM analysis).

3.7 Effect of polymer molecular weight and viscosity on T4 bacteriophage activity

Normally, the deeper an encapsulated component is within the core of a fibre the more sustained the release profile (Zhang 2005; Zhang 2006). However, despite the core/shell structure, a rapid release of T4 bacteriophage was observed when the PEO fibres were subjected to *in vitro* release experiments in aqueous medium buffer. As discussed above this is attributed to the rapid dissolution of the PEO fibres in the aqueous medium. As the dissolution process involves first the swelling of the PEO fibres by the aqueous medium, it may be possible to slow the rate of T4 bacteriophage liberation by increasing the fibre diameter, particularly that of the shell layer. In coaxial

electrospinning, the diameter of the electrospun fibres can be influenced by several factors such as the feeding ratio of the core and shell solutions, the polymer solution concentration, and/or polymer molecular weight (Seeram 2005; Liao 2006; Zhang 2006; Andrady 2008). **Figure 3.26** shows the T4 bacteriophage release profiles from immersed electrospun PEO fibres prepared using varying PEO molecular weights and concentrations. Although all fibres reach 100% T4 bacteriophage release within 30-40 min, there does appear to be a dependence on both PEO concentration and molecular weight.

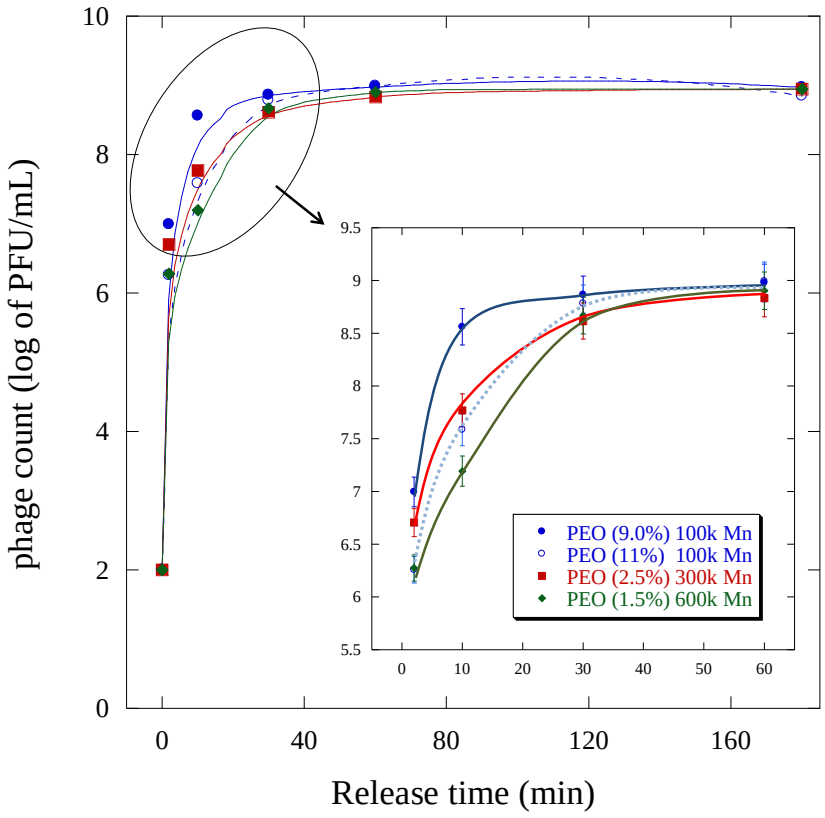

Figure 3-26: T4 bacteriophage release profiles from PEO electrospun fibres prepared using different PEO molecular weight and concentration. Error bars indicate standard deviation; *n*=3. T4 Bacteriophage counts of zero were recorded at 100 PFU/mL (or 2 log of PFU/mL), which is the limit of the detection in the assaying test.

While keeping all variables constant, an increase in PEO molecular weight (M_n) from 100 k to 600 k increased the electrospun fibre diameter from 1.25 to 2.25 µm (**Table 3.2** and **Figure 3.27**). This resulted in a relatively slower release rate of the T4 bacteriophage (**Figure 3.26b**), corresponding to almost an order of magnitude drop in bacteriophage activity (corresponding to 15% drop) at 10 min. Upon exposure to the aqueous media the hydrophilic PEO polymer within the electrospun fibres likely pass through a fast process of chain unfolding from the semi-crystalline phase to the amorphous phase, which leads to complete polymer chain disentanglement (Sperling 2006). Increasing the thickness of the polymer shell layer by increasing the PEO molecular weight retards the process of polymer chain unfolding and disentanglement and therefore a relatively slower release rate of the T4 bacteriophage is observed.

Table 3-3: Effect of polymer molecular weight and concentration on fibre diameter, solution viscosity and T4 bacteriophage release.

PEO (M_n)	**Concentration (%wt.)**	**Fibre diameter (µm)**	*** Viscosity (Pa.s) shear rate range of 1 to100 s^{-1}**	**Release at 10 min, log of PFU/mL,**	**Release at 10 min (%)**
100 k	9.0	1.35 ± 0.03	0.13 ± 0.01	8.56 ± 0.02	92
100 k	11	2.39 ± 0.02	0.36 ± 0.03	7.58 ± 0.15	83
300 k	2.5	1.80 ± 0.02	0.37 ± 0.01	7.76 ± 0.03	85
600 k	1.5	2.48 ± 0.05	0.65 ± 0.06	7.19 ± 0.14	78

* Measurements made on electrospun PEO fibre samples exposed to buffer medium for 10 min at which a 1mL aliquot (non-dissolved material remained settled at the bottom of the test tube) was removed and placed between the cone and plate geometries.

To better understand the effect of fibre diameter on the release rate, an attempt was made to increase fibre diameter at a constant PEO molecular weight (100 k (M_n)) by increasing PEO concentration. Increasing the PEO concentration from 9 to 11 %wt increased the fibre diameter from 1.35 to 2.39 µm, very similar to that of the PEO 600 k fibre (2.48 µm); however the release profile was only slightly slower at 11 %wt, very similar to release profile of the PEO 300 k fibres (confirmed through replicate experiments). Therefore, the release rate of T4 bacteriophage from the PEO electrospun fibres is not only governed by fibre diameter, it may be also affected by viscosity of the dissolving fibre/polymer solution.

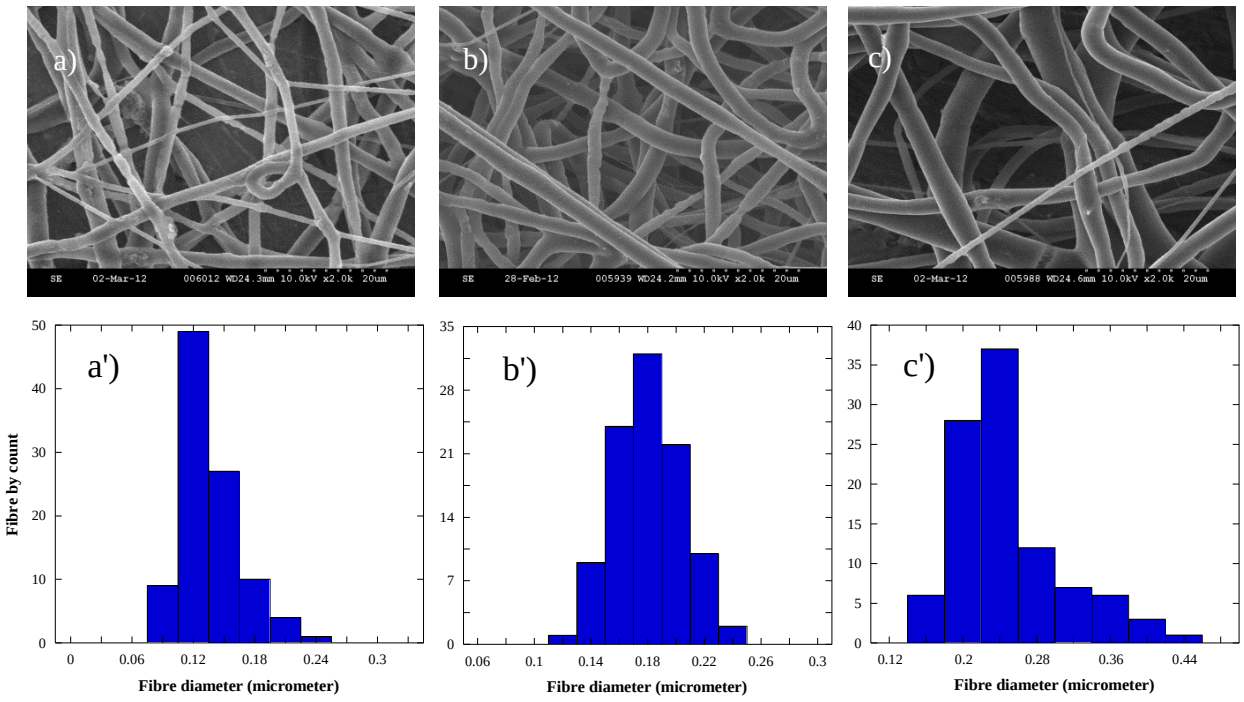

Figure 3-27: SEM images of coaxial electrospun PEO fibres obtained at using PEO molecular weights (M_n) of a)100 k, b) 300 k, c) 600 k along with the corresponding histogram plots of the PEO fibre distributions: a')100 k, b') 300 k, c') 600 k.

During the release profile measurements, the dissolution of PEO electrospun fibres could be observed through an increase in the viscosity of the buffer medium. The viscosity of the buffer was shown to be highly dependent on PEO molecular weight. Steady state rheology measurements showed an increase in viscosity from 0.11 to 0.71 (Pa·s) as PEO molecular weight (M_n) increased from 100 to 600 k, respectively **(Table 3.2** and **Figure 3.28)**. In general, bacteriophage motility and the ability to lyse bacteria decreases as solution viscosity increases (Hanlon 2001). Here, the rate of diffusion and activity of the T4 bacteriophage shifted to a slower release profile as the PEO solution viscosity increased (**Figure 3.26**). In the case of PEO 100 k increasing the concentration from 9 to 11%, resulted in a viscosity enhancement from 0.13 to 0.36 Pa·s, very close to the viscosity measured for the PEO 300 k electrospun fibres (0.37 Pa·s). Accordingly, the release profile of the 11 %wt PEO 100 k fibres was similar to that of the PEO 300 k fibres. Therefore, the viscosity of the swollen fibres and releasing environment could have a significant impact on the release profile of T4 bacteriophage.

The changes in PEO fibre morphology during the exposure to the buffer medium and release of T4 bacteriophage were also observed to be dependent on polymer molecular weight. **Figure 3.29** shows SEM images of fibres submerged in buffer medium at various time intervals. In the first 5 minutes, the PEO electrospun fibres began to swell, the extent to which was found to be slower as fibre diameter increased; 100 k (9 %wt) PEO fibres appearing more dissolved at 5 min than the corresponding 600 k PEO fibres. After 10 min of immersion in the buffer medium, the low molecular weight PEO (100 k) electrospun fibres were dissolved and isolated as polymer films after freeze-drying. By contrast, swollen electrospun fibres were still observed for the PEO 300 and 600 k fibres as evident by some traces of a fibrous structure. After 30 min of immersion in the buffer, all of the electrospun fibre morphologies were isolated as polymer films, correspond-

ing to the full release of T4 bacteriophage. These observed morphological changes in the PEO fibres were in good agreement with the measured T4 bacteriophage release profiles.

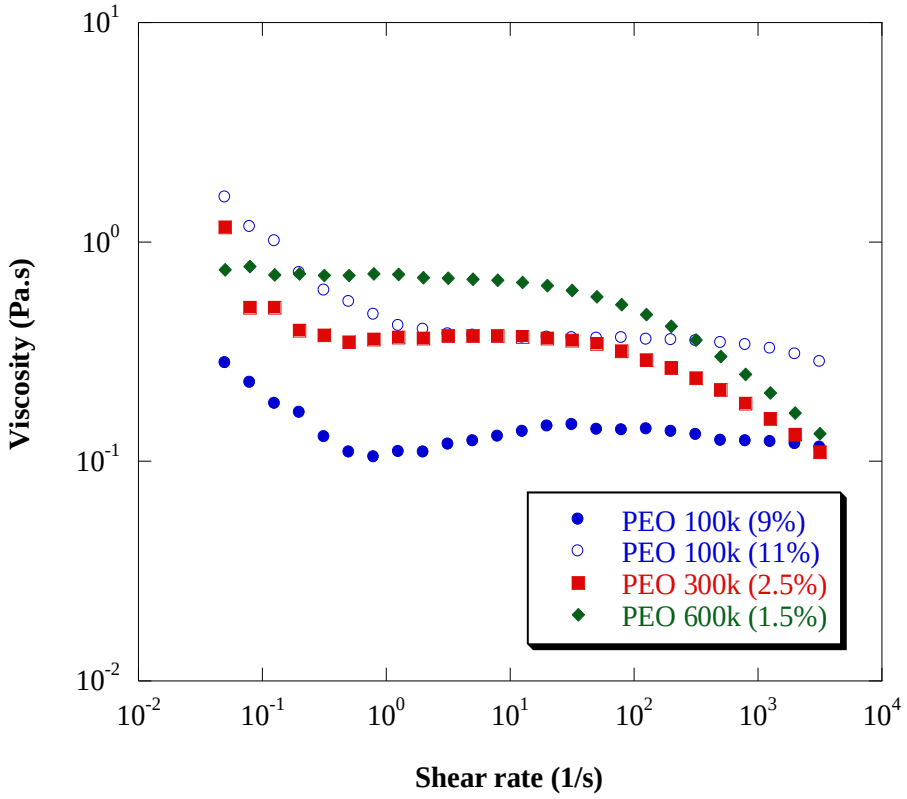

Figure 3-28: Steady state viscosity plots of PEO electrospun fibres in SM buffer. Measurements made on fibre samples exposed to buffer medium for 10 min.

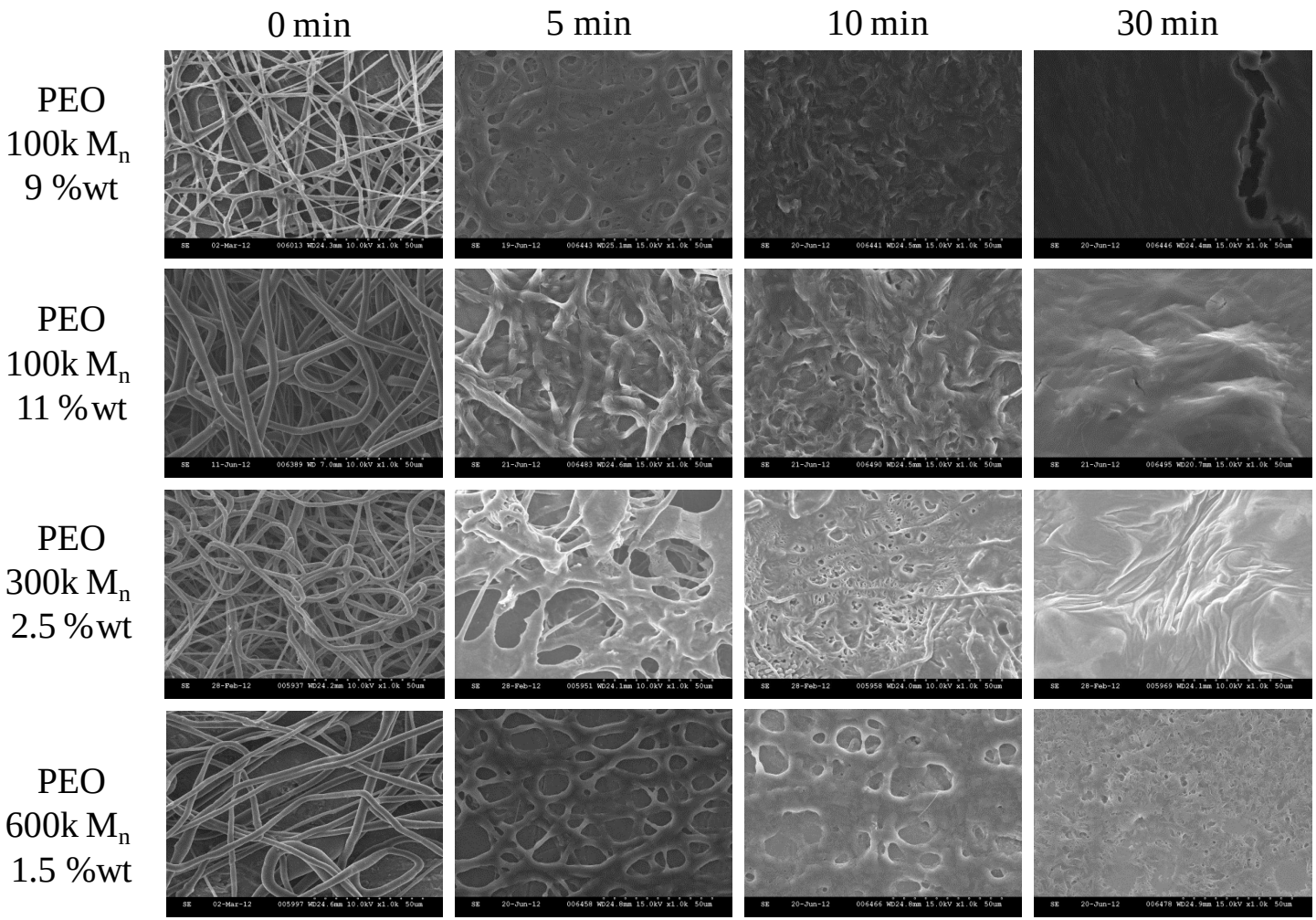

Figure 3-29: SEM images before and during the *in vitro* release experiments from the PEO electrospun fibres. Samples were freeze-dried prior to SEM analysis. Images were obtained at a magnification of 1.0 k.

3.8 Effect of hydrophilic/hydrphobic polymer blends on the release profiles of T4 bacteriophage

In order to further control the T4 bacteriophage release characteristics from the coaxial electrospun PEO fibres, it was devised to blend PEO with a more hydrophobic biopolymer, cellulose diacetate (CDA). Wild type and fluorescent-labeled T4 bacteriophage viruses were successfully encapsulated in PEO and PEO/CDA blend electrospun fibres using a coaxial electrospinning process. As compared to pure PEO electrospun fibres those prepared with a PEO/CDA polymer blend shell layer dramatically suppressed the burst release. The release rate was found to be dependent on the CDA/PEO ratio and PEO molecular weight; where increasing both parameters resulted in slower T4 bacteriophage release rates. Increasing the CDA content enhanced the hydrophobicity of the electrospun fibres, which resulted in less morphological alteration and a lower degree of fibre swelling in the post-release electrospun fibres. SEM and LSCM examination of the post-release fibre morphology suggested that the release mechanism is either solvent activation/fibre dissolution (in blends with high PEO content) or through a more fibre swelling/diffusional mechanism (in blends with high CDA content).

3.8.1 Effect of PEO/CDA blend ratios on the release of T4 bacteriophage

In previous experiments, the high hydrophilicity of PEO resulted in rapid fibre dissolution and immediate leaching of T4 bacteriophages into the surrounding buffer medium; a burst release was exhibited over a period of 30 min that resulted in almost 100% release of the T4 bacteriophage. To avoid the rapid release of T4 bacteriophage, the hydrophilicity of the shell polymer layer was decreased through the blending with hydrophobic cellulose diacetate (CDA). When CDA fibres were coaxially electrospun with a core containing T4 bacetriophage, the resulting

fibre did not exhibit any measurable bacteriophage activity or release even after two months of submersion in buffer medium. **Figure 3.30** shows the SEM images of the CDA fibres before and after immersion in buffer medium. It is clearly evident that no fibre swelling or degradation of the CDA polymer occurred. This is in agreement with the known properties of CDA, which can maintain its molecular integrity for a very long period (>2 years) before being hydrolytically degraded (Heinze 2004). Unlike the release of small molecules, a controlled release of large biological compound such as T4 bacteriophage requires relatively large fibre expansion and/or the creation of large macro-pores in the fibre. Therefore, by manipulating the ratio of hydrophilic/hydrophobic polymers in the shell layer a controlled diffusional release as a result of fibre swelling may be obtained. Thus, a series of hydrophilic/hydrophobic polymer (PEO/CDA) blends were prepared in an attempt to alter fibre morphology and provide better control over the release of T4 bacteriophage.

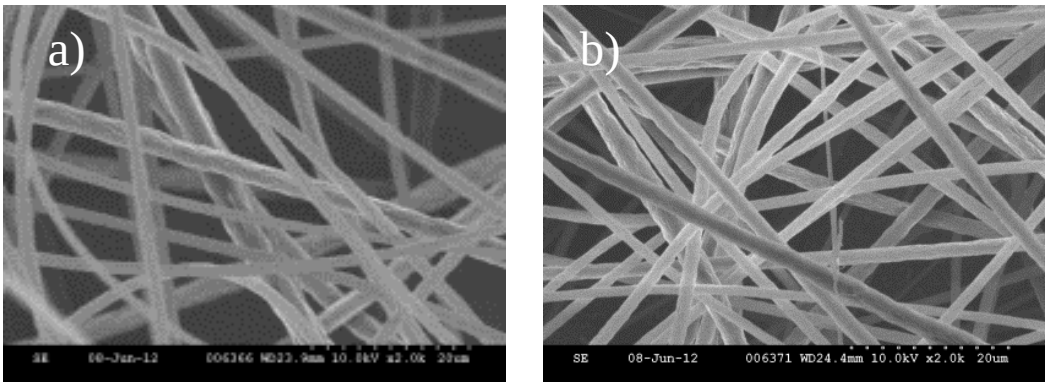

Figure 3-30: Coaxial electrospun cellulose diacetate fibres conatining T4 Bacteriophage a) before and b) after immersion in aqueous buffer for 72 hours.

The blending of CDA with PEO led to a reduction in release rate of T4 bacteriophage in all formulations as compared to the pure PEO fibre. As found for the pure PEO fibres the fastest T4 bacteriophage release was observed in the CDA/PEO blend fibres prepared using the 100 k PEO. Although PEO molecular weight had an effect on the release of T4 bacteriophage, the most significant effect was related to the CDA/PEO ratio (**Figure 3.31**).

The observed slower release with the addition of CDA is due to the increased hydrophobicity of the electrospun fibres, which decreases the fibre solubility/swelling in the aqueous media. Cellulose diacetate is often used as a filtration material for biological compounds due to its good dimensional stability. Here, the addition of CDA results in greater fibre resistance to the aqueous environment and prevents fibre dissociation. The improved control of the release of T4 bacteriophage was observed in a manner that is independent of loading concentration and core diameter.

By increasing the PEO molecular weight in the blend composition, further increased control over the release profile was possible. The increase in the PEO molecular weight likely leads to greater polymer entanglement (intermolecular interaction) between PEO-PEO and PEO-CDA polymer chains, which results in slower fibre swelling/dissolution and a slower release of T4 bacteriophage. Pervious investigations have shown that these two polymers are miscible (Jiang 2002; Pittarate 2011). Due to their miscibility, co-continuous electrospun fibre morphology was expected. For this type of fibre morphology, a post-treatment (submersion in aqueous buffer) results more in fibre swelling. In fact further analysis (SEM, DSC and IR) was performed to explain this phenomena and their results is explained in the next sections

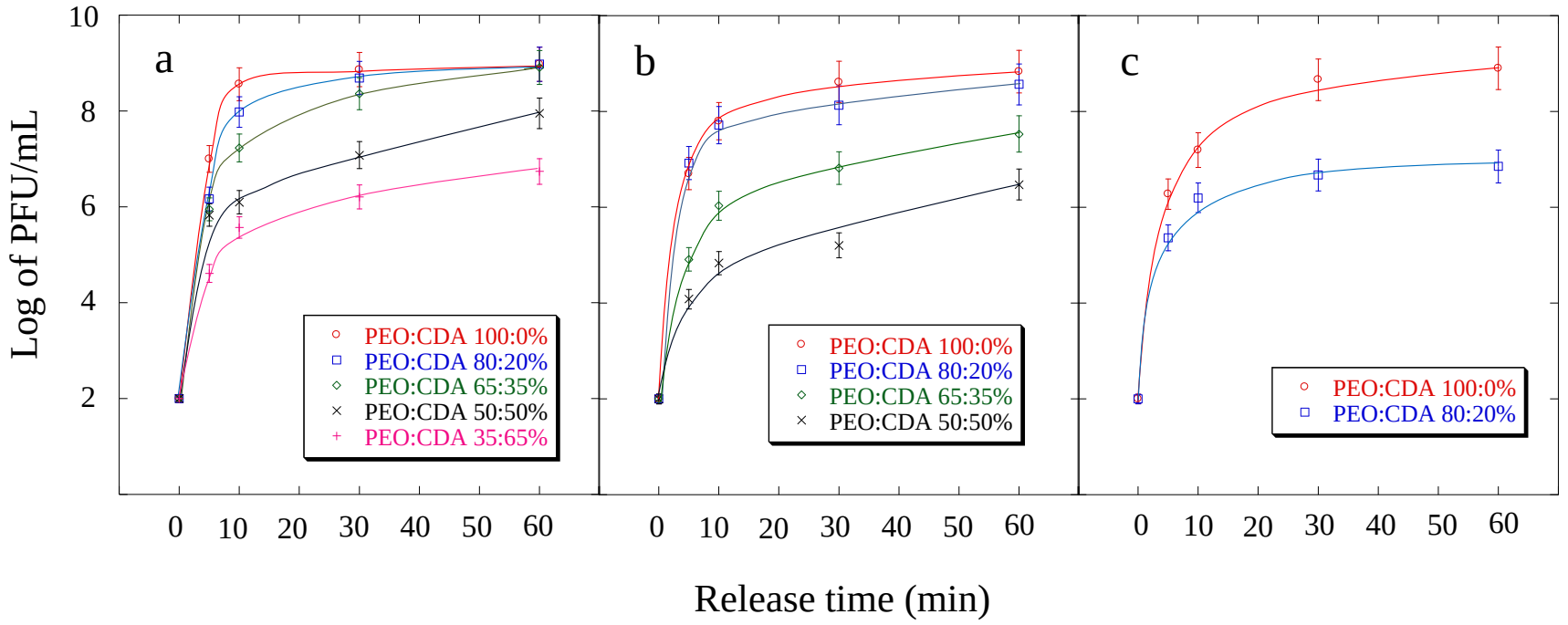

Figure 3-31: T4 bacteriophage release profiles from PEO/CDA co-axial electrospun fibres made using differentPEO/CDA blend ratios and PEO molecular weights (M_n): a) 100 k, b) 300 k, and c) 600 k. *n* = 2 and error bars represent the average absolute deviation from the mean of each data points . Bacteriophage counts of zero were recorded at 2 log of PFU/mL (or 100 PFU/mL) which is the limit of bacteriophage detection in the assay test.

The morphology of all of the polymer blend fibres before and after T4 bacteriophage release by submersion in buffer medium was investigated with scanning electron microscopy. The SEM images show uniform bead-free, as-spun fibres for all of the PEO/CDA blends. The morphological structure of the post-release blended fibres was then monitored during 6 hours of immersion in an aqueous buffer (**Figure 3.32**). The SEM images show that the changes in fibre morphology were dependent on the PEO content in the blend fibres; the higher the PEO content the more significant the change in fibre morphology. In the higher PEO contain blend fibres the morphological structure was again altered to a polymer film as the PEO polymer was dissolved away from the fibre. However, as the CDA content increased, swollen fibre morphology was observed, which was very much dependent on the molecular weight of the PEO used. In the case of the 100k PEO, PEO:CDA ratios of up to 50:50 (%wt) were fully dissolved in the buffer medium, while the 35:65 (PEO:CDA) blends showed evidence of only being swollen in the buffer medium. The behavior of the 300k and 600k PEO/CDA blend fibres was quite different; only the 300k 80:20 (%wt) PEO/CDA blend fibres dissolved, whereas the 65:35 and 50:50 300k PEO/CDA and 80:20 600k PEO/CDA blends retained a highly fibrous morphology. Again, the slow and limited change in fibre morphology between the different blends at a constant CDA content is attributed to the greater polymer entanglements associated with the increase in PEO molecular weight.

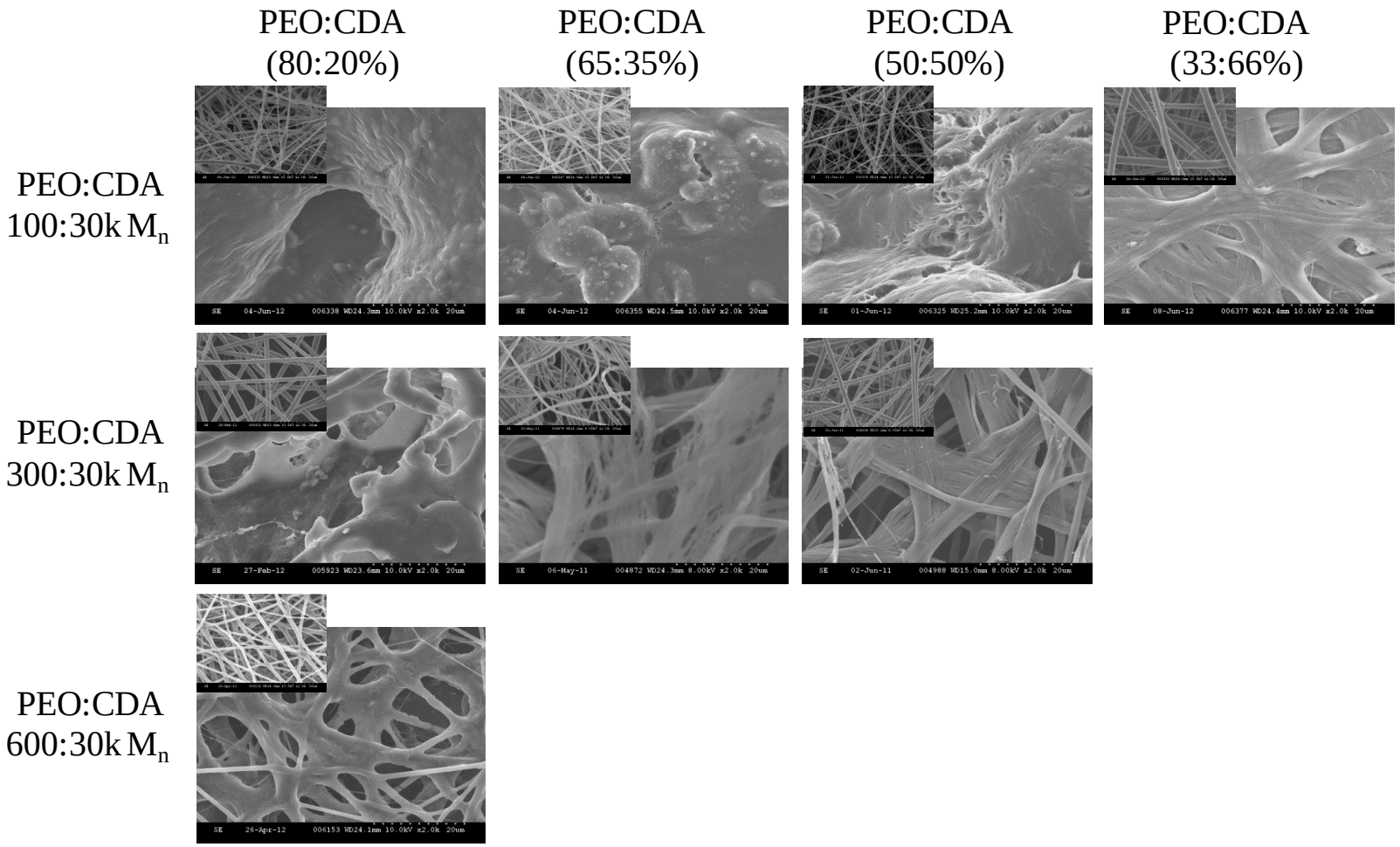

Figure 3-32: SEM images of electrospun fibre structure after 6 hours of immersion in buffer. The small inset images are of the electrospun fibre morphologies before immersion in buffer. All SEM images are obtained at magnification of 2.0k.

DSC analyses of various PEO/CDA polymers blend electrospun fibres are shown in **Figure 3.33**. The DSC scans show a depression in the crystallinity and a decrease in the melting temperature of PEO with increasing addition of CDA in the electrospun blend fibres. The decrease in crystallinity and melting temperature of the PEO phase implies miscibility and physical interaction (intermolecular forces and/or hydrogen bonding) between the two polymers (Ding 2001; Jiang 2002; Pielichowska 2011). Moreover, the shift in the melting temperature was found to increase with increasing PEO molecular weight (**Table 3.4**).

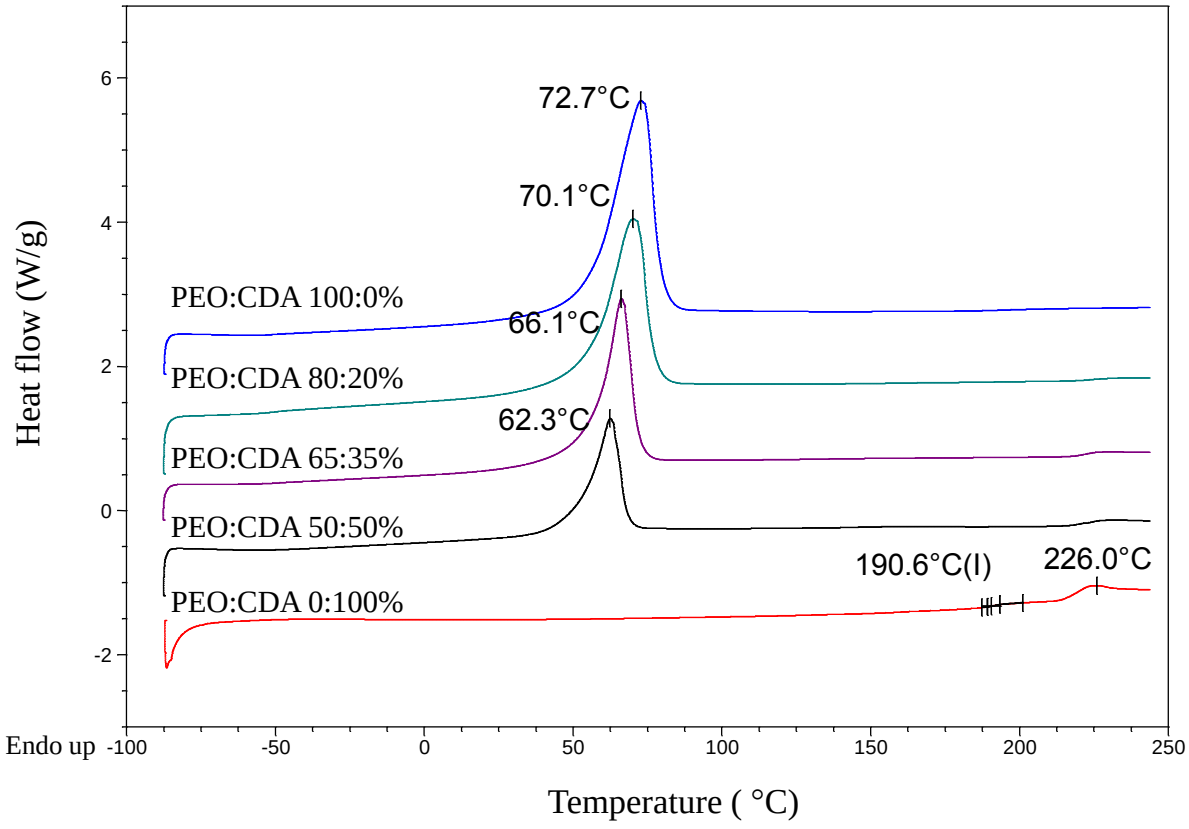

Figure 3-33: DSC analysis of electrospun fibres of PEO:CDA (300:30 k M_n) at different blend ratios. T_g and T_m were recorded as midpoint temperatures of the heat capacity transition and peak temperature of the heat capacity transition, respectively, from the second heating run. Samples were run in duplicate and they were within experimental error of each other (1.0 °C).

The observed melting point depression and decrease in crystallinity upon polymer blending has been widely studied in the literature (Pielichowska 2011). During the electrospinning process the solvent is rapidly removed and the polymer, PEO undergoes a certain degree of crystallization, which is dependent on the processing environment (Zhao 2004). In the presence of a miscible polymer like CDA, specific intermolecular interactions form between the PEO and CDA, which upon solvent removal, i.e. during electrospinning lead to a decrease in the crystallization of the PEO. In the case of polymer blends the decrease in the equilibrium melting point is largely enthalpic in nature wherein the greater the polymer/polymer interactions, the greater the melting point depression (Rim 1984). Although our experiments were not conducted under equilibrium conditions, our findings are in agreement with previous publications PEO/CDA blends (Ding 2001; Pielichowska 2011).

Table 3-4: PEO melting temperatures (T_m) observed for the various PEO/CDA blend electrospun fibres. Samples were run in duplicate and were within experimental error of each other (1.0 °C).

T_m of PEO °C	**PEO:CDA (100:0 %wt)**	**PEO:CDA (80:20 %wt)**	**PEO:CDA (65:35 %wt)**	**PEO:CDA (50:50 %wt)**	**PEO:CDA (35:65 %wt)**
PEO:CDA (600:30k M_n)	73.9 (153.6 J/g)	67.0 (105.7 J/g)	62.0 (78.98 J/g)	60.4 (47.7 J/g)	-
PEO:CDA (300:30k M_n)	72.7 (153.3 J/g)	70.1 (116.0 J/g)	66.1 (85.09 J/g)	62.3 (57.80 J/g)	-
PEO:CDA (100:30k M_n)	71.1 (160.1 J/g)	70.6 (123.4 J/g)	69.6 (110.6 J/g)	67.8 (85.4 J/g)	65.0 (67.6 J/g)

* Values in bracket show the area under the melting peak of PEO and it was measured using thermal universal analysis software from the DSC spectra.

Further support of the miscibility between PEO and CDA was obtained using Fourier-transform infrared spectroscopy (FTIR). FTIR analysis of the PEO/CDA electrospun fibres exhibited the various stretching bands associated with CDA; ester carbonyl and hydroxyl stretching bands at 1750 and 3300 cm^{-1}, respectively as well as those associated with PEO; methylene (CH_2) and C-O-C groups at 2900 and 1100 cm^{-1}, respectively. Of notable distinction was the shift in the C-O stretching band (at 1100 cm^{-1}) of PEO upon blending with CDA; it shifted to lower wave number with increasing CDA content (**Figure 3.34**). The shift to lower wavenumber is consistent with the formation of a strong intermolecular interaction involving the ether oxygen. The C-O-C bond can interact via hydrogen bonding with the free hydroxyl groups on CDA (Pittarate 2011). Thus the shift in C-O stretching band in the PEO/CDA blend clearly shows the presence of intermolecular hydrogen bonding between the CDA hydroxyl group and C-O functional group in PEO, and further supports the DSC results discussed above.

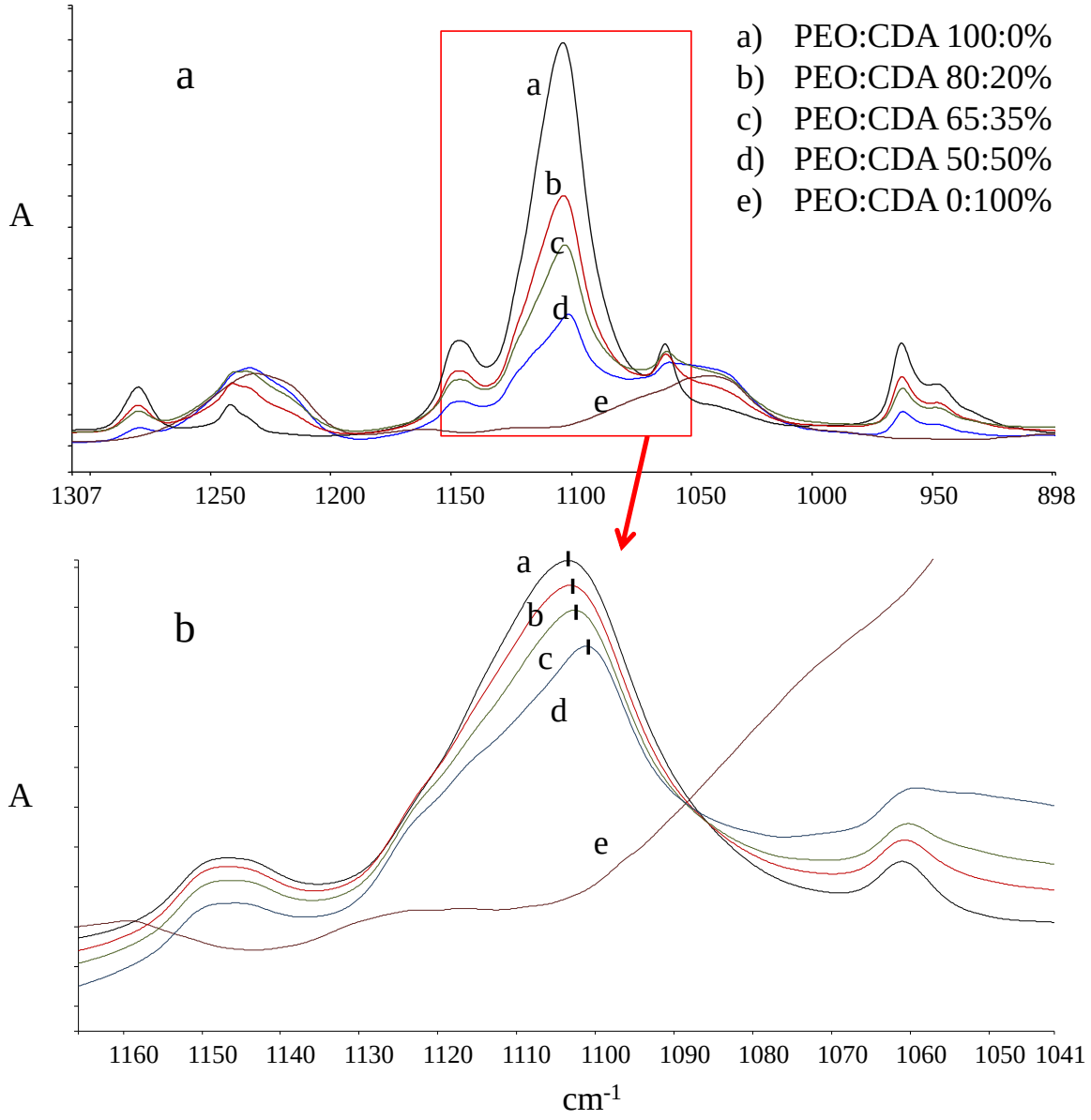

Figure 3-34: FTIR analysis of the various PEO/CDA polymer blend electrospun fibres. In plot b, all spectra were normalized to one at range of 1070 to 1135 cm^{-1} and they were separated from each other to show the hypsochromic shift, a change to shorter wavelength, with addition of CDA.

When two immiscible polymers are dissolved in a common solvent, a concentration-dependent phase separation occurs in solution (Guo 2003). Similar to cast polymer films, electrospun nanofibres from solution of two immiscible polymers also show the phase-separated morphology. Complete phase separation geometry (core-shell morphology) has been reported when two complete immiscible polymers are dissolved in a same solvent system and used for fibre formation (Bazilevsky 2007). A phase domain of one polymer distributed in electrospun fibre matrix of another polymer (nucleation growth phase separation) has been also observed (Bognitzki 2001). Therefore, phase geometry in the electrospun fibre is highly dependent on the degree of miscibility between the two polymers. In case of PEO/CDA blend, miscibility of these two polymers resulted in spinodal phase separation, which led to a co-continuous phase morphology electrospun fibre. The millisecond timescale in the electrospinning process together with the miscibility of PEO and CDA resulted in a narrow distribution of these two polymers in the form of a fine phase electrospun fibre morphology. Post-treatment of the fine phase geometry electrospun fibres of PEO/CDA blends and selective extraction of PEO with the aqueous solvent led to uniform fibre swelling and a well-formed morphology, as opposed to the creation of large pores (matrix-dispersed structure). However, the fibre swelling morphology in the post-treatment is highly dependent on the PEO/CDA blend composition, where at high PEO content (>80 %wt) the fibre structure was lost. The addition of CDA or increasing PEO molecular weight improve the structural integrity of the fibre and restricted the electrospun fibre expansion during the post-treatment. As a result, a lower degree of fibre swelling was observed as the CDA content and PEO molecular weight were increased.

According to **Figure 3.31b** increasing the CDA content in the PEO/CDA electrospun fibres resulted in a decrease in the amount of T4 bacteriophage released from the fibres upon immersion

in buffer. Moreover, the amount of T4 bacteriophage released from the PEO/CDA blend fibres appeared to plateau well below that expected based on the bacteriophage loading. Although the SEM images in **Figure 3.32** show the effect of CDA blending on fibre dissolution/swelling and are somewhat consistent with the decreased rate of bacteriophage release, they cannot provide detailed information on the release and release mechanism of the T4 bacteriophage. Therefore, laser confocal scanning microscopy (LCSM) was also employed to further support the release of the T4 bacteriophages from PEO/CDA (300 k:30 k M_n) electrospun fibres and possibly explain the release mechanism. The 300 k PEO blend system was used in this study as it showed the most variation in fibre morphology after immersion buffer (**Figure 3.32**). In these experiments the T4 bacteriophage was labeled with a fluorescent compound, FITC, which fluorescence green under the LCSM (**Figure 3.35**). Such fluorescently labeled compounds have been previously used to successfully identify the core/shell structures of large diameter (few hundred micrometer) fibres (Rahman 2004). Since the PEO/CDA-phage-FITC electrospun fibre is extremely small, details into the core-shell layer structure could not be clearly identified by LCSM. Under the confocal microscope all of the fibres exhibited the presence of the FITC-labeled T4 bacterio-phage throughout the fibre (**Figure 3.35,** top images). However, after immersion in buffer, the two electrospun fibres with high PEO content (100 and 80% PEO) revealed no fluorescent signal under LCSM imaging (**Figure 3.35**). This is consistent with the dissolved SEM images (**Figure 3.32**) and the 100% release of the T4 bacteriophage from the electrospun fibres (**Figure 3.31** and **Table 3.2**). As expected the two electrospun fibres with higher CDA content, exhibited some fluorescence under LCSM imaging; indicating T4 bacteriophage trapped/remaining in the fibre. The fluorescent signal was greater in PEO/CDA 50:50% as compared to the 65:35% blend fibre consistent with the SEM images (**Figure 3.32**) and release profiles (**Figure 3.31**). This confirms

that the release of T4 bacteriophage is highly dependent on the degree of swelling of the fibre, which, in turn, depends on the blend ratio of hydrophilic and hydrophobic polymers in the shell layer.

The core/shell structure of the PEO/CDA/T4 bacteriophage electrospun fibre is best described as a reservoir–type release design. This design has the advantage of providing a more controlled release that depends on shell thickness, shell permeability, size and amount of loaded bioactive agent, and defects in the shell layer such as thin spots and pinholes (Rahman 2004; Zhang 2006). In the polymer blend composition, the observed burst release of the T4 bacteriophage from low molecular weight and high PEO content fibres is clearly associated with solvent activation and rapid PEO dissolution. As the CDA content is increased, the fibre dissociation is eliminated, and the fibre swelling behaviour plays a primary role in the releasing of the T4 bacteriophage. In this case, the underlying release mechanism is likely governed by diffusional mechanisms. The initial instant release could be attributed to imperfections in the core/sheath structure (e.g., spots in the thin shell layer or shell failure), and the release from deeper regions of the electrospun polymer matrix is through diffusion and interconnected macro-pore network structures. The T4 bacterio-phage is a fairly large bioactive agent (200 x 400 nm) so its diffusion would be limited in the narrow pores. Therefore, the degree of fibre swelling and the size of the interconnected pores play a major role in the release profile of this large biological component.

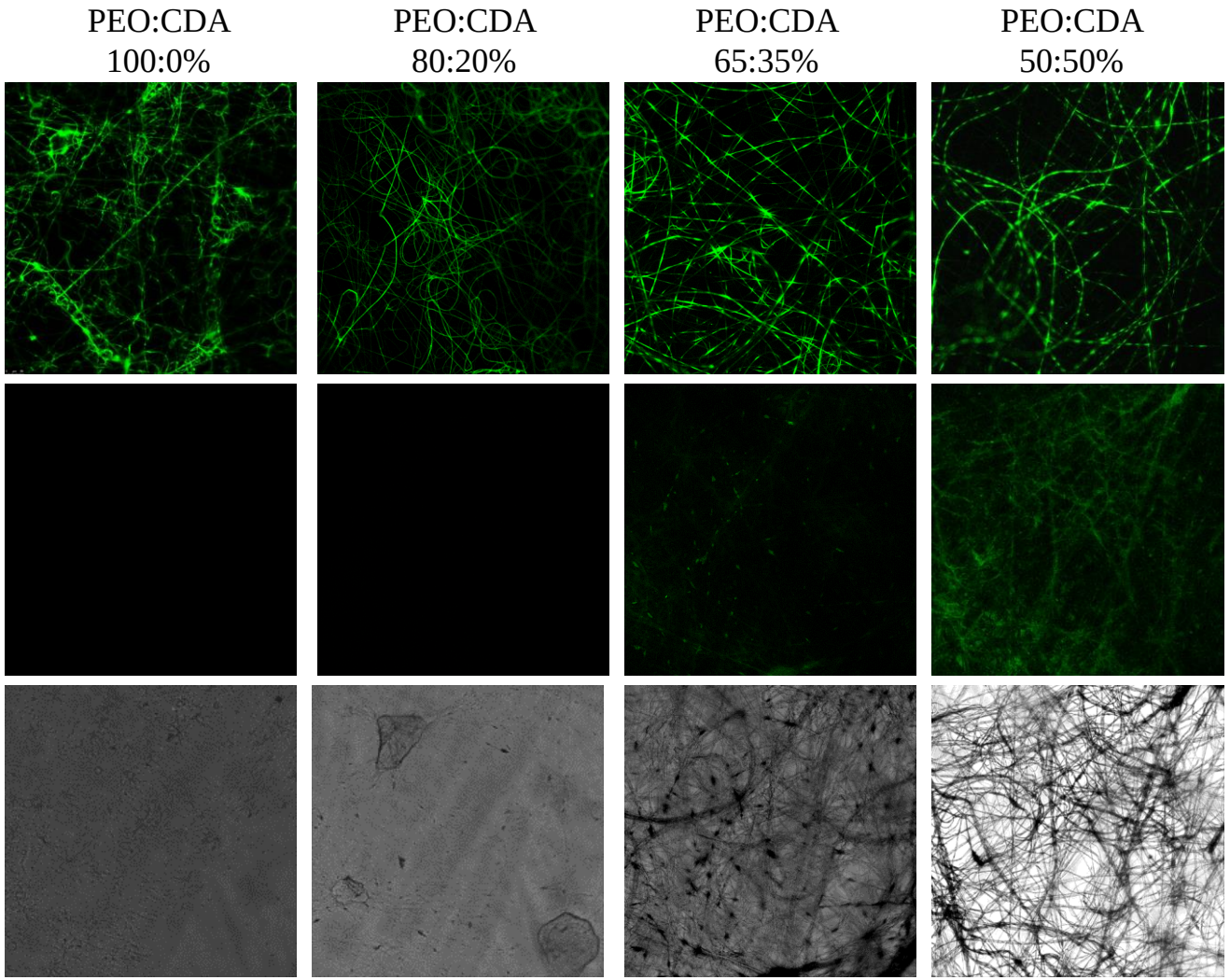

Figure 3-35: Laser confocal scanning microscopy images of PEO:CDA 300:30k M_n electrospun fibres before immersion in buffer (top), after 6 h immersion in buffer (middle) and the corresponding bright field images of the electrospun fibres after 6 hr immersion in buffer (bottom).

Another factor influencing the release of bacteriophage from the PEO/CDA blend fibre is the fact that there appears to be interaction between CDA and T4 bacteriophage (Minikh 2010; Tolba 2010). The binding between the CDA and T4 bacteriophage can affect the CDA thermodynamic transition and therefore the DSC analysis could detect changes in the thermal transitions of CDA. In fact, analysis of the DSC curve of electrospun fibres of pure CDA showed two distinct endothermic transitions, one at 190 °C (T_g) and the other at 225 °C (T_m) (**Figure 3.36**). The DSC scan of T4 bacteriophage did not show any obvious thermal transitions; however, the DSC curve of coaxial electrospun CDA fibres with T4 bacteriophage shifted the melting temperature of CDA from 226 °C to 222 °C (triplicate experiments) and the glass transition temperature disappeared. In fact, pervious work showed that T4 bacteriophage does bind to cellulosic materials and the interaction with cellulose occurs via the binding sites on the phage's long tail fibres, which are the bacterial binding sites. It was also shown that the subsequent activity of the bound T4 bacteriophage is lower than genetically-engineered T4 bacteriophage, which binds via its head (Sun 2001; Anany 2011). The binding of *wild type* T4 bacteriophage to the CDA polymer could explain the trapped bacteriophage in the electrospun fibre with high CDA content (observed confocal images) and it slow release profile.

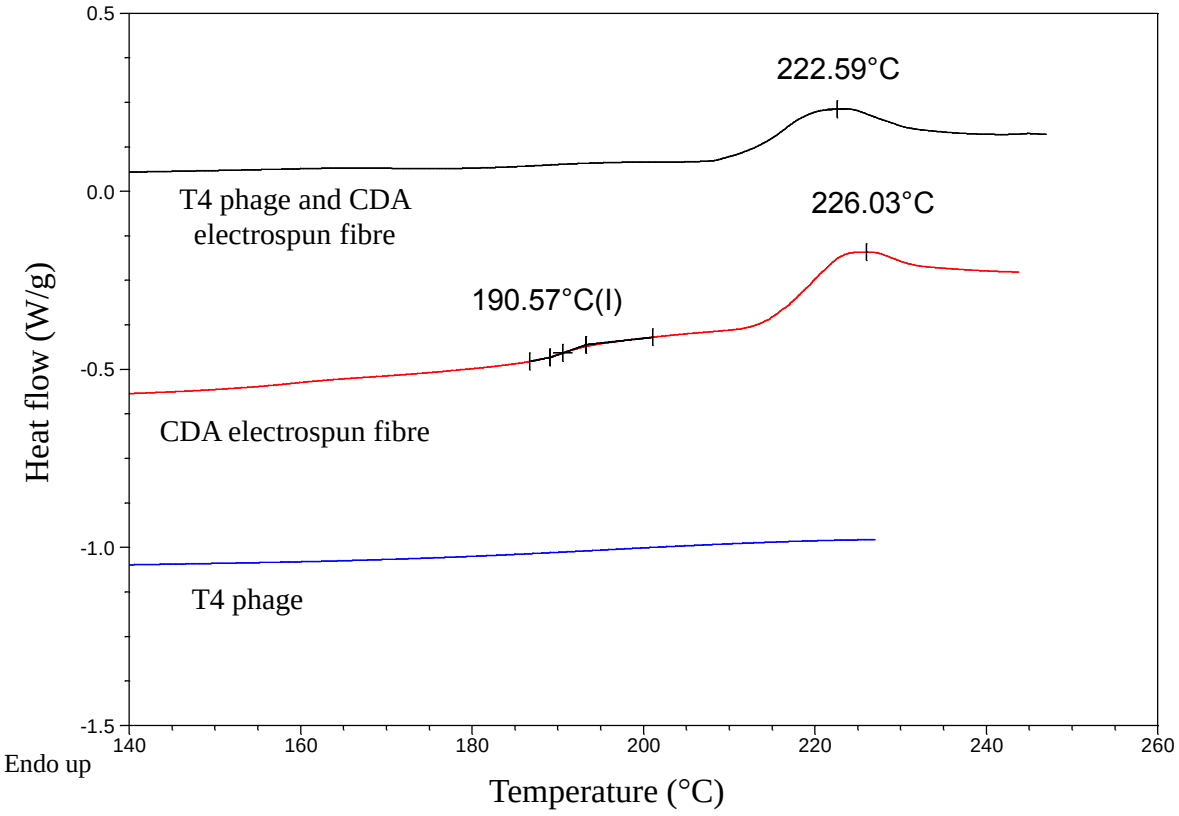

Figure 3-36: DSC analysis of dialysed freeze-dried T4 bacteriophage, electrospun CDA fibre and electrospun CDA fibre with encapsulated T4 bacteriophage. The T_g and T_m were recorded from the second heating run. Samples were run in duplicate and were within experimental error of each other (1.0 °C).

3.8.2 Effect of electrospun polymer blends on T4 bacteriophage infectivity

Phages are usually produced where the host (*E. coli*) population is infected by the phage, which grow until lysis. Therefore, continuous monitoring of the T4 bacteriophage production can be obtained by either cell density (cell count) or optical density (OD). Cell density measurements usually involve the removal of sample from the bulk liquid for off-line analysis and are relatively

slow, time consuming and costly (Sauvageau 2010). The optical density measurement (OD) is based on the amount of light scattered by the bacterial cells in culture or, in this case, non-infected proliferating bacteria (Matlock 2011). The OD measurement is relatively fast and inexpensive technique to monitor *E. coli* infectivity and it can be also operated for any on-going bacteriophage production systems. This method can be standardized to the minimum inhibitory concentration of phages required for the complete removal of bacterial contamination. This method could be valuable in bacteriophage therapy applications where bacteriophage production has to be carefully controlled.

The approach of using CDA/PEO blend electrospun fibres showed the ability to control T4 bacteriophage release. Therefore, the next step was to test the applicability of such bio-activated electrospun fibres in controlling *E. coli* populations. This was done by testing the efficacy of liberated T4 bacteriophage from four PEO/CDA blend electrospun fibre mats in the infection of *E. coli* cultures. In particular, this study allowed us to distinguish the inoculation capability of the different phage-activated-electrospun fibres using optical density measurements at 600 nm (OD600). This easy and rapid identification process allowed us to investigate the release-killing capacity of T4 bacteriophage and to compare these with pervious release profile measurements.

The OD600 was measured from undiluted and several diluted *E. coli* cultures (early stationary phase: after 18 hrs of incubation) to obtain a standard cell density curve. The OD600 values for the non-infected *E. coli* culture and dilution suspensions (6 fold dilution) were in the range of 0.92 to 0.21 absorbance units, which correspond to viable cell counts in the range of 3.8×10^7 to 1.0×10^9 colony forming units (CFU)/mL. The obtained standard curve was used to calculate the

CFU of *E. coli* infected with the bacteriophage impregnated fibres (**Table 3.3**). A drop in OD600 occurs when an infected *E. coli* cell is lysed, releasing a new brood of virus.

The *E. coli* infection trend, in the presence of bacteriophage activated PEO/CDA blend fibres, is illustrated in **Figure 3.37.** The optical density (OD600) of non-infected *E. coli* (negative control) showed a steady line at 0.93 AU, which was very similar to the stationary phase of the *E. coli* growth profile. The observed trend in optical density reflected the previously demonstrated differences in release characteristics from the different PEO/CDA blend fibres. The slow initial decline in the early hours (> 5 hrs) of inoculation indicates the time lag required for T4 bacteriophage infection to begin to overtake control of the *E. coli* cells (Sauvageau 2010). As it is shown in **Figure 3.37,** after the initial decline there are two distinguished phases in the OD 600 measurement. In phase I the primary infection is considered as responsible mechanism where the infection of bacteria is occurred by phages released from the inoculum or electrospun fibre (Payne 2003). The largest decrease in OD 600 was observed from the 100% PEO fibre, previously shown to have the fastest release rate (**Figure 3.31**). As the CDA content in electrospun fibres increased, the slope of the change in OD600 decreased significantly (**Table 3.5**); where the PEO/CDA 50:50 %wt fibre mats showed an OD600 bacteria cell density of almost one-half that of the 100% PEO electrospun fibre. In the phase II, the infection of bacteria is mainly occurred by phages that have been released by lysis of already infected cells (secondary infection). In this phase, there is an increase in T4 bacteriophage numbers via rapid viral self-replication (Payne 2003), and the exponential nature of a T4 bacteriophage growth bloom (Sauvageau 2010). In this phase, the calculated slope of the OD 600 curves showed to be similar for all electrospun fibre.

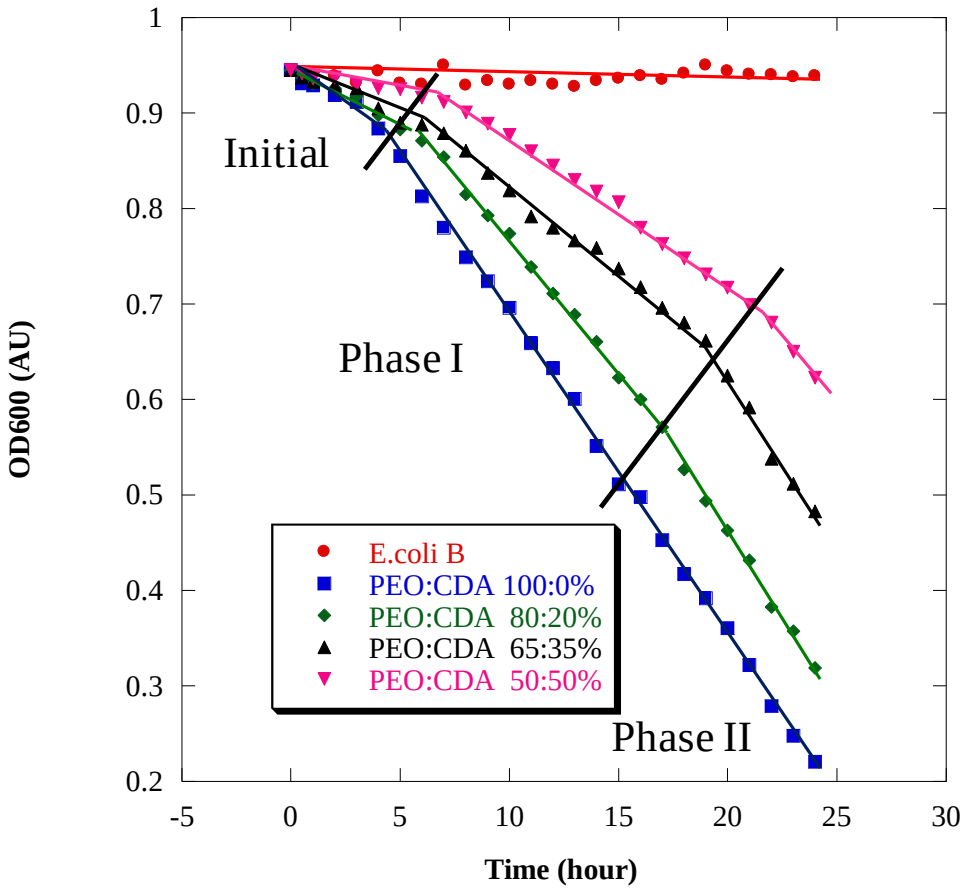

Figure 3-37: OD600 cell density measurements of the *E. coli* infected with T4 bacteriophage activated electrospun PEO/CDA blend fibres.

Table 3.5 shows the effect of the T4 bacteriophage activated fibre mats on *E. coli* activity and the overall infection rate. The infection rate was determined from the slope of curve as the OD600 of *E. coli* decreased. A large drop in *E. coli* activity from 4.1×10^9 to 7.0×10^7 CFU was observed in the infection curve with the full liberation of T4 bacteriophages from the dissolved 100 % PEO fibre mats. For this PEO fibre mat, the rate of infection was determined to be 0.033, compared to the infection rate in PEO:CDA 50:50 %wt which was roughly half as fast (0.015).

As the CDA content increases, the rate of infection slows, resulting from the lower degree of fibre swelling and better retention of T4 bacteriophage. Therefore, the improved retention of high CDA content polymer fibres has been demonstrated in data applicable to phage-based control of *E. coli*.

Table 3-5: Effect of the different T4 bacteriophage activated electrospun fibre mats on *E. coli* activity and inoculation rate.

***E. coli* B infectivity**	**PEO:CDA (100:0 %wt)**	**PEO:CDA (80:20 %wt)**	**PEO:CDA (65:35 %wt)**	**PEO:CDA (50:50 %wt)**
CFU after 24 hr of inoculation	7.0×10^7	3.6×10^8	4.2×10^8	5.5×10^8
Loss % (log of CFU)	20%	13%	9%	8%
Slope of curve phase I (A/hr)	0.033	0.028	0.017	0.015
Slope of curve phase II (A/hr)	0.034	0.035	0.036	0.029

3.9 Antibacterial activity test using disk diffusion test

The release-killing capacity of the T4 bacteriophage from the activated electrospun PEO/CDA fibres was also evaluated using disk diffusion testing (Chen 2008). In this test, the fibre mat incorporated T4 bacteriophage diffused out from the fibres killing the bacteria nearby until the minimum inhibitory concentration of bacteriophage is reached, below which bacteria can survive and proliferate. This results in the formation of a cleared zone around the fibre mat disk of varying area where bacterial growth was matched by infection and cell death (**Figure 3.38**). In the control experiment, a 100 µl of *E. coli* was inoculated in TSB_{ss} and spread on top of solid agar containing various PEO/CDA fibre discs and did not show any *E. coli* mortality (**Figure 3.38** left-most images). Similar treatments were applied using the PEO/CDA fibres with T4 bacteriophage, where again the zone of inhibition was dependent on the PEO/CDA blend. The largest zone of inhibition (ZoI) was observed for the 100% PEO fibres. The ZoI decreased significantly as the CDA content was increased, where the PEO:CDA 50:50% yielded only minor bacterial infection (**Figure 3.38d**).

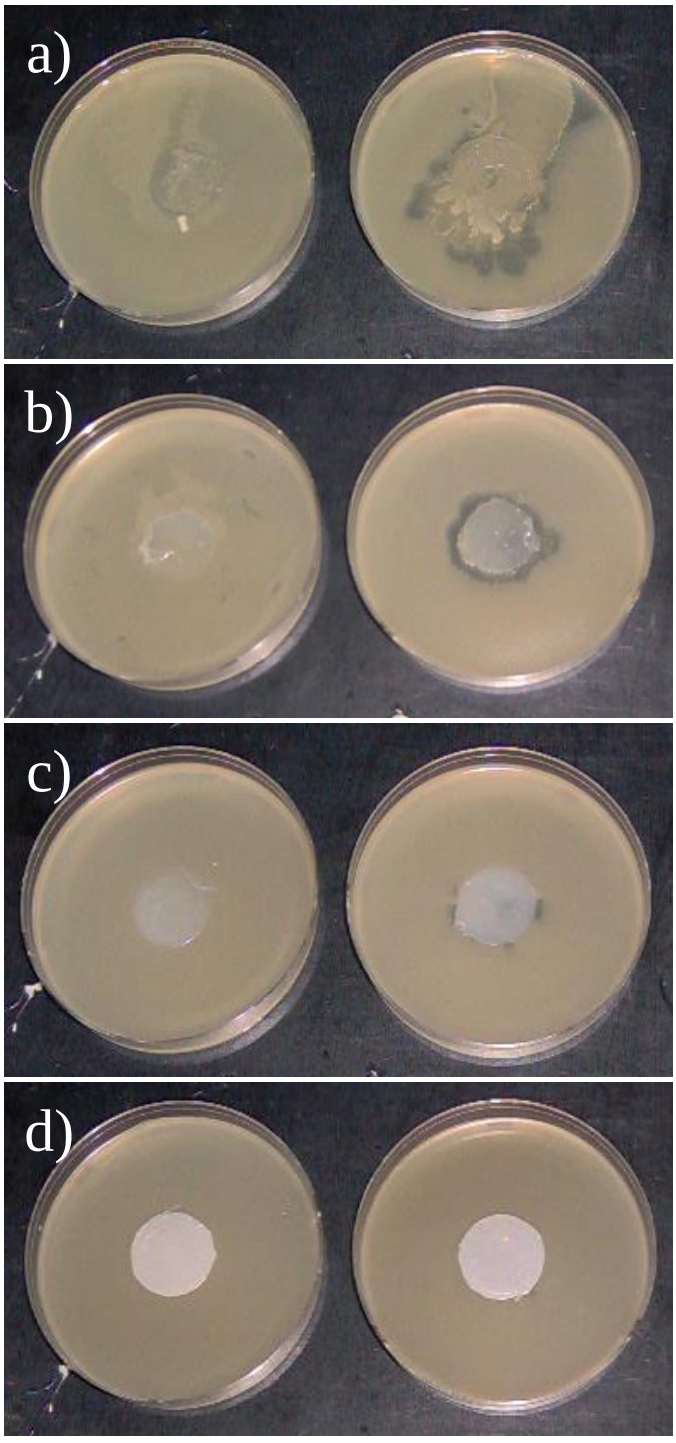

Figure 3-38: Images of agar plates after fibre disk diffusion tests. The right images are control plates containing electrospun fibres without T4 bacteriophage. The left images are plates containing electrospun fibres with T4 bacteriophage: (a) 300 k PEO:CDA 100:0 %wt, (b) 300 k PEO:CDA 80:20 %wt, (c) 300 k PEO:CDA 65:35 %wt, and (d) 300 k PEO:CDA 50:50 %wt.

From the disk diffusion test, our results indicate that the capability of the encapsulated T4 bacteriophage to kill bacteria is again dependent on the polymer properties of the electrospun fibres, as well as the moisture content of the surrounding environment. Here, the effect of aqueous solvent on the fibres was restricted by the fast solidification of the semisolid agar media used. However, the high solubility of the PEO electrospun fibres even in the semisolid media allowed for fast fibre dissolution and T4 bacteriophage release resulting in a relatively large area of disinfection. Increasing the CDA content lead to the structural integrity of the fibre mats being retained, but limited diffusion of the bacteriophage from the fibre mats occurred resulting in a very limited ZoI.

In real world applications, the initial rapid T4 bacteriophage release observed with the PEO / high PEO content fibrous mats may cause an undesired early inoculation, which can result in a dramatic reduction in the efficiency or complete failure in the T4 bacteriophage treatment. However, in the laboratory testing the water soluble PEO electrospun fibres were exposed to a large excess of aqueous buffer, resulting in rapid fibre dissolution and release of T4 bacteriophage. In practice, electropsun PEO fibre mats will be applied to the surfaces under much lower humidity conditions, i.e., the meat packaging, wherein a slower release profile of the T4 bacteriophages would likely be observed. In the electrospun fibre mats with higher CDA content only a very small proportion of the T4 bacteriophage were released to the surrounding environment. Again, in the treatment of surface infection with bacteriophages, there is always an increase in bacteriophage numbers via rapid viral self-replication, and in principle a small initial inocula would only be needed to set out an active bacteriophage therapy. Therefore, encapsulated viable T4 bacteriophage in electrospun fibre mat with high CDA content could be useful as slow delivery polymeric matrix device for long-term storage of food materials.

Chapter 4: Conclusion

Human mortality attributed to bacterial food poisoning, in particular *E. coli* O157:H7 tainted meat, has raised public awareness of the dangers of improperly handled food and has increased the demand for safer food packaging and outbreak prevention. Bacteriophage therapy, which uses viruses that are specific to bacteria, can be used to reduce the bacteria colonization on the surface of meat and has been used to treat systemic bacterial infections in animals. Iimmobilization of bacteriophages in fibrous materials could provide a reliable *in situ*, anti-bacterial surface beneficial for variety of applications, such as food packaging and as wound dressing material. For such applications, the major criterion is that bacteriophage be present in a dry form of non-woven fibre mat with highly preserved activity. Electrospinning process can be used as a key platform to achieve technical solution for this problem. The electrospinning process is a relatively simpleprocess for producing fibre mats with large surface area and good dimensional stability. This process can also be used to encapsulate large bioactive components, such as bacteria and viruses. This research examined how incorporated bacteriophage in electrospun fibres may provide a novel route to control foodborne bacterial contamination and prolong storage life.

The primary objective of this research was to examine different electrospinning techniques for encapsulating and maintaining the viability of T4 bacteriophage in biopolymers. The T4 bacteriobacteriophage was chosen as a model bacteriophage for this research, since it is one of the most delicate phages with sensitive structure. Previous work has shown that the T4 bacteriophage is not resilient enough to survive simple, unmitigated electrospinning. The exposure of bacteriophage to toxic organic solvents and/or evaporation of water during fibre formation results in dehydration and complete loss of activity. Therefore, this research demonstrates novel electrospinning techniques to encapsulate T4 bacteriophage and maintain high viability. The effect of all

processing conditions on fibre formation, viability and release profile of T4 bacteriophage is systematically investigated and briefly discussed herein.

Electrospinning PEO solution was first optimized under the following conditions: flow rate of 0.03 mL/min, distance of 15 cm and voltage of 1 kV/cm, generating smooth and uniform fibre. The same conditions were subsequently applied for suspension electrospinning of PEO/T4 bacteriophage to impregnate PEO fibre with phage. In this process, the T4 bacteriophages were initially dispersed in the aqueous polymer solution (PEO) and then subjected to electrospinning process. The SEM images showed smooth fibre with average diameter of 500±100 nm and no presence of T4 bacteriophages or any particles on the fibre surface. TEM analysis of the resulting fibres reveals the embedded T4 bacteriophages are non-uniformly distributed throughout the fibre matrix, i.e. not uniformly along the fibre nor from core to surface. This was attributed to the random orientation of T4 bacteriophages in the initial polymer suspension. After suspension electrospinning, the T4 bacteriophage activity was dropped by almost 5 orders of magnitude from 10^8 to 10^3 PFU/mL, corresponding to near complete loss of activity. This large drop in activity was attributed to the rapid dehydration of T4 bacteriophage during the electrospinning process, leading to the conclusion that a form of protective layer for the bacteriophage is required.

To avoid rapid dehydration of phages, pre-encapsulation of the T4 bacteriophage in alginate capsules (gelling agent) was performed using the emulsification process. The pre-encapsulated bioactive-alginate components were incorporated into PEO electrospun fibre via emulsion electrospinning process. A simulation study was also performed first, to investigate pre-encapsulation efficiency of BSA as protein model and to optimize the emulsion electrospinning process. The same methodology was applied to encapsulate T4 bacteriophage in emulsion electrospun fibre.

The morphology of pre-encapsulated BSA in the alginate was characterized with TEM microscopy, revealing 2D images of 3D nano-capsules of AOT/alginate and AOT/alginate/BSA-FITC with average diameter of 200 nm. These images also revealed that the AOT/alginate capsules had a spherical structure with a dense core, while the BSA-FITC (fluoresce-labeled BSA) capsules had a much darker and denser spherical core. The high electron density of labeled BSA-FITC resulted in a darker region in the core of spheres, which demonstrated the successful encapsulation of BSA in AOT/alginate capsule. The encapsulation of BSA in alginate capsules was further confirmed using DSC analysis which showed good agreement with the observed TEM morphology. The pure BSA revealed an endothermic transition at 152 °C followed by a fast degradation at 200 °C. However, the incorporated BSA in the AOT/calcium alginate capsules showed a single broad transition at 173 °C and no evidence of BSA degradation transition at 200 °C. These characteristics are best explained to result from the formation of nanocapsules with the entrapment of BSA.

Fibres were then formed using the emulsion system with either hydrophilic or hydrophobic polymers (PEO and CDA) for the external solvent with the alginate encapsulated BSA. The SEM images showed bead-in-string fibre morphology for both polymers and the fibre structure depended on the polymer concentration. TEM images showed the presence of darker areas within fibre not observed in the fibres produced without alginate capsules. Although detailed structure information of the encapsulated components was not clearly observed in TEM imaging, these dark areas most likely represented the encapsulated BSA. Under the LCSM microscope, green fluorescence was observed from the beaded areas of the polymer, demonstrating the presence of FITC-labeled BSA.

The encapsulation process was then applied to T4 bacteriophage using the same established procedure of emulsification process and completed by *in situ* alginate crosslinking using calcium chloride solution to form three-dimensional gel network of alginate capsules. The dried alginate capsules loaded with T4 bacteriophage were obtained by evaporating the external phase of the emulsion system and freeze dried. The morphological structure of the alginate capsules under the SEM microscopy showed a uniform alginate beads with no T4 bacteriophage on the surface. The average size of the alginate capsule was found to be 800±150nm which is larger than BSA/alginate capsules (200 nm), which could be explained bythe greater size of the T4 bacteriophage (200×300 nm). After emulsification, the bacteriophage activity was maintained to some extent, but dropped by an order of magnitude from 10^8 PFU/mL to 10^7 PFU/mL. This drop in T4 bacteriophage activity could be due to a loss during bacteriophage loading in the alginate capsules, the low mechanical strength of alginate and/or leaching of the bacteriophage from the capsules.

The physical stability of the cross-linked alginate capsules was evaluated by emulsion electrospraying and SEM analysis showed that most of capsules could not endure the electrospraying process and were deformed. Similarly, when encapsulated T4 bacteriophages were emulsion electrosprayed, there was a significant drop in activity. This could be attributed to the relatively low mechanical strength of alginate capsules and/or fast drying process which occurs during the electrospraying process. However, when the T4 bacteriophage/alginate capsules were incorporated in electrospun fibre, this protective coating increased bacteriophage activity by three orders of magnitude. In total, the infectivity assay showed only a 22% drop following electrospinning. The T4 bacteriophage activity significantly improved as compared to the activity measured from the suspension electrospun fibres. The decrease in bacteriophage activity relative to the original

bacteriophage activity is attributed to the low mechanical strength of the alginate capsules, wherein some were likely disrupted during the electrospinning process.

Coaxial electrospinning was found to be the most reliable process to encapsulate T4 bacteriophages with high bioactivity. TEM image confirmed the core/shell fibre structure possessed T4 bacteriophage incorporated into the core fibre. The improved viability was due to the allocation of the T4 bacteriophages to the core where they were protected by polymer shell layer from dehydration. The lytic activity of the encapsulated T4 bacteriophage was found to be unchanged from the initial activity (across three separate batches). The full activity of T4 bacteriophages was apparent after submerging the fibre in buffer and releasing the phages from the core/shell of the fibre. In coaxial electrospinning, the solvent evaporation from the core is very slow and therefore, drastic change in the osmotic environment during spinning is prevented. Consequently, the encapsulated T4 bacteriophages remained highly infective as a component of the core of the coaxial polymer.

Once the method of polymer production had proved effective, the long-term storage of the fibre mat was assessed. The stability of free and encapsulated T4 bacteriophage were investigated during storage at 20, 4, and −20 °C. The survival of free phages in the freeze-dried form decreased rapidly from 10^8 to 10^2 PFU/mL after 1 day of storage at 20°C. While free phages stored at 4°C had their activities decreased relatively slower from 10^8 to 10^5 PFU/mL during one month of storage. Storage at the lowest temperature tested (−20 °C), revealed no decrease in viability over a month of storage. Following storage, the PEO/T4 bacteriophage fibres demonstrated overall improved viability relative to free phage, with a moderate decrease in viability in samples stored at room temperature, and those stored at 4 and −20°C were essentially stable for up to one month

(longest time tested). The encapsulation of T4 bacteriophage in a dry form while preserving their activity is important for prolonged storage in applications such as food packaging.

Despite the core/shell structure, a rapid release of T4 bacteriophage was observed when the PEO fibre was subjected to in vitro release study in aqueous medium buffer. The burst release of T4 bacteriophages is attributed to the high hydrophilicity of PEO polymer and therefore the liberation of T4 bacteriophages occurs through solvent activation followed by fibre dissolution. After experimentation with polymer molecular weight, the SEM images demonstrated that the dissolution rate of electrospun fibre is influenced by molecular weight. Increasing the PEO molecular weight increases the diameter of polymer shell layer and the viscosity of the releasing medium. This resulted in a relatively slower release rate of the T4 bacteriophages, corresponding to an order of magnitude (15%) drop in bacteriophage activity after 10 min of soaking. Increasing thickness of polymer shell layer retards the process of polymer chain unfolding and disentanglement and therefore slows the release of T4 bacteriophages.

To further retard the dissolution of polymer and retain the T4 bacteriophage within the fibre for longer periods, the high hydrophilicity of PEO polymer had to be tempered with more hydrophobic characteristics. The controlled release of the T4 bacteriophage was designed based around blending PEO with the hydrophobic polymer cellulose diacetate (CDA). Incorporation of CDA into the PEO phase led to a decrease in the release kinetic of T4 bacteriophage in all formulations regardless of PEO molecular weight. The reduction was found to be highly dependent on the CDA/PEO composition ratio and to some extent on PEO molecular weight. Addition of CDA polymer in the blend composition increases the hydrophobicity of the resultant electrospun fibres, and decreases the fibre solubility/swelling in aqueous media. Here, the addition of CDA

resulted in greater fibre resistance to aqueous environment and prevented fibre dissociation. The controlled release of T4 bacteriophages was observed in a manner independent of loading concentration and core diameter. SEM and LSCM examination of the post-release fibre morphology suggested that the release mechanism is either solvent activation/fibre dissolution (blend with high PEO content) or through a more fibre swelling/diffusional mechanism (blend with high CDA content).

This research has provided the correct specifications for creating electrospun fibres which can maintain the viability of delicate biologically active entities, and assessed the conditions which are important for maintaining this viability. The research has also demonstrated the feasibility of creating fibres which can imbue significant anti-bacterial properties onto products with an appropriate level of storage for commercial application in meat packaging (no loss in T4 bacteriophage activity during refrigerated for one month).

Chapter 5: Future Work

This research has examined the various methods of encapsulation via electrospinning process to incorporate a highly viable T4 bacteriophage in electrospun fibres. The activity and release profile of the T4 bacteriophage was examined after each encapsulation processes. However, there are several other parameters that could be considered to improve the encapsulation efficiency and release profile of T4 bacteriophage from electrospun fibre.

The coaxial electrospinning was found to be the most reliable process to encapsulate the T4 bacteriophage within the core of the fibre. The encapsulation efficiency and release characteristic of the T4 bacteriophage could be even more drastic and interesting in triaxial electrospinning, since a lager mass of T4 bacteriophage can be incorporated in the innermost layer as well as the middle layer of a biocompatible polymer. The outermost layer would be a single hydrophobic polymer to enhance the electrospinability and to induce a diffusional release characteristic.

Triaxial electrospinning could also be used as a simple technique for immobilization of the T4 bacteriophage on the surface of electrospun fibres. In this process, the innermost layer would be a hydrophobic polymer such as CDA, and the T4 bacteriophage in the middle layer with PEO polymer as the outermost layer. After removing or washing PEO from the surface of fibre, a fibre with the immobilized T4 bacteriophages on a CDA electrospun core would be obtained. It could provide a comprehensive approach for the fabrication of different bacteriophages in/on electrospun fibres for high-performance multifunctional applications.

Another possible approach would be to use block copolymers as the electrospun polymer shell layer to better control the release profile. The effect of using a grafted or block copolymer is particularly prominent in critical application such as wound dressing or in meat packaging applica-

tion. In this type of fibre structure the covalently bonded hydrophilic polymer tends to bend around the fibre axis and release the encapsulated components. Using this method, the complete dissolution of the hydrophilic polymer on the surface of meat or skin is avoided and therefore less contamination would occur.

Cellulose diacetate (CDA) was used as hydrophobic polymer in blend with PEO to reduce release rate of the T4 bacteriophage from electrospun polymer. Cellulose acetate with different degree of substitution exhibits different solubility. For example, cellulose diacetate with a degree of substitution of 2.5 is soluble in most organic solvent; however, cellulose monoacetate (CMA) with degree of substitution below 1 is only soluble in water. Blending these two polymers as an electrospun polymer shell layer would be interesting to see if the release rate can be further controlled. Graft copolymerizing CMA on a backbone of CDA would be another interesting approach for a controlled release study. Grafting different molecular weights of CMA would induce variable pore sizes on the surface of the electropsun fibre and therefore exhibit different release profiles.

This exciting report suggests that high surface area of fibre with high T4 bacteriophage bioactivity produced by coaxial electrospinning could be useful in food packaging and/or as wound dressing materials. The overriding question for utilization of these materials in food packaging is whether or not PEO/CDA blend polymer based materials can exhibit high mechanical strength with reliable performance that equals or exceeds of standard paper packaging materials. Therefore, testing the mechanical properties of all blends electrospun fibre is still a great deal of work which remains to be done in future.

Most of commercialized paper food packaging materials are composed of cellulosic components. In our development, T4 bacteriophageactivated electrospun fibres were composed of various blend ratios of PEO/CDA polymers. The cellulose diacetate was added as hydrophobic polymer to avoid burst release and to obtain a sustained release profile. Lignin as second largest biopolymers can be also added as hydrophobic polymer into PEO electrospun fibre and to substitute CDA polymer. The PEO/lignin polymers can easily form electrospun fibre and various blend ratio of these two polymers could show a better and more sustained release of T4 bacteriophage.

References

Ackermann H. W., D. M. S. (1987). "Viruses of Prokaryotes." Boca Raton, FL: CRC Press **vols. 1 and 2**.

Ackermann, H. W., DuBow, M.S. (1987). "Viruses of Prokaryotes." Boca Raton, FL: CRC Press **vols. 1 and 2**.

Ahvenainen, R. (2003). "Novel Food Packanging Techniques." Woodhead Publishing.

Anany, H., Chen, W., Pelton, R., and Griffiths M. W. (2011). "Biocontrol of Listeria monocytogenes and Escherichia coli O157:H7 in Meat by Using Phages Immobilized on Modified Cellulose Membranes." APPLIED AND ENVIRONMENTAL MICROBIOLOGY **77**(18): 6379-6387.

Andrady, A. L. (2008). Science and Technology of Polymer Nanofibres. Hoboken, New Jersey, Published by John Wiley & Sons, Inc.

Ang, S. S., Salleh, A. B., Bakar, A. F., Yusof, N. A., and Heng, L. Y. (2012). "Characteristics of β-glucosidase production by Paecilomyces variotii and its potential application in bioassay system for boric acid determination." African Journal of Biotechnology **11**(14): 3394-3401.

Atterbury, R. J., M. A. P. Van Bergen, F. Ortiz, M. A. Lovell, J. A. Harris, A. De Boer, J. A. Wagenaar, V. M. Allen, and P. A. Barrow (2007). "Bacteriophage therapy to reduce Salmonella colonization of broiler chickens." Appl. Environ. Microbiol **73**: 4543-4549.

Ayutsede, J., M. Gandhi, S. Sukigara, M. Micklus, H.-E. Chen, and F. Ko (2005). "Regeneration of Bombyx mori silk by electrospinning and characterization of electrospun nonwoven mat." Polymer **46**(5): 1625-1634.

Baumgarten, P. K. (1971). "Electrostatic Spinning of Acrylic Microflbers." J. Colloid Interf. Sci. **36**: pp. 75-79.

Bazilevsky, A. V., Yarin, A. L., Megaridis, C.M. (2007). "Co-electrospinning of Core−Shell Fibers Using a Single-Nozzle Technique." Langmuir **23**(5): 2311-2314.

Benoy, B. B. B., Sa; Arup, Mukherjee (2006). "Preparation and in vitro characterization of slow release testosterone nanocapsules in alginates." Acta Pharm. **56**: 417–429.

Bognitzki, M., Czado, W., Frese, T., Schaper, A., Hellwig, M., Steinhart, M., Greiner, A. and Wendorff, J. H. (2001). "Nanostructured Fibers via Electrospinning." Adv. Mater. **13**: 70-72.

Bognitzki, M., T. Frese, M. Steinhart, A. Greiner, J. H. Wendorff, A. Schaper, and M. Hellwig (2001). "Preparation of fibers with nanoscaled morphologies: electrospinning of polymer blends." Polymer Engineering and Science **41**(6): 982-989.

Buchko, C. J., Chen, L. C, Shen, Y. and Martin, D. C. (1999). "Processing and microstructural characterization of porous biocompatible protein polymer thin films." Polymer **40**: 7397-7407.

Chapman, M. (2010). "The Electrospinning Company Ltd." from http://www.electrospinning.co.uk/.

Chen, L. B., Lev; Hatton, Alan; Rutledge, Gregory. (2008). "Electrospun cellulose acetate fibers containing chlorhexidine as a bactericide." Polymer **49**: 1266-1275.

Chew, S. Y., J. Wen, E. K. F. Yim, and K. W. Leong (2005). "Sustained release of proteins from electrospun biodegradable fibers." Biomacromolecules **6**(4): 2017-2024.

Choi, S. W., Kim, J.R, Jo, S.M., Lee, W.S. and Kim, B.C. (2004). "Electrospun PVdFbased fibrous polymer electrolytes for lithium ion polymer batteries." Electrochim. Acta. **50**(1): 69-75.

Comyn, J. (1985). "Polymer Permeability. ." Elsevier Applied Science Publishers, New York.

Coppi G., I. V., Leo E., Bernabei M. T. and Cameroni R. (2002). "Protein immobilization in crosslinked alginate microparticles." Microencapsulation **19**(1): 37-44.

Crank, J. (1980). "The Mathematics of Diffusion. ." Oxford University Press.

Crcarevska, M. S. D., Marija Glavas; Goracinova, Katerina (2008). "Chitosan coated Ca–alginate microparticles loaded with budesonide for delivery to the

inflamed colonic mucosa." European Journal of Pharmaceutics and Biopharmaceutics **68**: 565-578.

Deitzel, J. M., Kleinmeyer, J., Harris, D. and Tan, N. C. B. (2001). "The effect of processing variables on the morphology of electrospun nanofibers and textiles." Polymer **42**: 261-272.

Demir, M. M., Yilgor, I., Yilgor, E. and Erman, B. (2002). "Electrospinning of polyurethane fibers." Polymer **43**: 3303-3309.

Ding, E. Y., Jiang, Y., Li, G. K. (2001). "Comparative studies of the structures and transition characteristics of cellulose diacetate modified with polyethylene glycol prepared by chemical bonding and physical blending methods." J. Macromol. Sci. Physic **40**(6): 1053-1068.

Donaldson (1915). "Donaldson Company, Inc." from http://www.donaldson.com/en/contactus/index.html.

Doshi, J. R., Darrell H. (1995). "Electrospinning process and applications of electrospun fibers." Journal of Electrostatics **35**: 151–160.

Dror, Y., Kuhn, J., Avrahami, R., and Zussman, E. (2008). "Encapsulation of Enzymes in Biodegradable Tubular Structures." Macromolecules **41**: 4187-4192.

Dubrovskii, S. A., Rakova, G.V., Lagutina, M.A., Kazanskii, K.S. (2001). "Osmotic properties of poly(ethylene oxide) gels with localized charged units

" Polymer **49**(19): 8075-8083.

eSpin (2010). "eSpin Technologies Inc." from http://espintechnologies.com/.

Fang, X. a. D. H. R. (1997). "DNA fibers by electrospinning." Journal of Macromolecular Science: Physics **36**(2): 169–173.

Fong, H., Chun, I., Reneker, D. H. (1999). "Beaded nanofibers formed during electrospinning." Polymer **40**: 4585-4592.

Formhals, A. (1934). "Process and apparatus for preparing artificial threads." US Patent **1,975,504**.

Frazier, L. M. (2007). "SNS Nano Fiber Technology LLC ". from http://www.snsnano.com.

Freitas, S. M. H. P. G., B. (2005). "Microencapsulation by solvent extraction/evaporation: reviewing the state of the art of microsphere

preparation process technology." J. Controlled Release **102**: 313-332.

Gomez, S., Fleury, E., Vignon, M. R. (2004). "Preparation of cellouronic acids and partially acetylated cellouronic acids by TEMPO/NaClO oxidation of water-soluble cellulose acetate." Biomacromolecules **5**(2): 565-571.

Goode, D., V. M. Allen, and P. A. Barrow (2003). "Reduction of experimental Salmonella and Campylobacter contamination of chicken skin by application of lytic bacteriophages." Appl. Environ. Microbiol **69**: 5032-5036.

Greer, G. G. (2005). "Bacteriophage Control of Foodborne Bacteria." Journal of Food Protection **68**(5): 1102-1111.

Guo, Q. P. (2003). "A DSC study on miscible blends containing two crystalline components: poly(1-caprolactone)/poly[3,3-bis(chloromethyl) oxetane." Die Makromolekulare Chemie **191**(11): 2639–2645.

Gupta, P., C. Elkins, T. E. Long, and G. L. Wilkes (2005). "Electrospinning of linear homopolymers of poly(methyl methacrylate): exploring relationships between fiber formation, viscosity, molecular weight and concentration in a good solvent." polymer **46**(13): 4799–4810.

Haas, D. H., Stefan; Greil, Peter (2010). "Solvent control of cellulose acetate nanofibre felt structure produced by electrospinning." J Mater Sci **45**: 1299–1306.

Hammad, A. M. M. (1998). "Evaluation of alginate-encapsulated Azotobacter chroococcum as a phage-resistant and an effective inoculum." J. Basic Microbiol. **38**(1): 9–16.

Han, S. O., Son, W. K,. Youk, J. H., Park, W. H. (2008). "Electrospinning of ultrafine cellulose fibers and fabrication of poly(butylene succinate) biocomposites reinforced by them." Journal of Applied Polymer Science **107**(3): 1954-1959.

Hanlon, G. W. D., Stephene P.; Olliff Cedric J.; and Ibrahim, Lamia J. (2001). "Reduction in Exopolysaccharide Viscosity as an Aid to Bacteriophage Penetration through Pseudomonas aeruginosa Biofilms." Applied and Environmental Microbiology **67**(6): 2746–2753.

Heinze, T. L., T. (2004). "Chemical characteristics of cellulose acetate

" Macromolecular Symposia **208**: 167-237.

Hong Chena, L. Y., Wei Songa, Zhongkui Wub, Dan Li (2008). "Biocompatiblepolymer materials: Role of protein–surface interactions." Progress in Polymer Science **33**(11): 1059–1087.

Hongxu, Q., Hu, P., Xu, J., and Wang, A. (2006). "Encapsulation of drug reservoirs in fibers by emulsion electrospinning : Morphology characterization and preliminary release assessment." Biomacromolecules **7**: 2327-2330.

Huang, Z. M., Zhang, Y. Z., Kotaki, M., Ramakrishna, S. (2003). "A review on polymer nanofibers by electrospinning and their applications in nanocomposites." Composites Science and Technology **63**(15): 2223-2253.

Huanga, Z.-M. Z. Y. Z. K., M.; Ramakrishna, S. (2003). "A review on polymer nanofibers by electrospinning and their applications in nanocomposites." Composites Science and Technology **63**: 2223-2253.

Jiang, H., Fang, D., Hsiao, B.S., Chu, B. and Chen, W. (2004). "Optimization and characterization of dextran membranes prepared by electrospinning." Biomacromolecules **7**: 326-333.

Jiang, H. L., D. F. Fang, B. Hsiao, B. Chu, and W. Chen (2004). "Preparation and characterization of ibuprofen-loaded poly(lactide-co-glycolide)/poly(ethylene glycol)-g-chitosan electrospun membranes." Journal of Biomaterials Science: Polymer Edition **15**(3): 279–296.

Jiang, H. L., Y. Q. Hu, Y. Li, P. C. Zhao, K. J. Zhu, andW. L. Chen (2005). "A facile technique to prepare biodegradable coaxial electrospun nanofibers for controlled release of bioactive agents." Journal of Controlled Release **108**((2–3)): 237–243.

Jiang, Y., Ding, E., Li, G. (2002). "Study on transition characteristics of PEG?CDA soild-solid phase change materials." Polymer **43**: 117-122.

Jiang, Z. Z., Yufei; Li, Jian; Jiang, Wen; Yang, Dong and Wu Hong (2007). "Encapsulation of â-Glucuronidase in Biomimetic alginate Capsules for Bioconversion of Baicalin to Baicalein." Ind. Eng. Chem. Res. **46**: 1883-1890.

Jin, H. J., Fridrikh, S. V., Rutledge, G. C. and Kaplan, D. I. (2002). "Electrospinning Bombyx mori silk with poly(ethylene oxide),." Biomacromolecules **3**: 1233-1239.

Joerger, R. D. (2003). "Alternatives to antibiotics: bacteriocins, antimicrobial peptides and bacteriophages." Poult. Sci. **82**: 640–647.

Kamide, K., Saito, M. (1985). "Thermal-Analysis of Cellulose-Acetate Solids with Total Degrees of Substitution of 0.49, 1.75, 2.46, and 2.92." Polymer Journal **17**(8): 919-928.

Katti, D. S., K. W. Robinson, F. K. Ko, and C. T. Laurencin (2004). "Bioresorbable nanofiber-based systems for wound healing and drug delivery: optimization of fabrication parameters." Journal of Biomedical Materials Research Part B: Applied Biomaterials **70**(2): 286–296.

Kenawy, E. R., Bowlin, G.L., Mansfield, K., Layman, J., Simpson, D.G., Sanders, E.H. and Wnek, G.E. (2002). "Release of tetracycline hydrochloride from electrospun poly(ethylene-co-vinylacetate), poly(lactic acid), and a blend." J. Control. Release **81**: 57-64.

Khurana, H. S., Patra, P.K. and Warner, S.B. (2003). "Nanofibers from melt electrospinning." Abstr. Pap. Am. Chem. Soc, **226**(U425-U425 464-POLY).

Kim, C. W., M. W. Frey, M. Marquez, and Y. L. Joo (2005). "Preparation of submicron-scale, electrospun cellulose fibers via direct dissolution." Journal of Polymer Science Part B: Polymer Physics **43**(13): 1673–1683.

Kim, J. R., Choi, S. W., Jo, S. M., Lee, W. S. and Kim, B. C. (2005). "Characterization and Properties of P(VdF-HFP)-Based Fibrous Polymer Electrolyte Membrane Prepared by Electrospinning." J. Electrochem. Soc. **152**: A295-A300.

Kim, K. S., Y. K. Luu, C. Chang, D. F. Fang, B. S. Hsiao, B. Chu, and M. Hadjiargyrou (2004). "Incorporation and controlled release of a hydrophilic antibiotic using poly(lactide-co-glycolide)-based electrospun nanofibrous scaffolds." Journal of Controlled Release **98**(1): 47-56.

Klein, S., Kuhn, J., Avrahami, R., Tarre, S., Beliavski, M., Green, M., and Zussman, E. (2009). "Encapsulation of Bacterial Cells in Electrospun Microtubes." Biomacromolecules **10**: 1751–1756.

Ko, F. G., Y. Ali, A. Naguib, N. Ye, H. H. Yang, G. L. Li, C. Willis, P. (2003). "Electrospinning of continuons carbon nanotube-filled nanofiber yarns." Advanced Materials **15**(14): 1161-1175.

Ko, Y. G. a. F. (2006). Nanotubes and Nanofibres, chapter 8, published by Taylor and Francis Group, LLC.

Kohn, A. S. a. A. (1974). "The Effects of Freeze-Drying on Bacteriophage T4." CRYOBIOLOGY **11**: 452-464.

Kutter, E., Sulakvelidze, A. (2004). "Bacteriophages: Biology and Applications." CRC Press, Boca Raton, FL.

Lameiro, M. H., R. Malpique, A. C. Silva, P. M. Alves, and E. Melo (2006). "Encapsulation of adenoviral vectors into chitosan-bile salt microparticles for mucosal vaccination." J. Biotechnol **126**: 152-162.

Langer, R. (2003). "Biomaterials in drug delivery and tissue engineering: One laboratory's experience." Acc. Chem. Res. **3**(94): 94-101.

Langer, R., Rhine, W., Hsieh, D. S. T. & Bawa, R. (1980). "Controlled Release of Bioactive Materials,." ed. Baker, R. (Academic, New York).

Langer, R. F., J. (1978). "Polymeric Delivery Systems, ." ed. Kostelnik, R. J. (Gordon & Breach, New York),.

Larrondo, L. a. M. R. S. I. (1981a). "Electrostatic Fiber Spinning from Polymer Melts. I. Experimental Observations on Fiber Formation and Properties." J. Polym. Sci. Pol. Phys. **19**: pp. 909-920.

Lee, S.-W. a. B., Angela M. (2004). "Virus-Based Fabrication of Micro- and Nanofibers Using Electrospinning." J Nano Lett. **4**(3): 387–390.

Li, W. J., Laurencin, C.T., Caterson, E.J., Tuan, R.S. and Ko, F.K. (2002b). "Electrospun nanofibrous structure: A novel scaffold for tissue engineering." J. Biomed. Mater. Res. **60**: 613-621.

Liang Chen, L. B., T. Alan Hatton, Gregory C. Rutledge (2008). "Electrospun cellulose acetate fibers containing chlorhexidine as a bactericide." Polymer **49**: 1266-1275.

Liang, D. H., Y. K. Luu, K. S. Kim, B. S. Hsiao, M. Hadjiargyrou, and B. Chu (2005). "In vitro non-viral gene delivery with nanofibrous scaffolds." Nucleic Acids Research **33**(19): 170.

Liao, I. C. C., S. Y.; and Leong, K. W. (2006). "Aligned core–shell nanofibers delivering bioactive proteins." Nanomedicine **4** 465–471.

Liu, H. Q., Hsieh, Y. L. (2002). "Ultrafine fibrous cellulose membranes from electrospinning of cellulose acetate." Journal of Polymer Science Part B-Polymer Physics **40**(18): 2119-2129.

Lu, H. W. L., S. H.; Wang, X. L.; Qian, X. F.; Yin, J.; Zhu, Z. K. (2003). "Silver nanocrystals by hyperbranched polyurethane-assisted photochemical reduction of Ag " Materials Chemistry and Physics **81**(1): 107-107.

Lu, Y. a. S. C. C. (2004). "Micro and nano-fabrication of biodegradable polymers for drug delivery." Advanced Drug Delivery Reviews **56**(11): 1621–1633.

Luong-Van, E., L. Grøndahl, K. N. Chua, K. W. Leong, V. Nurcombe, and S. M. Cool (2006). "Controlled release of heparin from poly(1-caprolactone) electrospun fibers." Biomaterials **27**(9): 2042–2050.

Luu, Y. K., K. Kim, B. S. Hsiao, B. Chu, and M. Hadjiargyrou (2003). "Development of a nanostructured DNA delivery scaffold via electrospinning of PLGA and PLA–PEG block copolymers." Journal of Controlled Release **89**(2): 341–353.

Matlock, B. C., Beringer, Richard W., Ash, David L., Page, Andrew F. (2011). "Differences in Bacterial Optical Density Measurements between Spectrophotometers." Thermo Scientific Technical Note 52236.

Matthews, C. K., Kutter, E. M., Mosig, G. and Berget, P. B. (1983). "Bacteriophage T4." (Washington, DC: American Society for Microbiology).

Matthews, J. A., Wnek, G.E., Simpson, D.G. and Bowlin, G.L. (2002). "Electrospinning of collagen nanofibers." Biomacromolecules **3**: 232-238.

McKee, M. G., Wilkes, G.L., Colby, R.H. and Long, T.E. (2003). "Correlations of solution rheology with electrospun fiber formation of linear and branched polyesters." Macromolecules **37**: 1760-1767.

Megelski, S., Stephens, J.S., Chase, D.B. and Rabolt, J.F. (2002). "Micro- and nanostructured surface morphology on electrospun polymer fibers,." Macromolecules. **35**: 8456-8466.

Min, B.-M., L. Jeong, Y. S. Nam, J.-M. Kim, J. Y. Kim, and W. H. Park (2004). "Formation of silk fibroin matrices with different texture and its cellular response to normal human keratinocytes." International Journal of Biological Macromolecules **34**(5): 223-230.

Minikh, O., M. Tolba, L. Y. Brovko, and M. W. Griffiths (2010). "Bacteriophage-based biosorbents coupled with bioluminescent ATP assay for rapid concentration and detection of Escherichia coli." J. Microbiol. Methods **82**: 177-183.

Mo, X. M., Xu, C. Y., Kotaki, M, Ramakrishna, S. (2004). "Electrospun P(LLA-CL) nanofiber: a biomimetic extracellular matrix for smooth muscle cell and endothelial cell proliferation." Biomaterials **25**: 1883-1890.

Moser, C. A., T. J. Speaker, and P. A. Offit (1998). "Effect of water-based microencapsulation on protection against EDIM rotovirus challenge in mice." J. Virol **72**: 3859-3862.

Park, K. a. R. J. M. (2000). "Controlled drug delivery: designing technologies for the future." ACS Symposium Series, Volume 752, American Chemical Society, Washington, DC.

Park, T. G. A., M. J.; Langer, R (1994). "Controlled-Release of Proteins from Poly(L-Lactic Acid) Coated Polyisobutylcyanoacrylate Microcapsules." J. Appl. Polym. Sci. **52**: 1797-1807.

Pattama, T. U., Rungsardthong; Pitt, Supaphol. (2007). "Vitamin-loaded electrospun cellulose acetate nanofiber mats as transdermal and dermal therapeutic agents of vitamin A acid and vitamin E." European Journal of Pharmaceutics and Biopharmaceutics **67**: 387-397.

Pavlov, M. P., J. F. Mano, N. M. Neves, and R. L. Reis (2004). "“Fibers and 3D mesh scaffolds from biodegradable starch-based blends:production and characterization." Macromolecular Bioscience **4**(8): 776–784.

Payne, R. J. H., Jansen, V.A.A. (2003). "Pharmacokinetic principles of bacteriophage therapy." Clin. Pharmacokinet **42**: 315-325.

Pham, Q. P., U. Sharma, and A. G. Mikos (2006). "Electrospinning of polymeric nanofibers for tissue engineering applications: a review." Tissue Engineering **2**(15): 1197–1211.

Pielichowska, K., Pielichowski, k. (2011). "Biodegradable PEO/cellulose-based solid–solid phase change materials." Polymer Adv. Technol. **22**: 1633-1641.

Pintaric, B., Rogosic, M. and Mencer, H. J. (2000). "Dilute solution properties of cellulose diacetate in mixed solvents." Journal of Molecular Liquids **85**(3): 331-350.

Pittarate, C., Yoovidhya, T., Srichumpuang, W., Intasanta N., and Wongsasulak S., (2011). "Effects of poly(ethylene oxide) and ZnO nanoparticles on the morphology, tensile and thermal properties of cellulose acetate nanocomposite fibrous film." Polymer Journal **43**: 978-986

Pizzoli, M. S., M. Ceccorulli, G. Pezzin, G. (1985). "Rate of Absorption of Di-N-Butylphthalate in Glassy Poly(Vinylchloride)." Polymer Communications **26**(4): 107-109.

Price, R. L., Haberstroh, K.M., Webster, T.J. (2003). "Selective bone cell adhesion on formulations containing carbon nanofibers,." Biomaterials **24**: 1877-1887.

Puapermpoonsiri, U., Spencer, J., van der Walle, C.F. (2009). "A freeze-dried formulation of bacteriophage encapsulated in biodegradable microspheres." European Journal of Pharmaceutics and Biopharmaceutics **72**: 26-33.

Qi Hongxu, P. H., Jun Xu, and Aijun Wang (2006). "Encapsulation of drug reservoirs in fibers by emulsion electrospinning : Morphology characterization and preliminary release assessment." Biomacromolecules **7**: 2327-2330.

Qi, H. X., Hu, P. Xu, J., Wang, A. J. (2006). "Encapsulation of drug reservoirs in fibers by emulsion electrospinning: Morphology characterization and preliminary release assessment." Biomacromolecules **7**(8): 2327-2330.

Rahman, N. A., and Mathiowitz, E. (2004). "Localization of bovine serum albumin in double-walled microspheres." Journal of Controlled Release **94**(1): 163–175.

Ramakrishna Seeram, K. F., Wee-Eong Teo, Teik-Cheng Lim and Zuwei Ma (2005). An Introduction to Electrospinning and Nanofibres, Printed in Singapore by World Scientific Printers (S) Pte Ltd.

Rathbone, M. J., J. Hadgraft, and M. S. Roberts (2003). "Modified-Release Drug Delivery Technology." Drugs and the Pharmaceutical Sciences Series **Volume 126**(Marcel-Dekker, Inc., New York).

Reneker, D. H., Yarin, A. L., Fong, H. and Koombhongse, S. (2000). "Bending instability of electrically charged liquid jets of polymer solutions in electrospinning." J. Appl. Phys. **87**: 4531-4547.

Reneker, D. H. a. C., I. (1996). "Nanometre diameter fibres of polymer, produced by electrospinning." Nanotechnology **7**: pp. 216-223.

Rim, P. B., Runt J. P., (1984). "Melting point depression in crystalline/compatible polymer blends." Macromolecules **17**(8): 1520-1526.

Rustemeyer, P. (2004). "CA filter tow for cigarette filters." Macromolecular Symposia **208**: 267-291.

Rustemeyer, P. (2004). "History of CA and evolution of the markets." Macromolecular Symposia **208**: 1-6.

Rutledge, G. C., Li, Y., Fridrikh, S., Warner, S. B., Kalayci, V. E. and Patra, P. (2000). "Electrostatic Spinning and Properties of Ultrafine Fibers, National Textile Center,." 2000 Annual Report (M98-D01), National Textile Center: 1-10.

Salalha, W., Kuhn, J., Dror, Y. and Zussman, E. (2006). "Encapsulation of bacteria and viruses in electrospun nanofibres." Nanotechnology **17**: 4675-4681.

Sauvageau, D., Allain, B., Cooper, D.G. (2010). "Using the rate of respiration to monitor events in the infection of Escherichia coli cultures by bacteriophage T4." Biotechnol. Prog. **26**(3): 865-871.

Seeram, R. F., Kazutoshi; Teo, Wee-Eong; Lim, Teik-Cheng and Ma, Zuwei (2005). An Introduction to Electrospinning and Nanofibres, Printed in Singapore by World Scientific Printers (S) Pte Ltd.

Shenoy, S. L., Bates, W. D., Frisch, H. L. and Wnek, G. E. (2005). "Role of chain entanglements on fiber formation during electrospinning of polymer solutions: good solvent, non-specific polymer-polymer interaction limit." Polymer **46**: 3372-3384.

Smith, H. W., and M. B. Huggins (1983). "Effectiveness of phages in treating experimental Escherichia coli diarrhoea in calves, piglets and lambs." J. Gen. Microbiol **129**: 2659-2675.

Soares, J. P. S., J. E.; Chierice G. O.; Cavalheiro, T. G. (2004). "Thermal behavior of alginic acid and its soduim salt " Ecletica **29**(2): 57-63.

Sombatmankhong, K., Sanchavanakit, P. Pavasant, and P. Supaphol (2007). "Bone scaffolds from electrospun fiber mats of poly(3-hydroxybutyrate), poly(3-hydroxybutyrate-co-3-hydroxyvalerate) and their blend." Polymer **48**(5): 1419-1427.

Son, W. K., J. H. Youk, T. S. Lee, and W. H. Park (2004). "Preparation of antimicrobial ultrafine cellulose acetate fibers with silver nanoparticles." Macromolecular Rapid Communications **25**(18): 1632–1637.

Son, W. K. Y., J. H. Lee, T. S. Park, W. H. (2004). "Electrospinning of ultrafine cellulose acetate fibers: Studies of a new solvent system and deacetylation of ultrafine cellulose acetate fibers." Journal of Polymer Science Part B-Polymer Physics **42**(1): 5-11.

Soothill, J., Hawkins, C., Anggard, E., Harper, D. (2004). "Therapeutic use of bacteriophages." Lancet Infect. Dis. **4**: 544-545.

Soothill J., H. C., Anggard E., Harper D. (2004). "Therapeutic use of bacteriophages." Lancet Infect. Dis. **4**: 544-545.

Sperling, L. H. (2006). "INTRODUCTION TO PHYSICAL POLYMER SCIENCE." A JOHN WILEY & SONS, INC. PUBLICATION(ISBN: 978-0-471-70606-9, FOURTH EDITION).

Srikar R., Y. A. L., Megaridis C. M. , Bazilevsky A. V., and Kelley E. (2008). "Desorption-Limited Mechanism of Release from Polymer Nanofibers." Langmuir **24**: 965-974.

Sturesson, C., and L. Wikingsson. (2000). "Comparison of poly(acryl starch) and poly(lactide-co-glycolide) microspheres as drug delivery system for a rotavirus vaccine." J. Control. Release **68**: 441-450.

Sun, W. (2001). "Use of bioluminescent Salmonella for assessing the efficiency of constructed phage-based biosorbent. ." J. Ind. Microbiol. Biotechnol. **27**: 126.

Sun, Z. C. Z., E.; Yarin, A. L.; Wendorff, J. H.; Greiner, A. (2003). "Compound core shell polymer nanofibres by co-electrospinning." Advance Material **15**: 1929.

Tang, L. G., D. N. S. Hon, et al. (1996). "Polymorphic transformations of cellulose acetates prepared by solution acetylation at an elevated temperature." Journal of Macromolecular Science-Pure and Applied Chemistry **33**(2): 203-208.

Taylor, G. (1964). "Disintegration of Water Drops in an Electric Field." Proc. R. Soc. Lond. A.(280): pp. 383-397.

Tolba, M., O. Minikh, L. Y. Brovko, S. Evoy, and M. W. Griffiths (2010). "Oriented immobilization of bacteriophages for biosensor applications." Appl. Environ. Microbiol. **76**: 528–535.

Tungprapa, S. J., Ittipol; Supaphol, Pitt. (2007). "Release characteristics of four model drugs from drug-loaded electrospun cellulose acetate fiber mats, Polymer 2007; 48, 5030-504." Polymer **48**: 5030-5040.

Van de Weert, M. V. t. H., R.; Van der Weerd, J.; Heeren R.M.; Posthuma G.; Hennink W.E.; Crommelin D.J. (2000). "Lysozyme distribution and conformation in a biodegradable polymer matrix as determined by FTIR techniques." J. Control. Release **68**: 31-40.

Vega Lugo, A.-C. L., Loong-Tak (2012). "Effects of poly(ethylene oxide) and pH on the electrospinning of whey protein isolate." Journal of Polymer Science Part B: Polymer Physics **15**(16): 1188–1197.

Venugopal, J., and Ramakrishna, S. (2005). "Applications of polymer nanofibers in biomedicine and biotechnology." Appl. Biochem. Biotechnol. **125**: 147-157.

Verreck, G., I. Chun, J. Rosenblatt, J. Peeters, A. Van Dijck, J. Mensch, M. Noppe, and M. E. Brewster (2003). "Incorporation of drugs in an amorphous state into electrospun nanofibers composed of a water-insoluble, nonbiodegradable polymer." Journal of Controlled Release **92**(3): 349–360.

Wang, Y. H. H., Y. L. (2004). "Enzyme immobilization to ultra-fine cellulose fibers via Amphiphilic polyethylene glycol spacers." Journal of Polymer Science Part a-Polymer Chemistry **42** (17): 4289–4299.

Wayne, J. S., C. L. McDowell, K. J. Shields, and R. S. Tuan (2005). "In vivo response of polylactic acid–alginate scaffolds and bone marrow-derived cells for cartilage tissue engineerin " Tissue Engineering **11**(5-6): 953–963.

Xiao, M. and M. W. Frey (2007). "The role of salt on cellulose dissolution in ethylene diamine/salt solvent systems." Cellulose **14**(3): 225-234.

Xiuling, X. L., Yang; Xiaoyi, Xu; Xin, Wang; Xuesi, Chen; Qizhi, Liang; Jing, Zeng; Xiabin. Jing (2005). "Ultrafine medicated fibers electrospun from W/O emulsions." Journal of Control Release **108**: 33-42.

Xu, X., Zhuang, X., Chen, X. (2006). "Preparation of core-sheath composite nanofibres by emulsion electrospinning." Macromolecular Rapid Communications **27**: 1637-1642.

Yongsheng Ma, J. C. P., Qi Wang, Yongping Xu, Xiaoqing Huang, Anton Korenevsky, and Parviz M. Sabour (2008). "Microencapsulation of Bacteriophage Felix O1 into Chitosan-Alginate Microspheres for Oral Delivery." Applied and environmental microbiology **74**(15): 4799-4805.

Yongsheng, M. J., C., Pacan; Qi Wang; Yongping, Xu; Xiaoqing, Huang; Anton, Korenevsky and Parviz, M. Sabour (2008). "Microencapsulation of Bacteriophage Felix O1 into Chitosan-Alginate Microspheres for Oral Delivery." Applied and environmental microbiology **74**(15): 4799-4805.

Yoo, H. S., E. A. Lee, J. J. Yoon, and T. G. Park (2005). "Hyaluronic acid modified biodegradable scaffolds for cartilage tissue engineering." Biomaterials **26**(14): 1925–1933.

Yoshimoto, H., Shin, Y. M., Terai, H. and Vacanti, J. P. (2003). "biodegradable nanofiber scaffold by electrospinning and its potential for bone tissue engineering." Biomaterials **24**: 2077-2082.

You, Y., Min, B. M, Lee, S. J., Lee, T. S. and Park, W. H. (2005). "In Vitro Degradation Behavior of Electrospun Polyglycolide, Polylactide, and Poly(lactide-coglycolide)." J. Appl. Polym. Sci. **95**: 193-200.

Zeng, J., A. Aigner, F. Czubayko, T. Kissel, J. H. Wendorff, and A. Greiner (2005). "Poly(vinyl alcohol) nanofibers by electrospinning as a protein delivery

system and the retardation of enzyme release by additional polymer coatings." Biomacromolecules **6**(3): 1484–1488.

Zeng, J., L. X. Yang, Q. Z. Liang, X. F. Zhang, H. L. Guan, X. L. Xu, X. S. Chen, and X. B. Jing (2005). "Influence of the drug compatibility with polymer solution on the release kinetics of electrospun fiber formation." Journal of Controlled Release **105** ((1-2)): 43-51.

Zeng, J., X. Y. Xu, X. S. Chen, Q. Z. Liang, X. C. Bian, L. X. Yang, and X. B. Jing (2003). "Biodegradable electrospun fibers for drug delivery." Journal of Controlled Release **92**(3): 227–231.

Zhang, C. X., X. Y. Yuan, L. L. Wu, and J. Sheng (2005a) (2005). "Drug-loaded ultrafine poly(vinyl alcohol) fibre mats prepared by electrospinning." e-Polymers 072.

Zhang, Y. Z. W., S. X.; Feng, Y.; Li, J.; Lim, C. T.; and Ramakrishna, S. (2006). "Coaxial Electrospinning of (Fluorescein Isothiocyanate-Conjugated Bovine Serum Albumin)-Encapsulated Poly(E-caprolactone) Nanofibers for

Sustained Release." Biomacromolecules **7** 1049-1057.

Zhao, S. L., Wu, X. H., Wang, L. G. and Huang, Y. (2004). "Electrospinning of Ethyl-Cyanoethyl Cellulose/Tetrahydrofuran Solutions." J. Appl. Polym. Sci. **91**: 242-246.

Zuwei, M. K., M., Ramakrishna, S. (2005). "Electrospun cellulose nanofiber as affinity membrane." Journal of Membrane Science **265**: 115-123.

Appendix

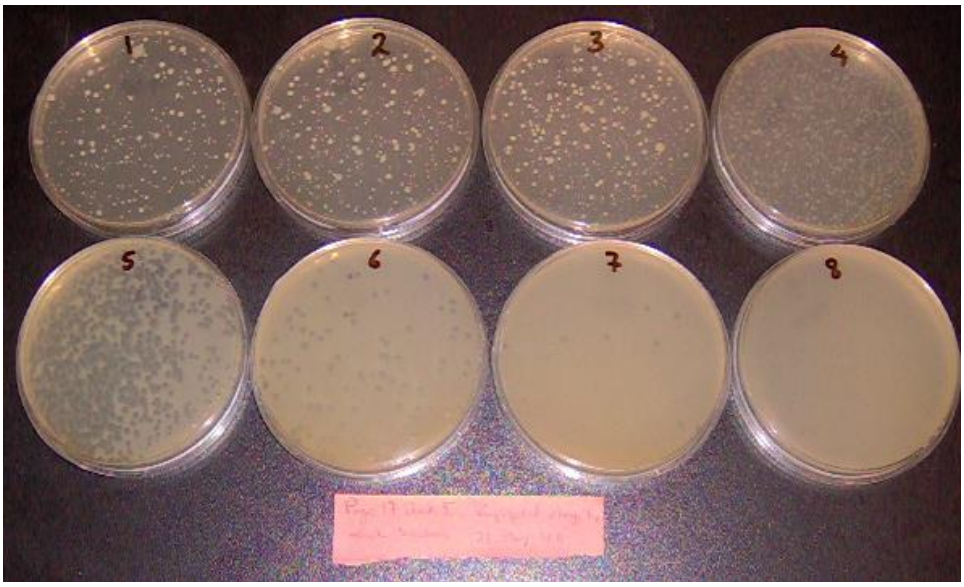

Figure A1: T4 Bacteriophage activity of original stock (10^8 PFU/mL).

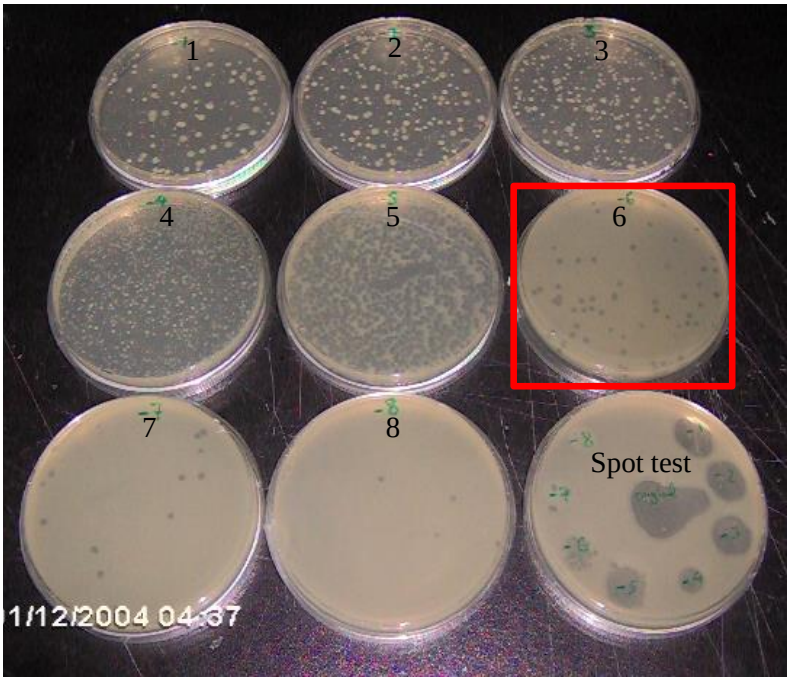

Figure A2: T4 bacteriophage activity after vortexing at 10k rpm and freeze drying (10^8 PFU/mL).

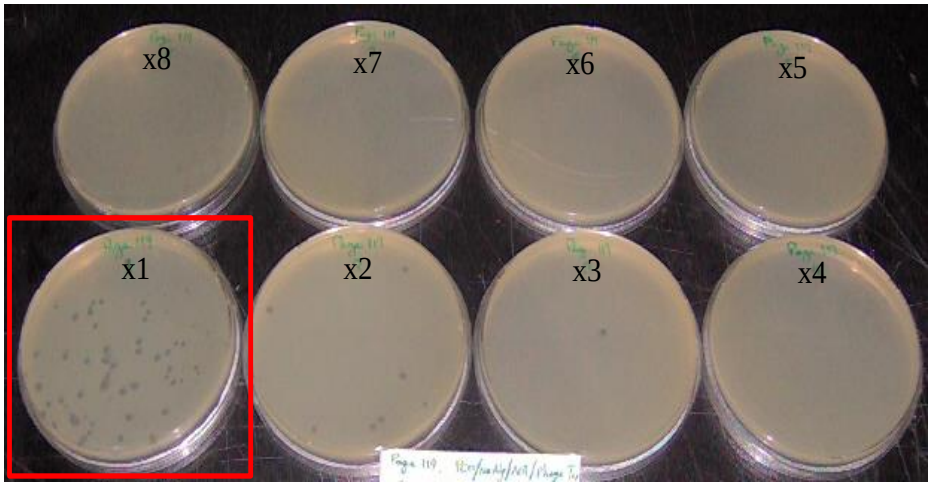

Figure A3: T4 bacteriophage activity after emulsification electrospinning in absence of calcium chloride, as cross-linker agent for alginate (10^3 PFU/mL).

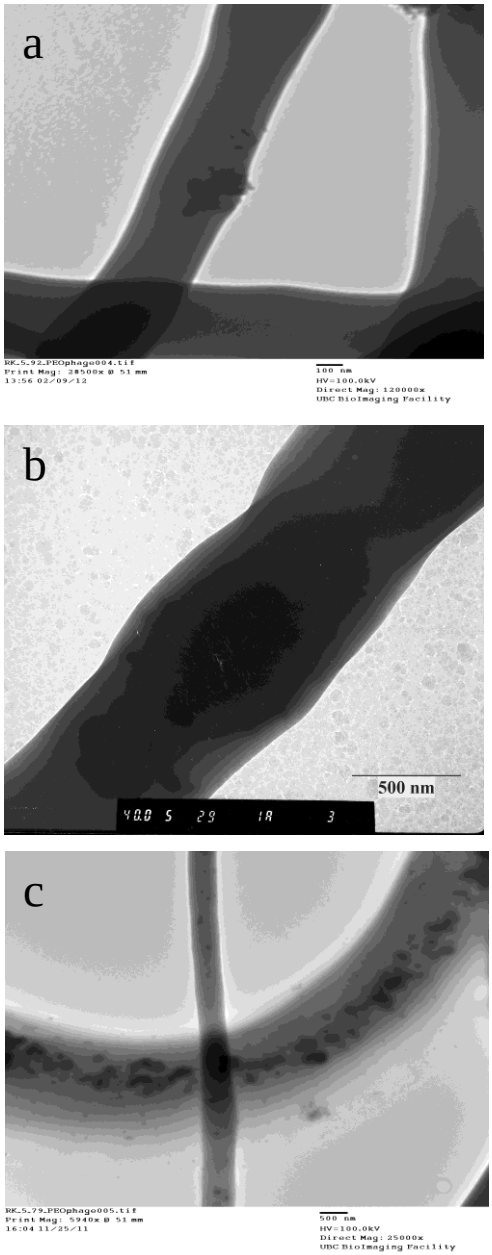

Figure A4: TEM microscopy analysis of encapsulated T4 bacteriophage in electrospun fibre after a) suspension electrospinning, b) emulsion electrospinning, and c) coaxial electrospinning.

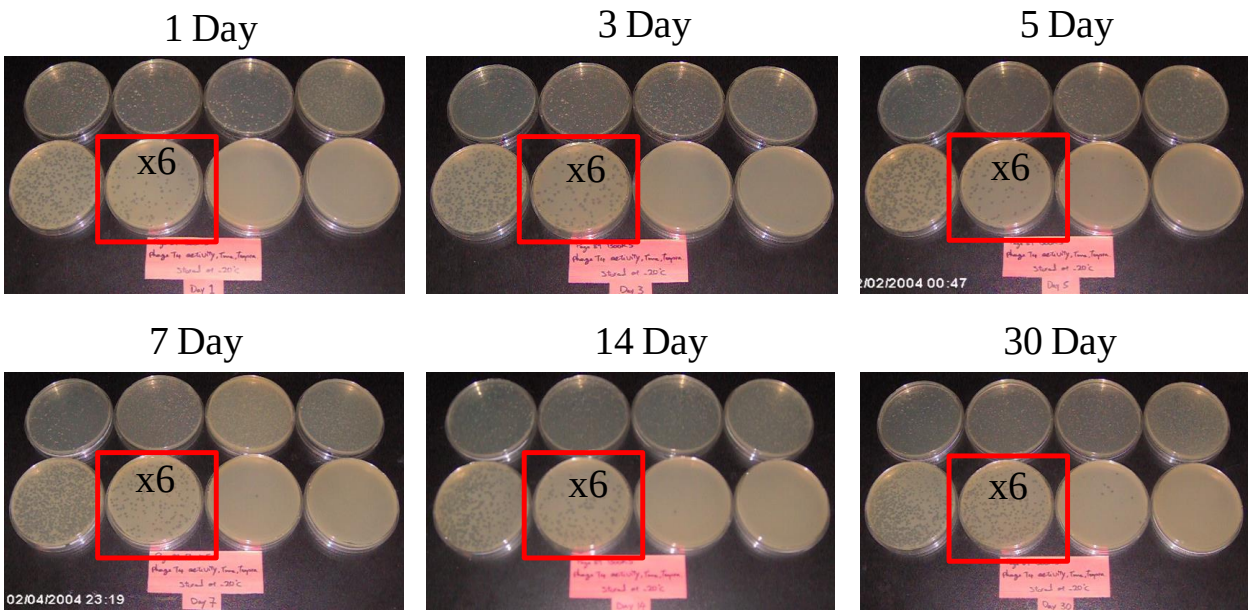

Figure A5: Stability of freeze dried T4 bacteriophage stored at -20 °C. Activity measurement was performed by serial dilution test.

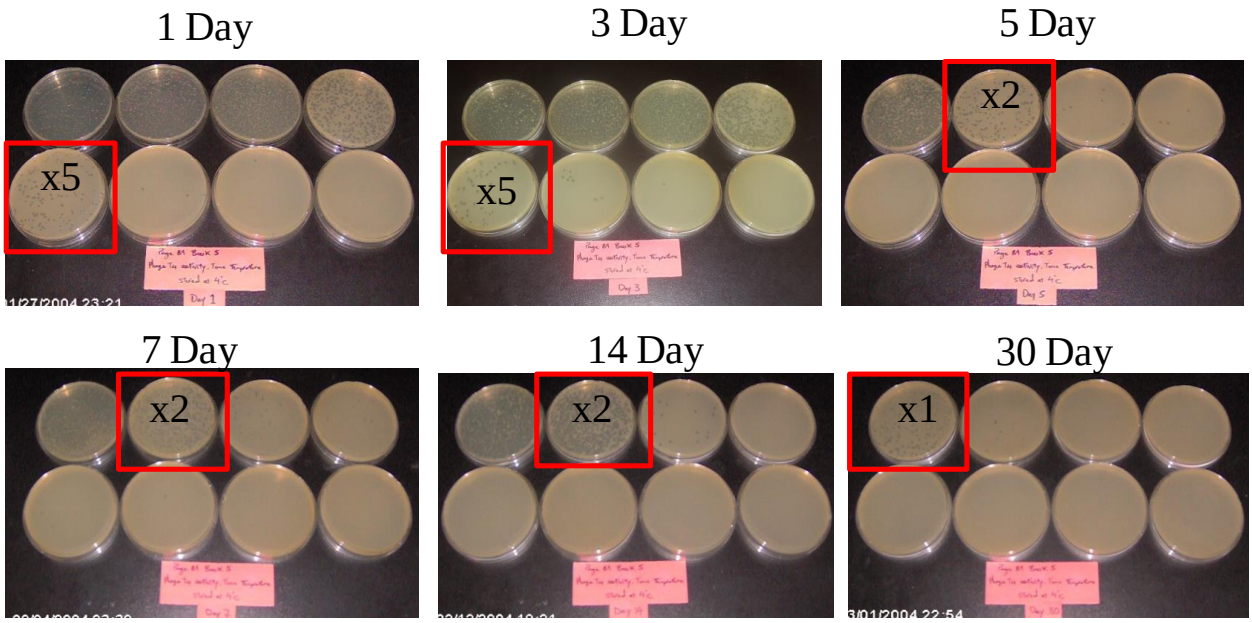

Figure A6: Stability of freeze dried T4 bacteriophage stored at 4 °C. Activity measurement was performed by serial dilution test.

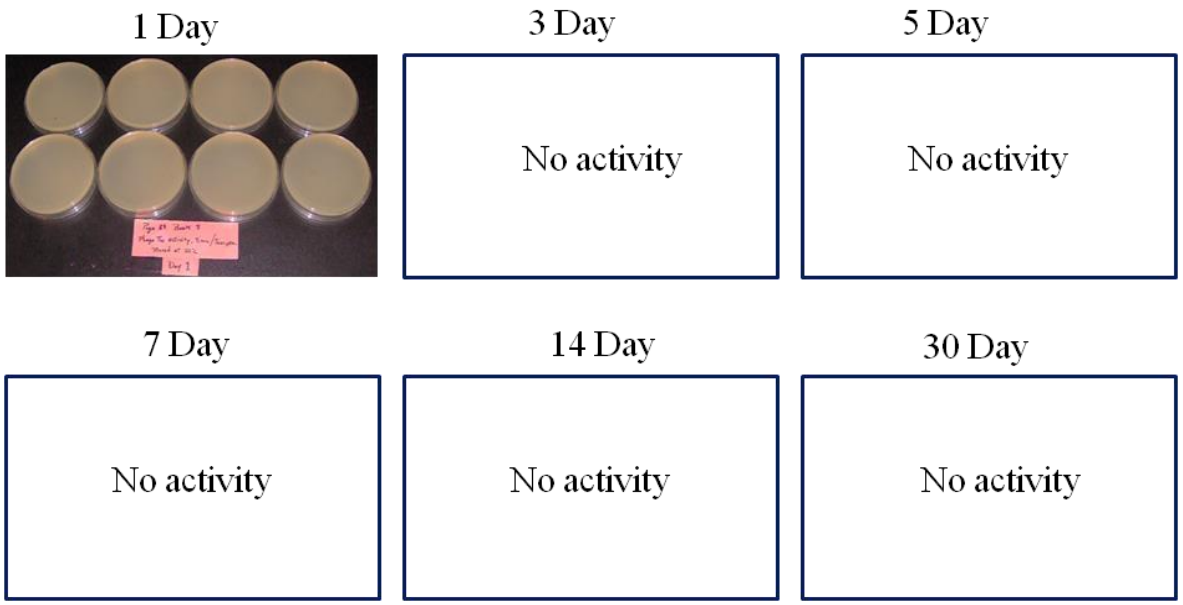

Figure A7: Stability of freeze dried T4 bacteriophage stored at 20 °C. Activity measurement was performed by serial dilution test.

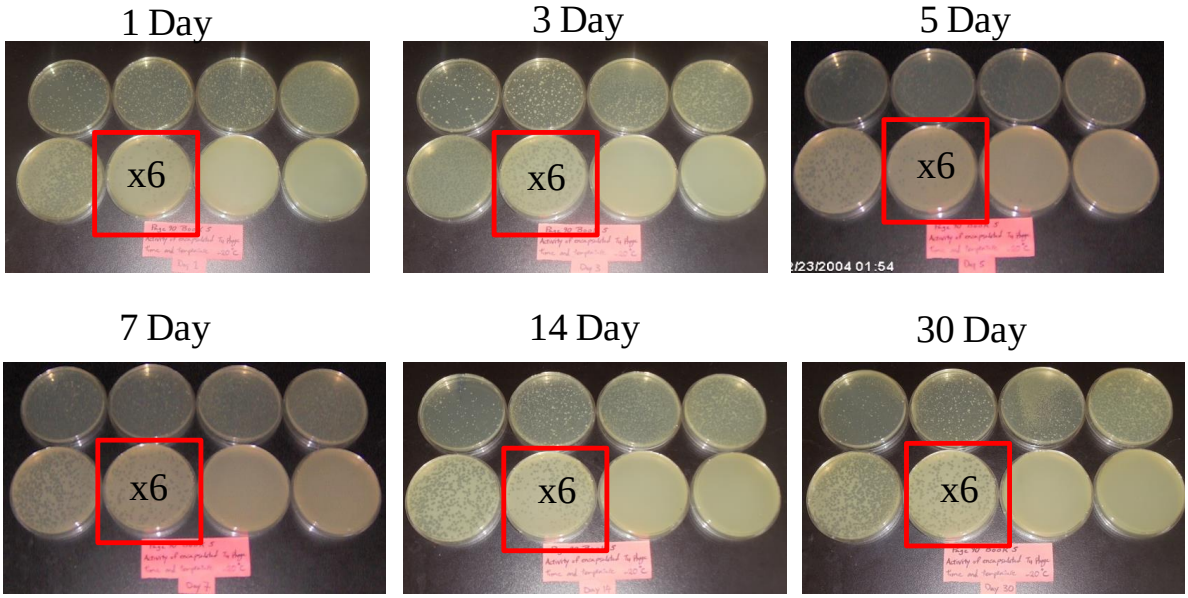

Figure A8: Stability of encapsulated T4 bacteriophage in core/shell electrospun fibre stored at -20 °C. Activity measurement was performed by serial dilution test.

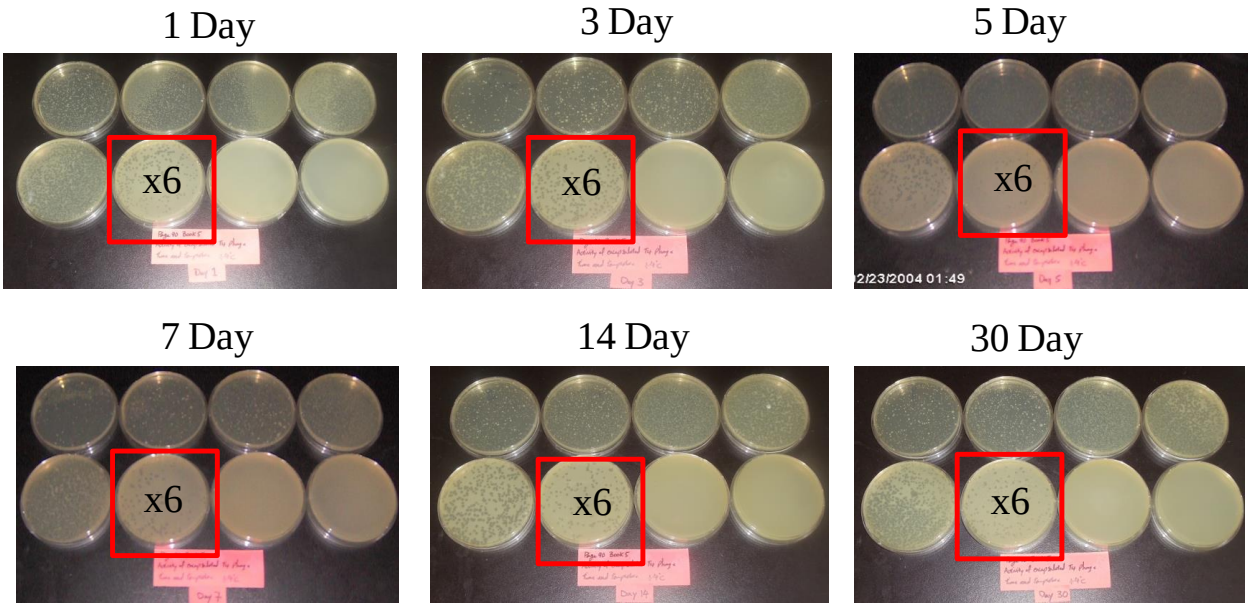

Figure A9: Stability of encapsulated T4 bacteriophage in core/shell electrospun fibre stored at 4 °C. Activity measurement was performed by serial dilution test.

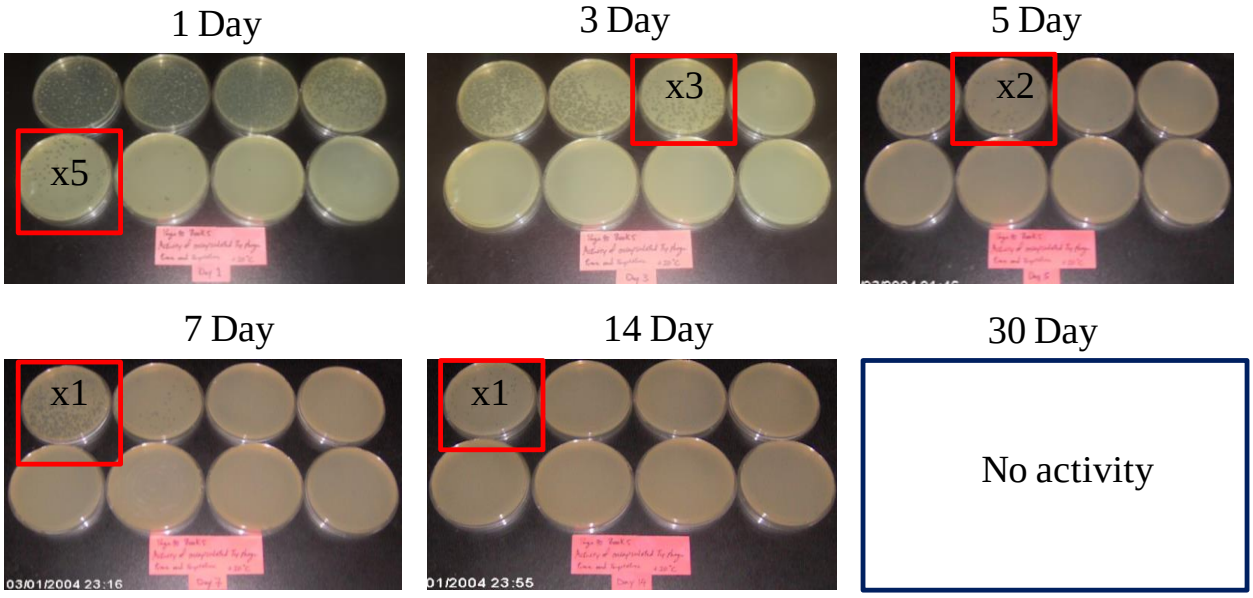

Figure A10: stability of encapsulated T4 bacteriophage in core/shell structure electrospun fibre stored at 20 °C. Activity measurement was performed by serial dilution test.

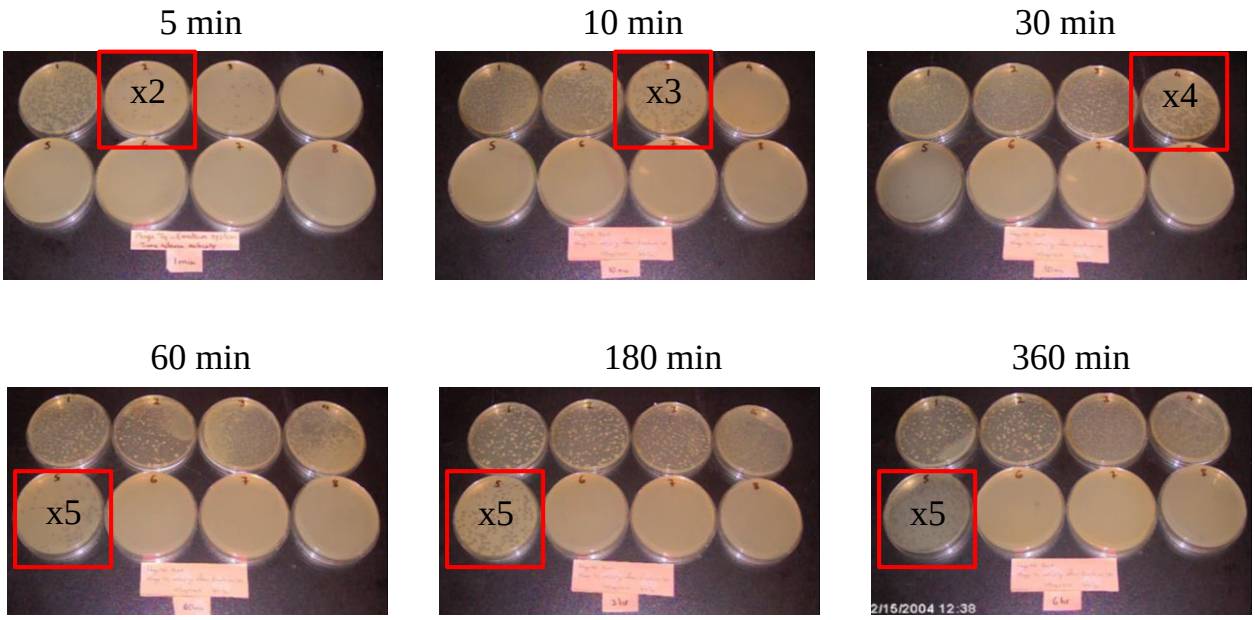

Figure A11: Activity measurement of T4 bacteriophage at different time of release from calcium-alginate capsules (after emulsification process).

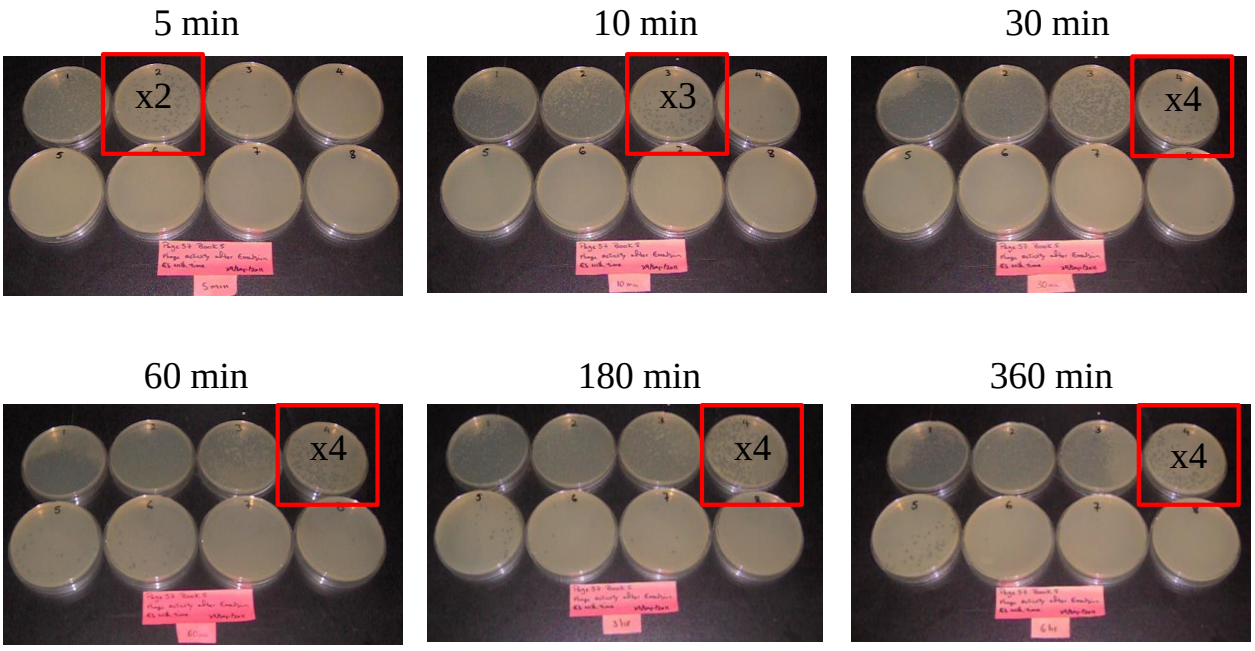

Figure A12: Activity measurement of T4 bacteriophage at different time of release from emulsion electrospun PEO fibre (after emulsion electrospinning process).

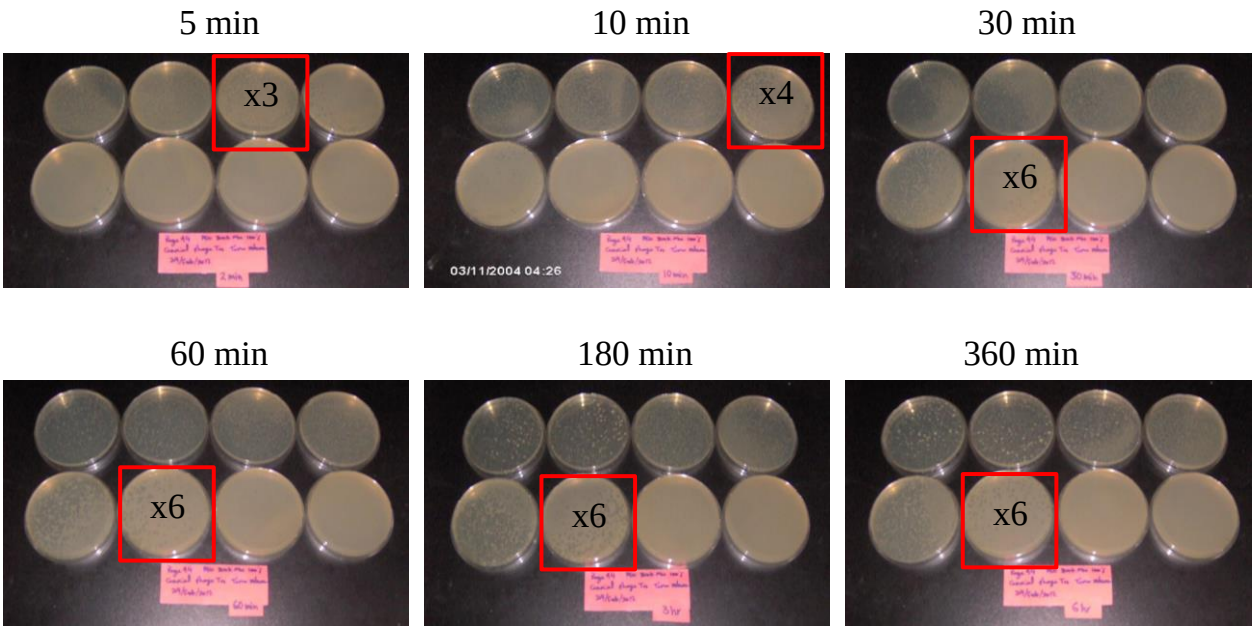

Figure A13: Activity measurement of T4 bacteriophage at different time of release from core/shell electrospun PEO fibre, 300k M_n (after coaxial electrospinning process).

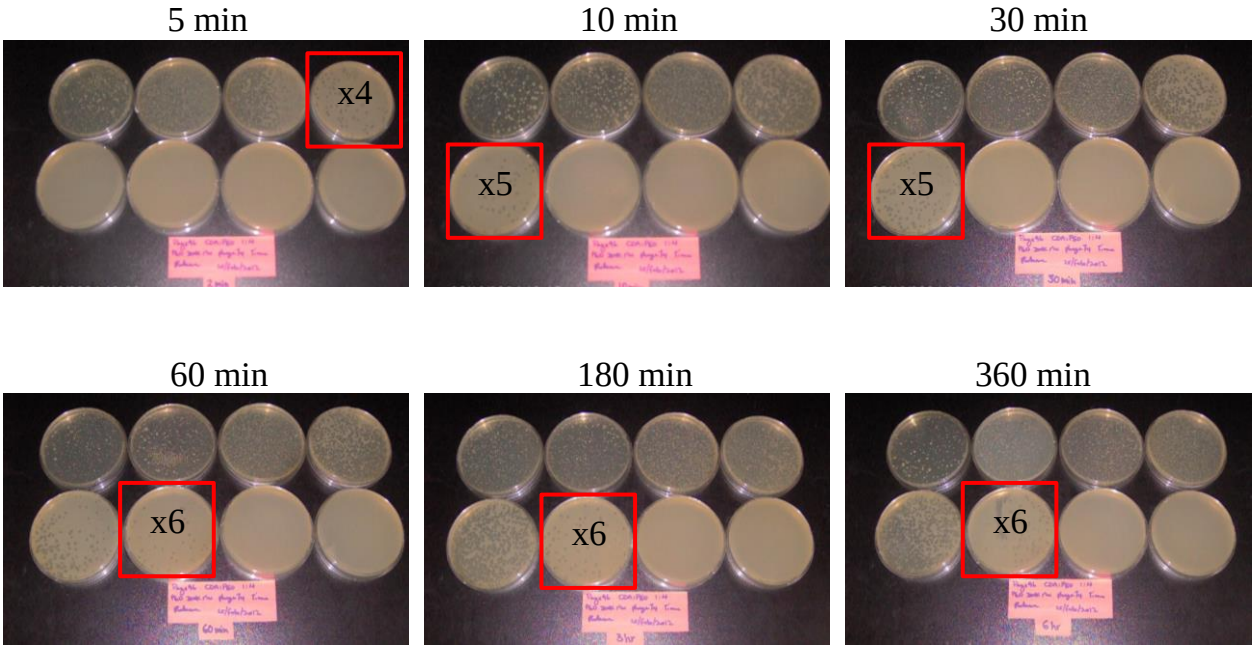

Figure A14: Activity measurement of T4 bacteriophage at different time of release from core/shell electrospun PEO:CDA fibre, 80:20 %wt, 300:30k Mn, respectively.

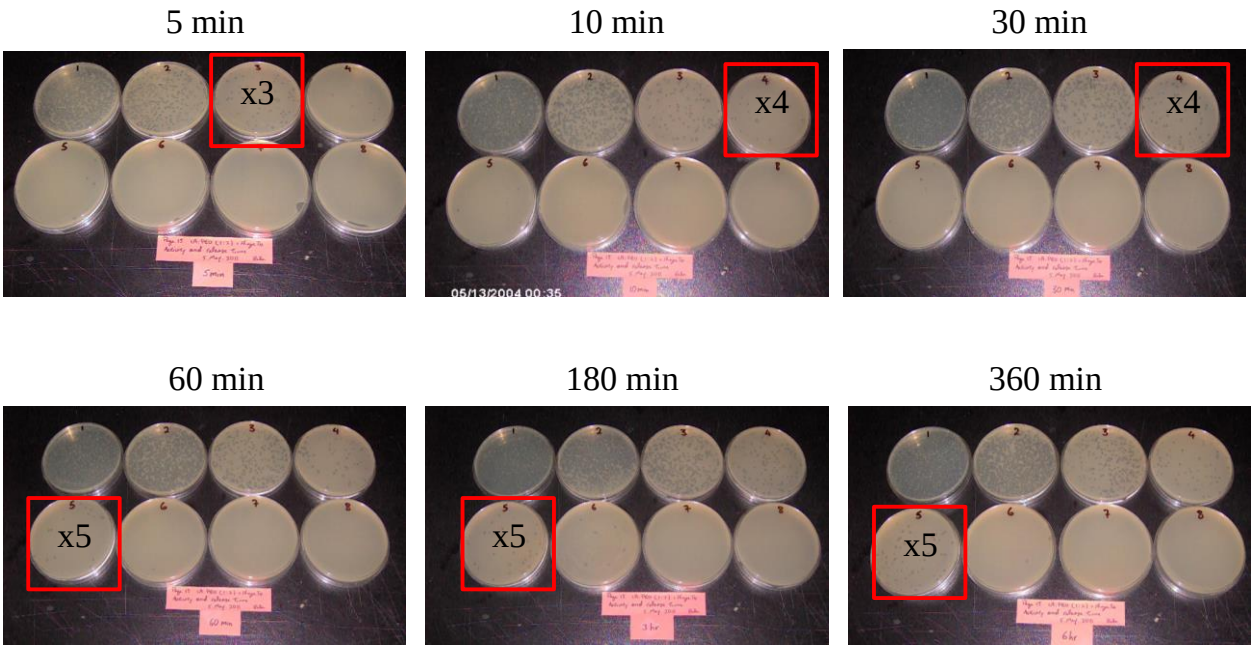

Figure A15: Activity measurement of T4 bacteriophage at different time of release from core/shell electrospun PEO:CDA fibre, 65:35 %wt, 300:30k M_n, respectively.

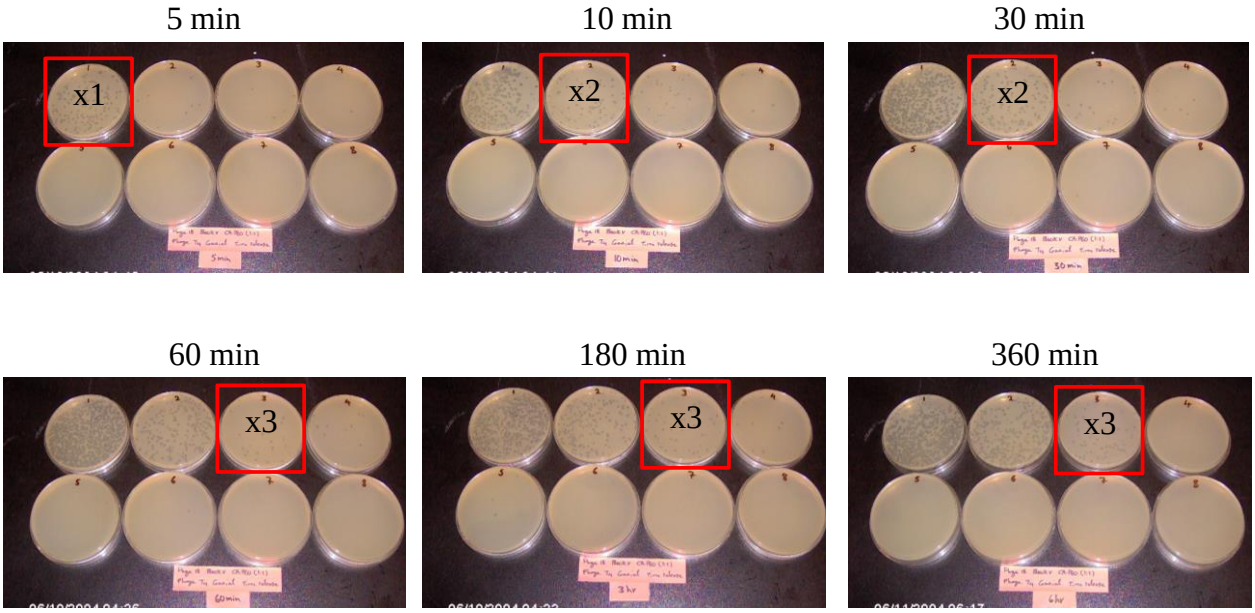

Figure A16: Activity measurement of T4 bacteriophageat different time of release from core/shell electrospun PEO:CDA fibre, 50:50 %wt, 300:30k M_n, respectively.

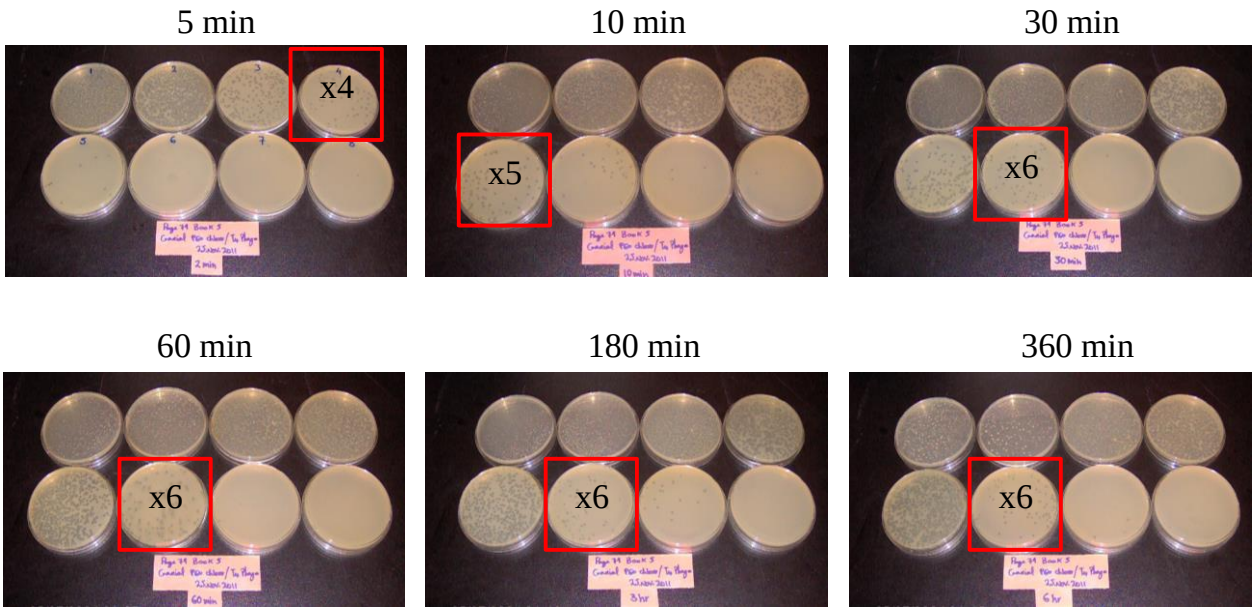

Figure A17: Activity measurement of T4 bacteriophage at different time of release from core/shell electrospun PEO fibre, 100k M_n at 9 %wt concentration (after coaxial electrospinning process).

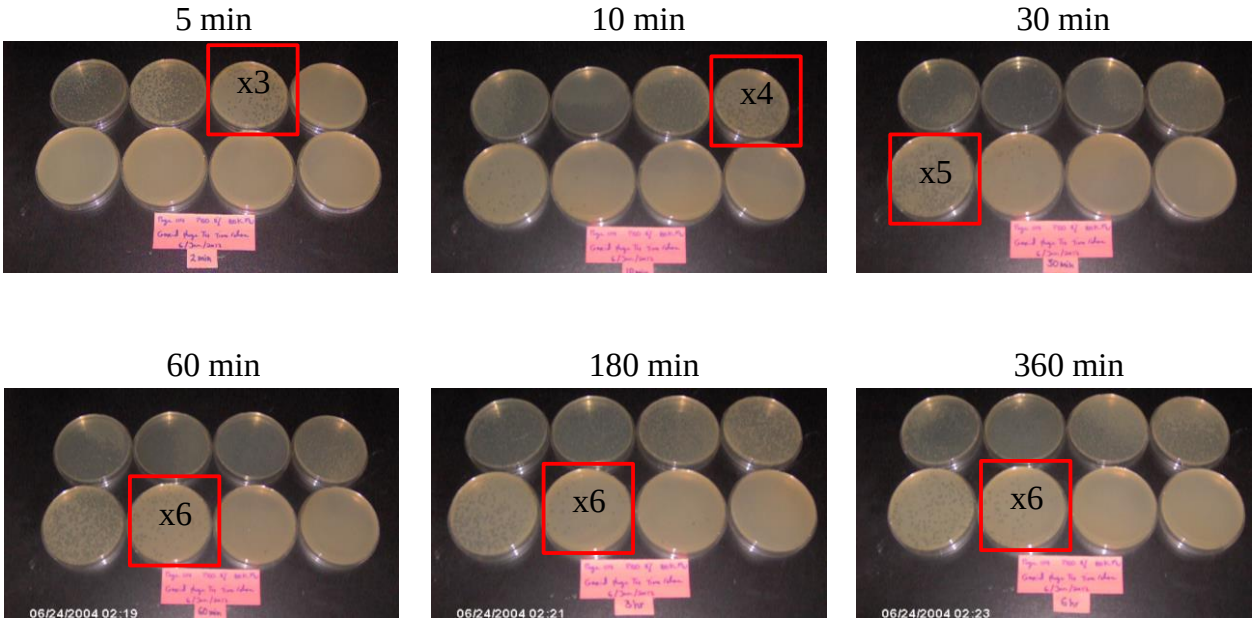

Figure A18: Activity measurement of T4 bacteriophage at different time of release from core/shell electrospun PEO fibre, 100k M_n at 11 %wt concentration (after coaxial electrospinning process).

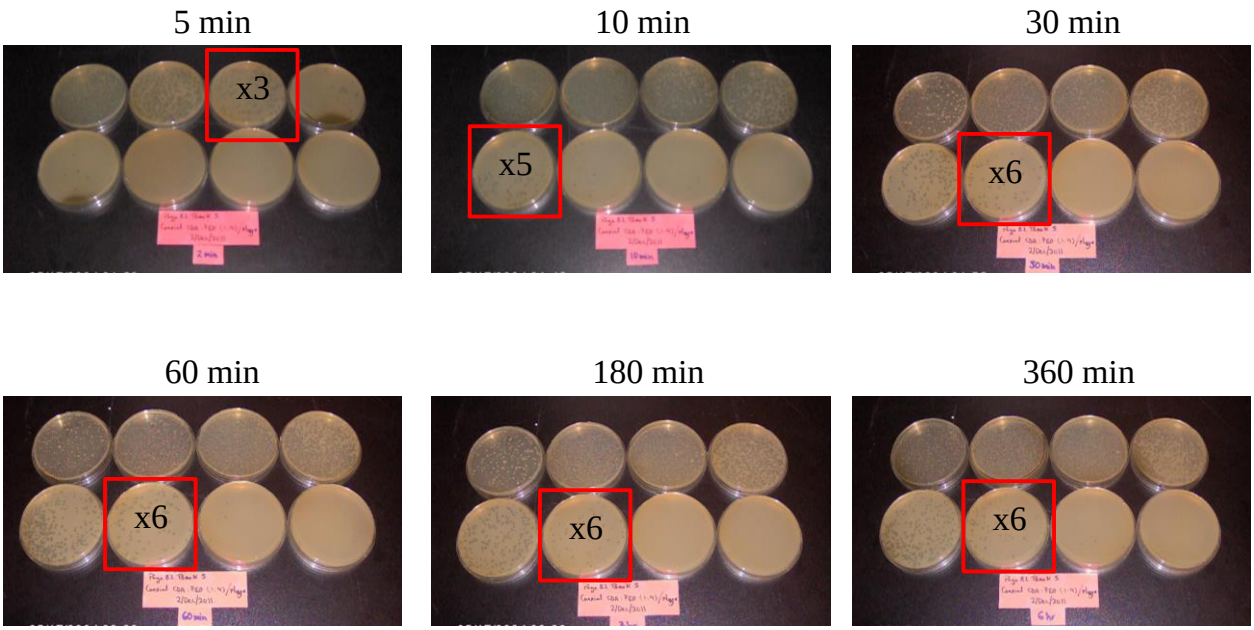

Figure A19: Activity measurement of T4 bacteriophage at different time of release from core/shell electrospun PEO:CDA fibre, 80:20 %wt, 100:30k M_n (after coaxial electrospinning process).

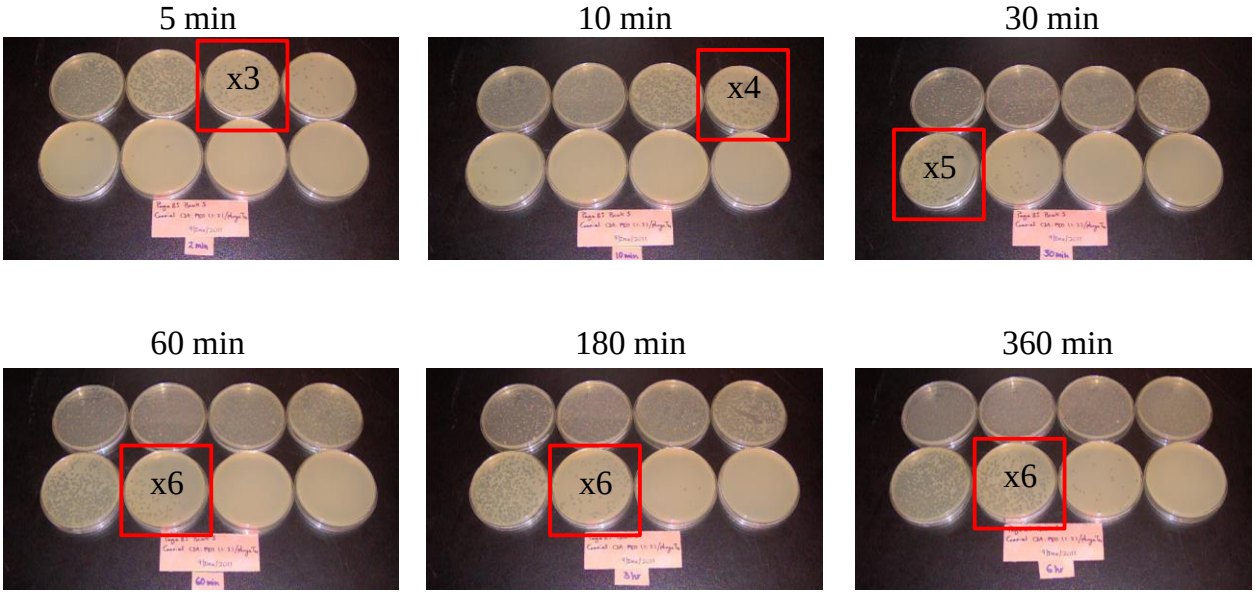

Figure A20: Activity measurement of T4 bacteriophage at different time of release from core/shell electrospun PEO:CDA fibre, 65:35 %wt, 100:30k M_n (after coaxial electrospinning process).

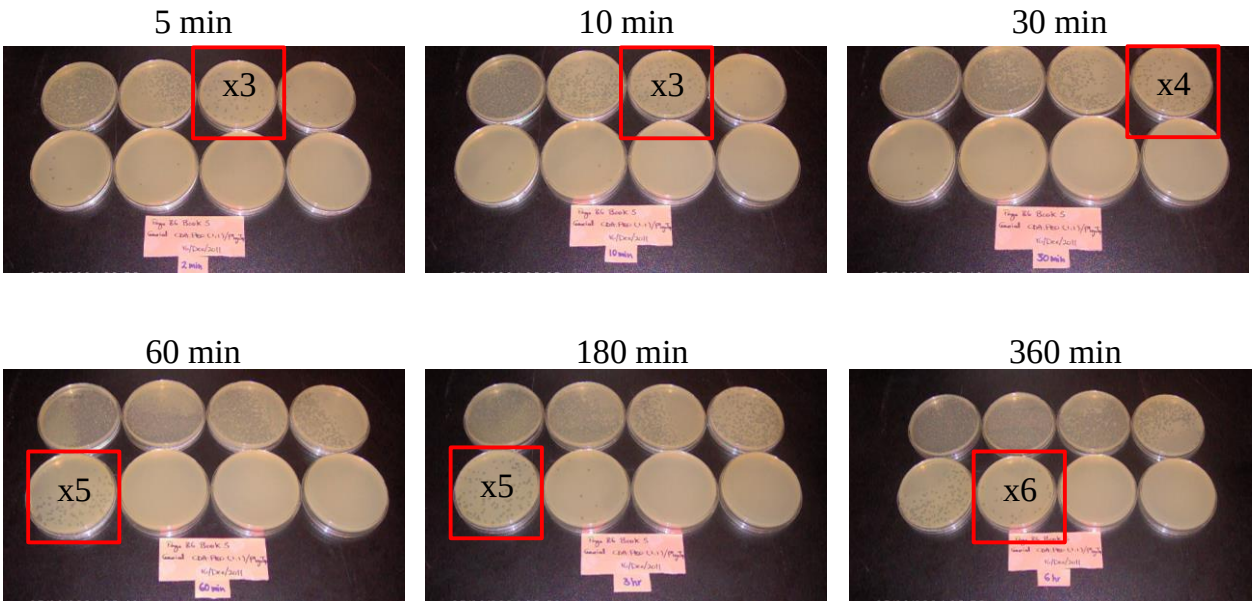

Figure A21: Activity measurement of T4 bacteriophage at different time of release from core/shell electrospun PEO:CDA fibre, 50:50 %wt, 100:30k M_n (after coaxial electrospinning process).

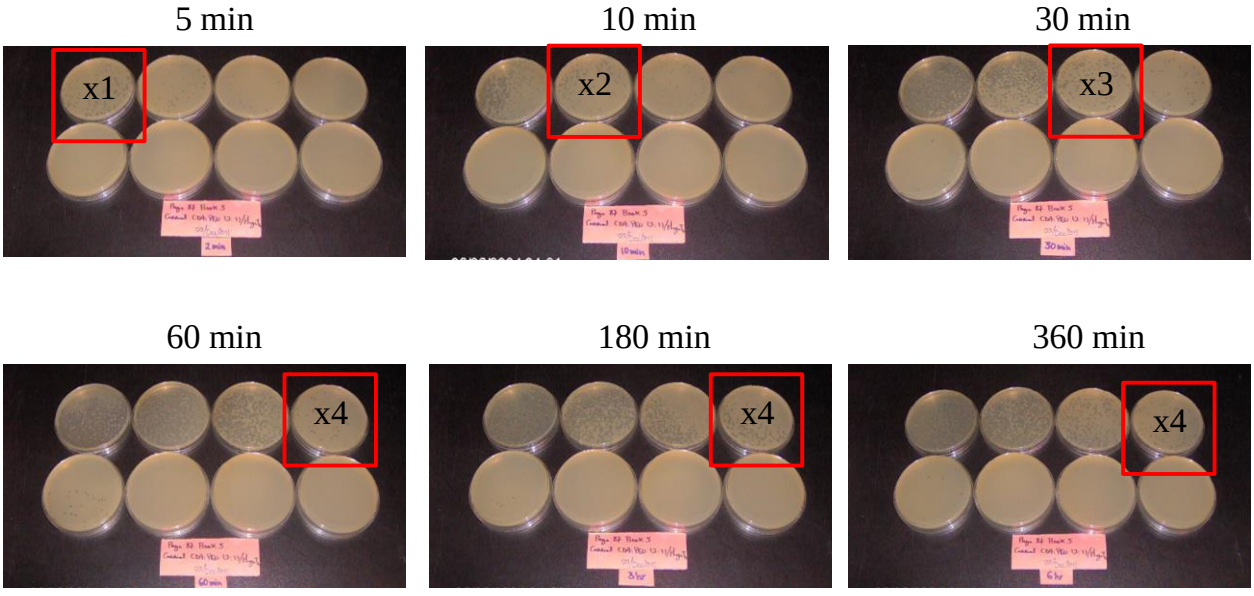

Figure A22: Activity measurement of T4 bacteriophage at different time of release from core/shell electrospun PEO:CDA fibre, 35:65 %wt, 100:30k M_n (after coaxial electrospinning process).

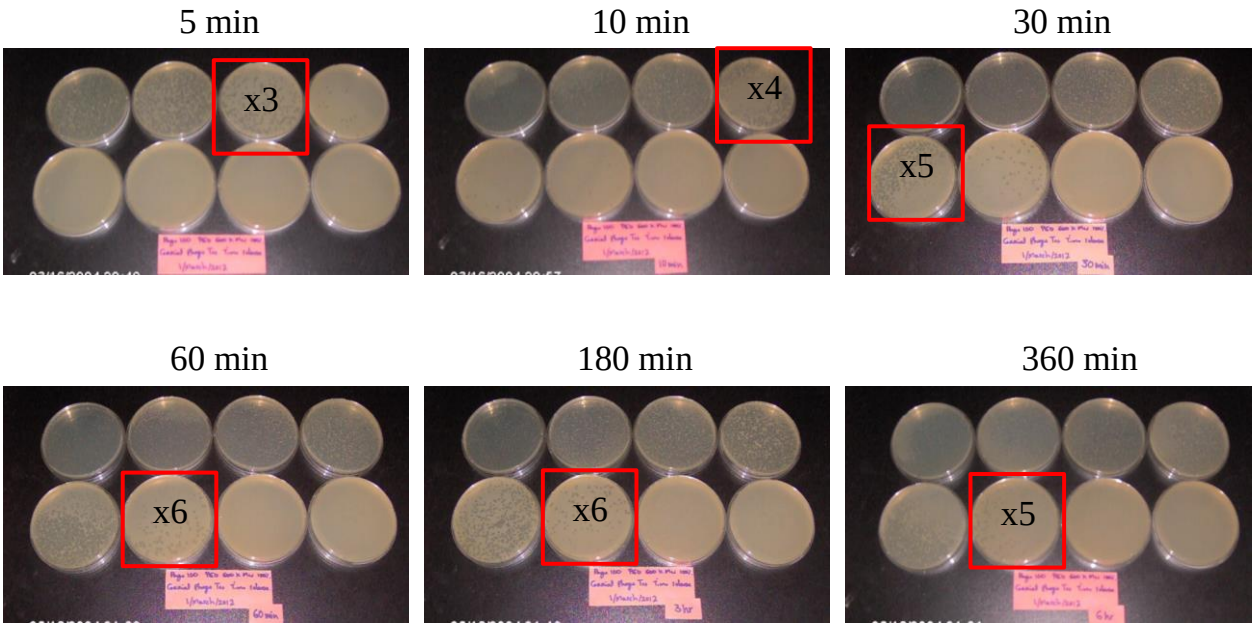

Figure A23: Activity measurement of T4 bacteriophage at different time of release from core/shell electrospun PEO fibre, 600k M_n (after coaxial electrospinning process).

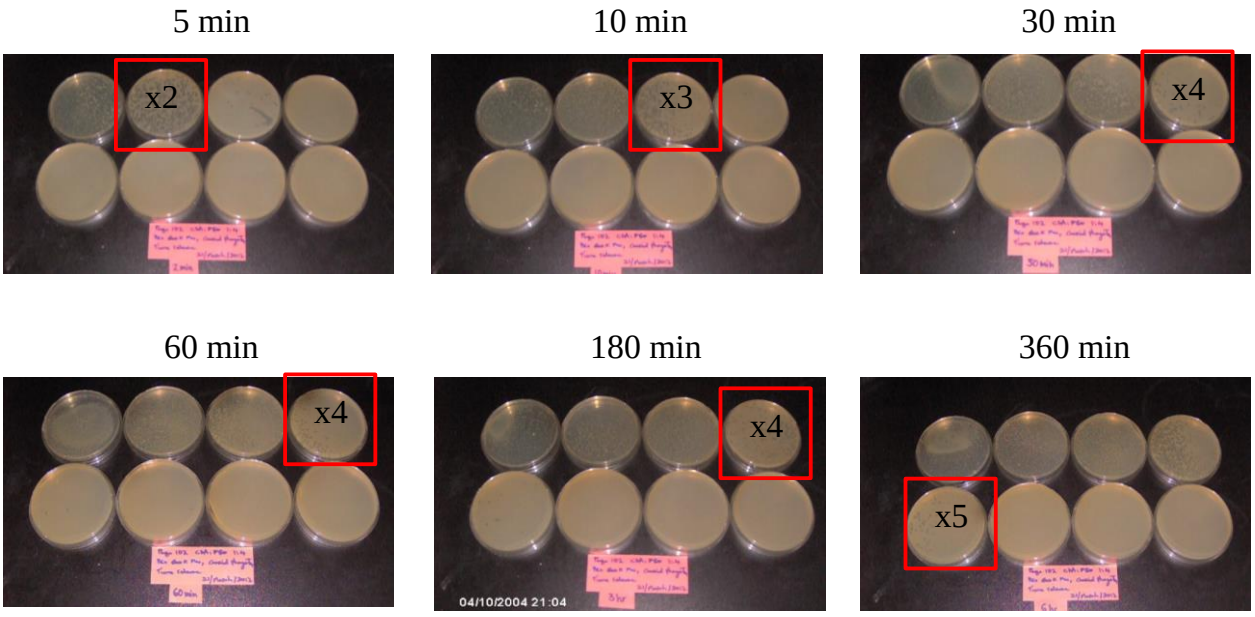

Figure A24: Activity measurement of T4 bacteriophage at different time of release from core/shell electrospun PEO:CDA fibre, 80:20 %wt, 600:30k M_n (after coaxial electrospinning process).

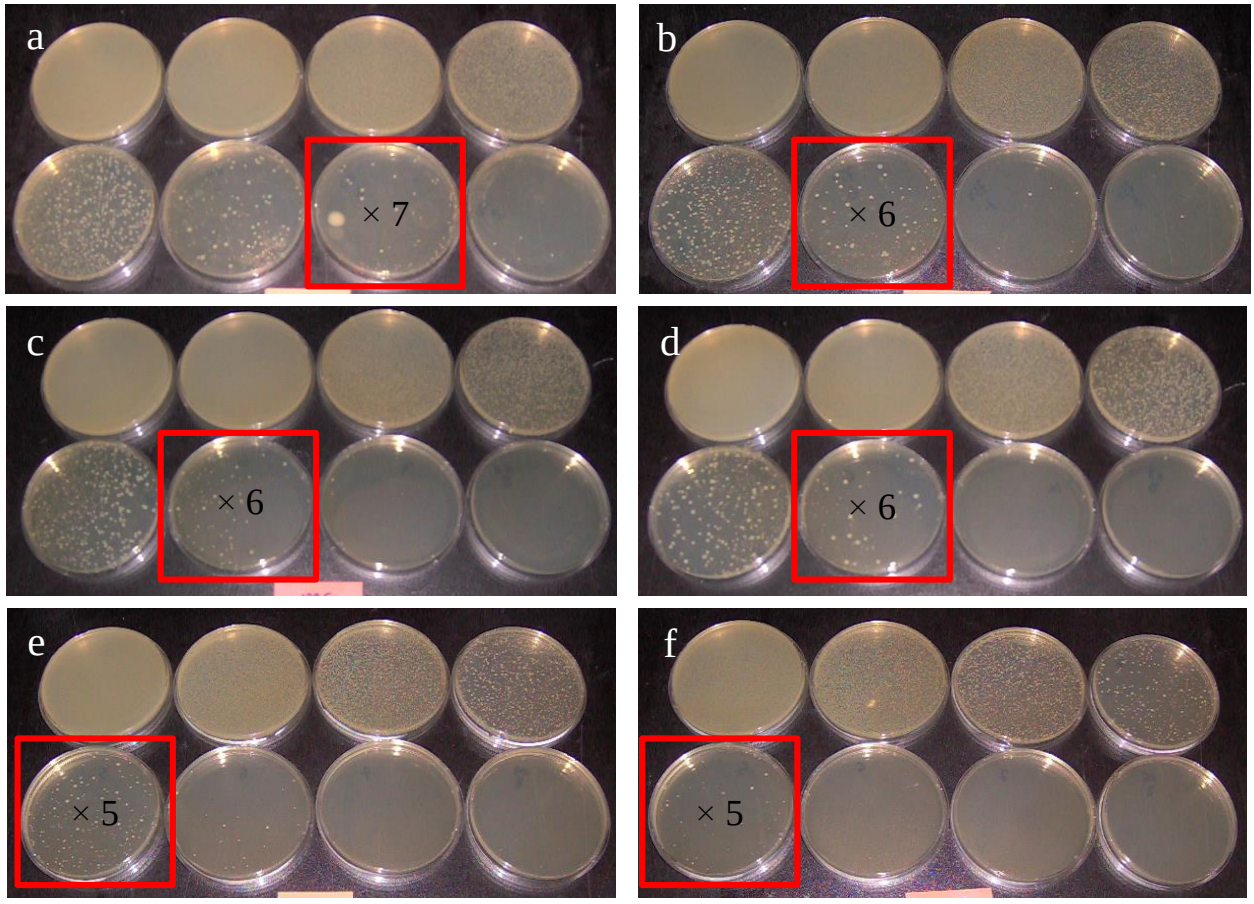

Figure A25: *E. coli* activity measurement performed by serial dilution test for a) original stock of overnight cultured in TSB, b) ×2 dilution in TSB, c) ×3 dilution in TSB, d) ×4 dilution in TSB, e) ×5 dilution in TSB and f) ×6 dilution in TSB.

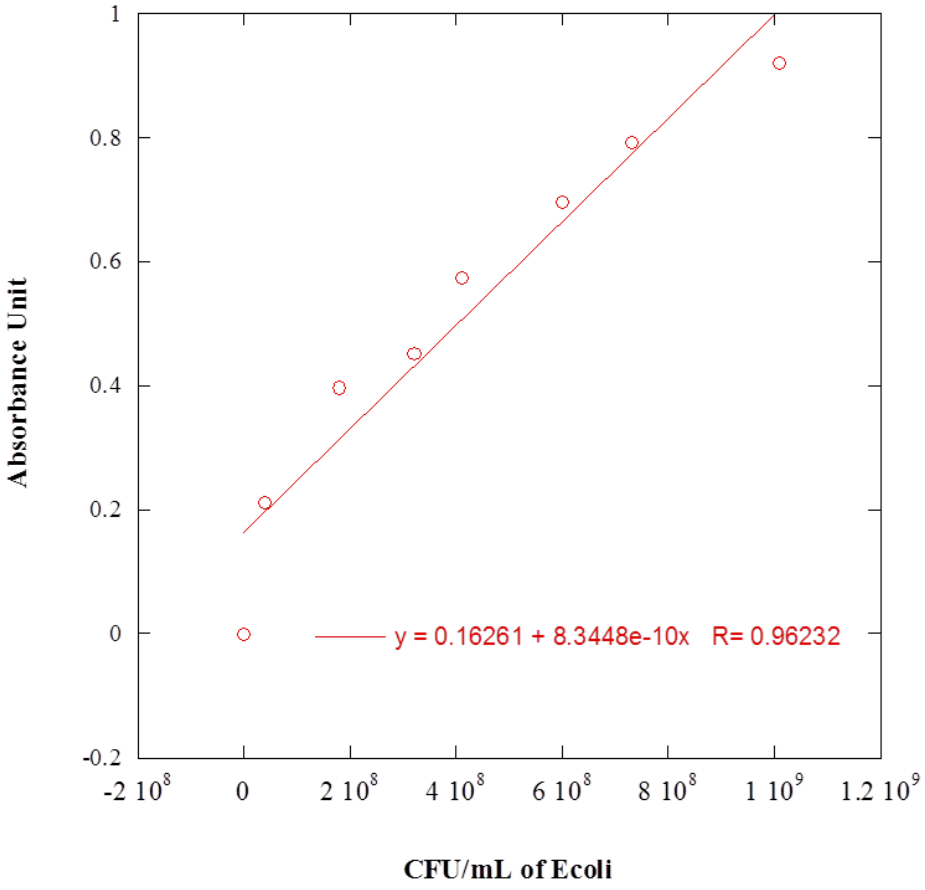

Figure A26: Concentration conversion standard curve for *E. coli* grown in TSB media.

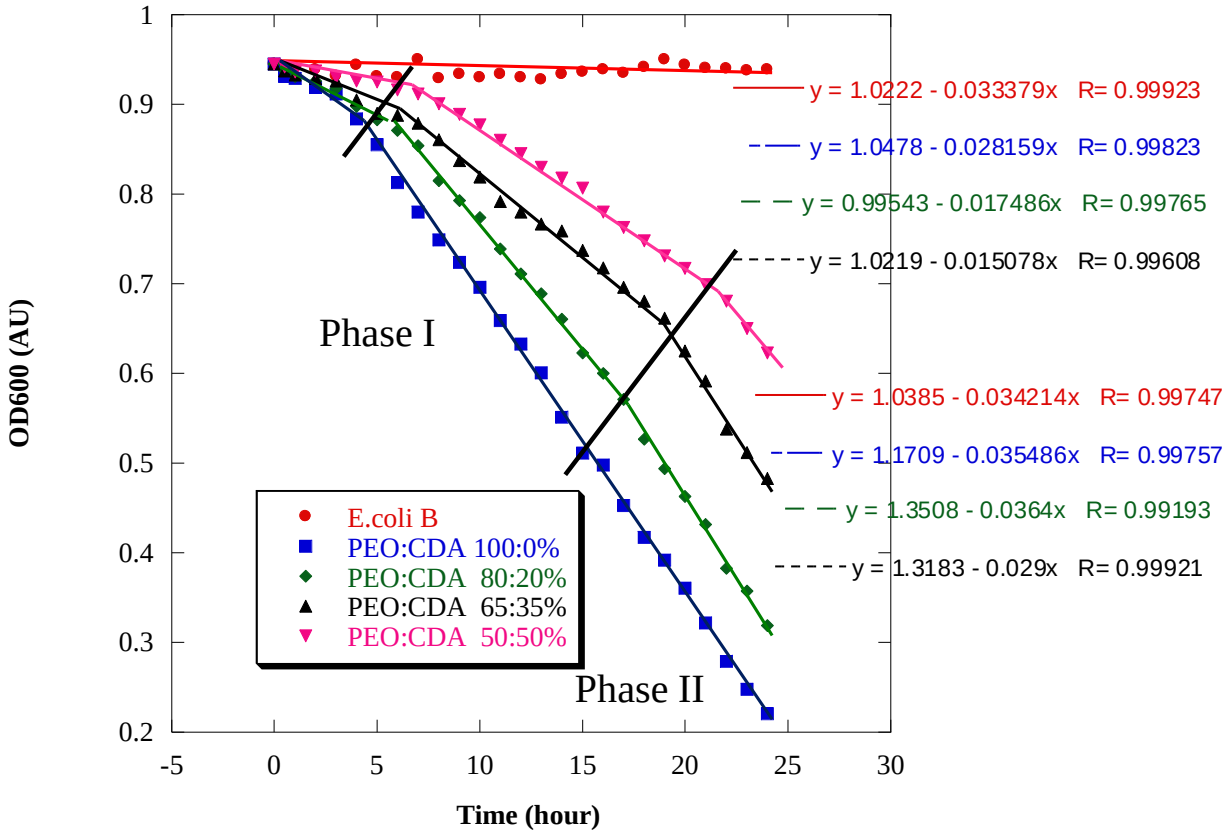

Figure A27: Slope of curve from OD600 cell density of the infected *E. coli* with T4 bacteriophage activated electrospun PEO/CDA blend fibre

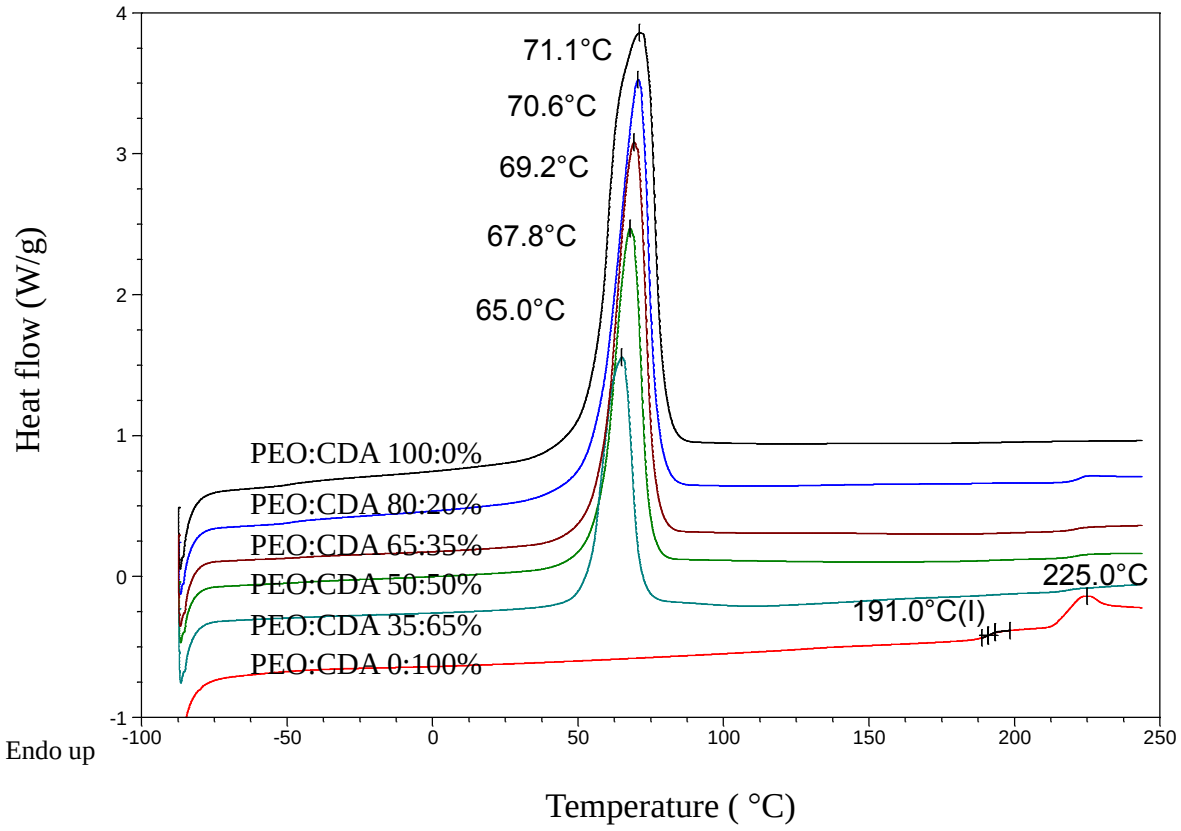

Figure A28: DSC analysis of electrospun fibres of PEO:CDA (100:30 k M_n) at different blend ratios. T_g and T_m were recorded as midpoint temperatures of the heat capacity transition and peak temperature of the heat capacity transition, respectively, from the second heating run. Samples were run in duplicate and they were within experimental error of each other (1.0 °C).

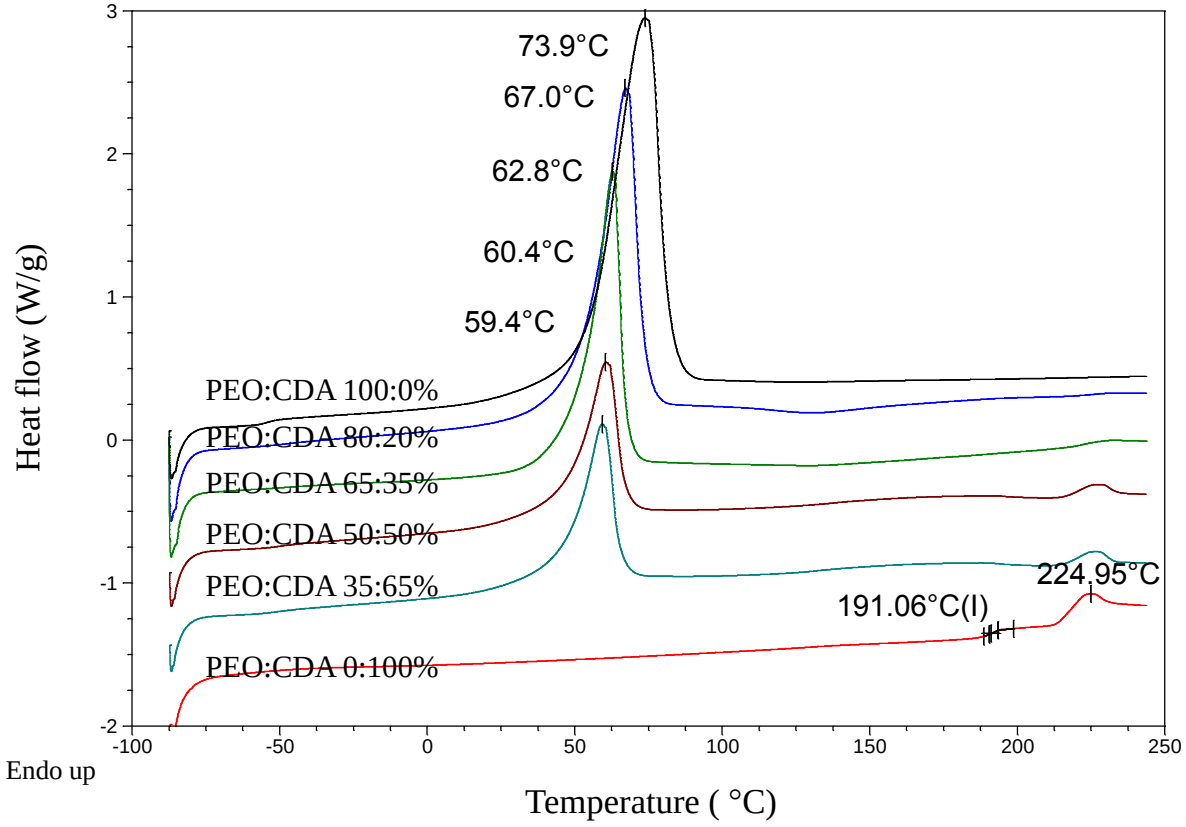

Figure A29: DSC analysis of electrospun fibres of PEO:CDA (600:30 k M_n) at different blend ratios. T_g and T_m were recorded as midpoint temperatures of the heat capacity transition and peak temperature of the heat capacity transition, respectively, from the second heating run. Samples were run in duplicate and they were within experimental error of each other (1.0 °C).

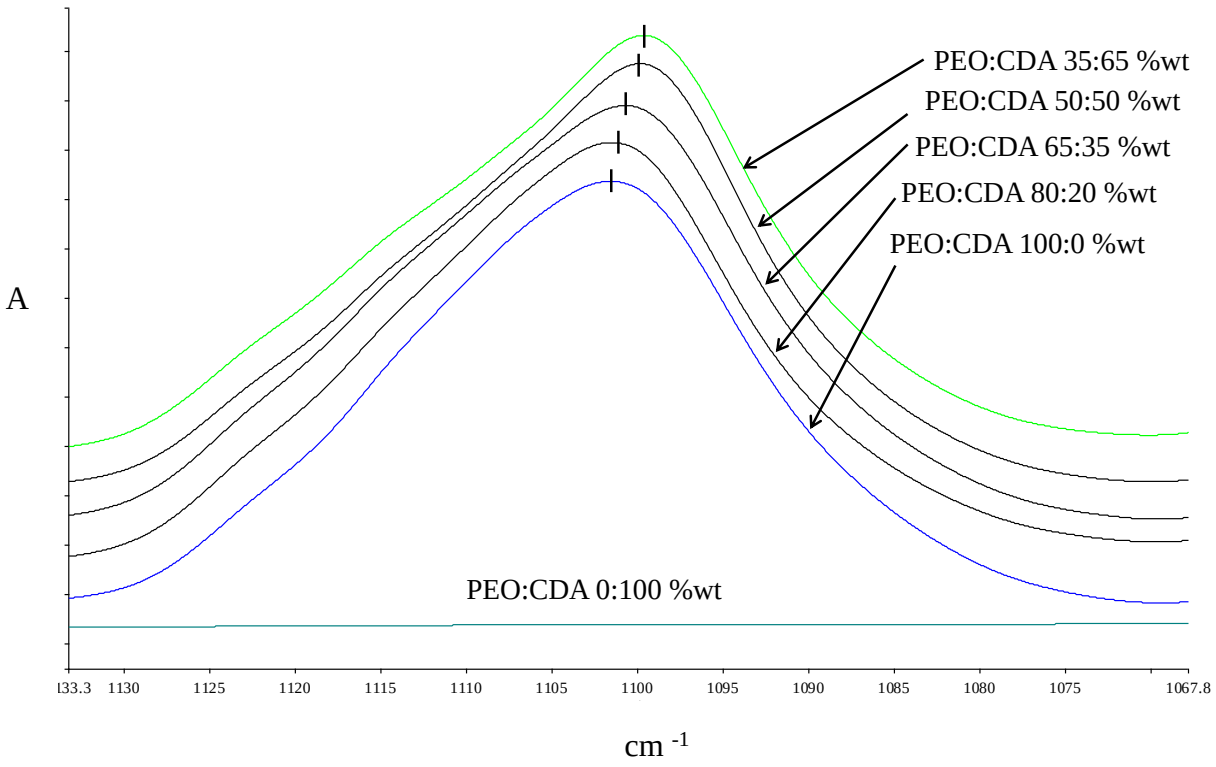

Figure A30: FTIR analysis of the various PEO/CDA (100:30 k M_n) polymer blend electrospun fibres. All spectra were normalized to one at range of 1069 to 1138 cm^{-1} and they were separated from each other to show the hypsochromic shift, a change to shorter wavelength, with addition of CDA.

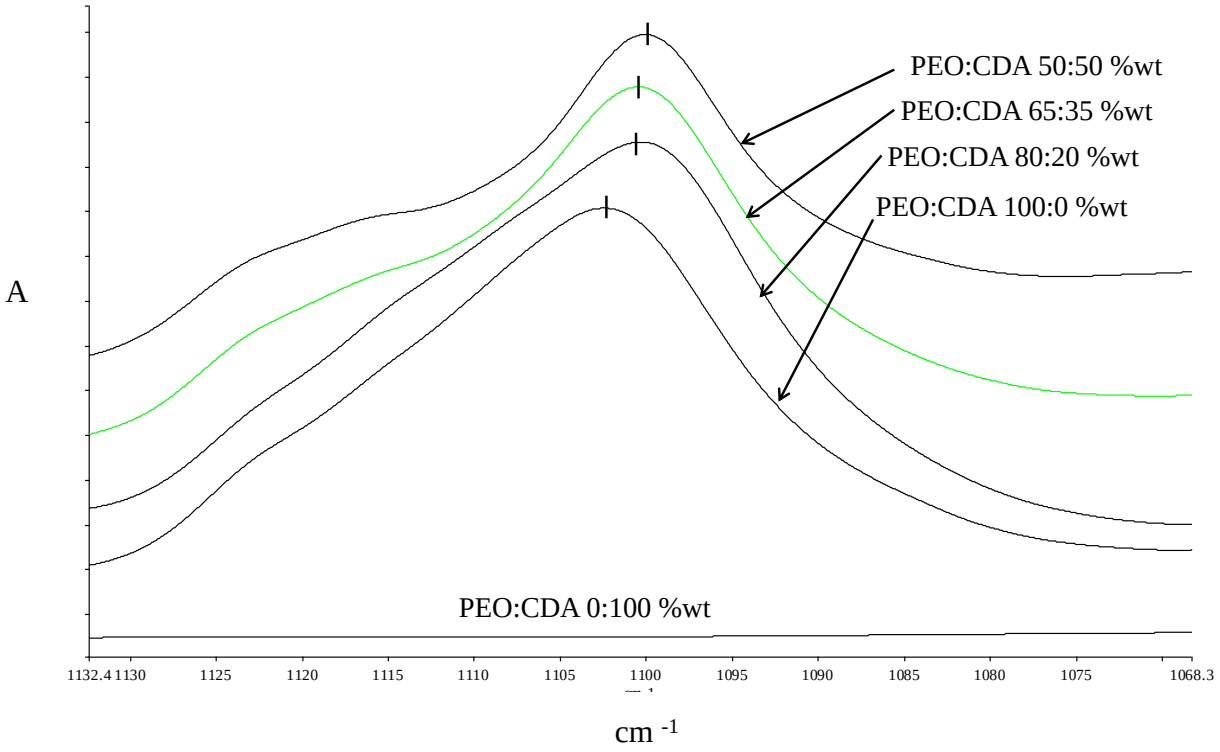

Figure A31: FTIR analysis of the various PEO/CDA (600:30 k M_n) polymer blend electrospun fibres. All spectra were normalized to one at range of 1069 to 1138 cm^{-1} and they were separated from each other to show the hypsochromic shift, a change to shorter wavelength, with addition of CDA.

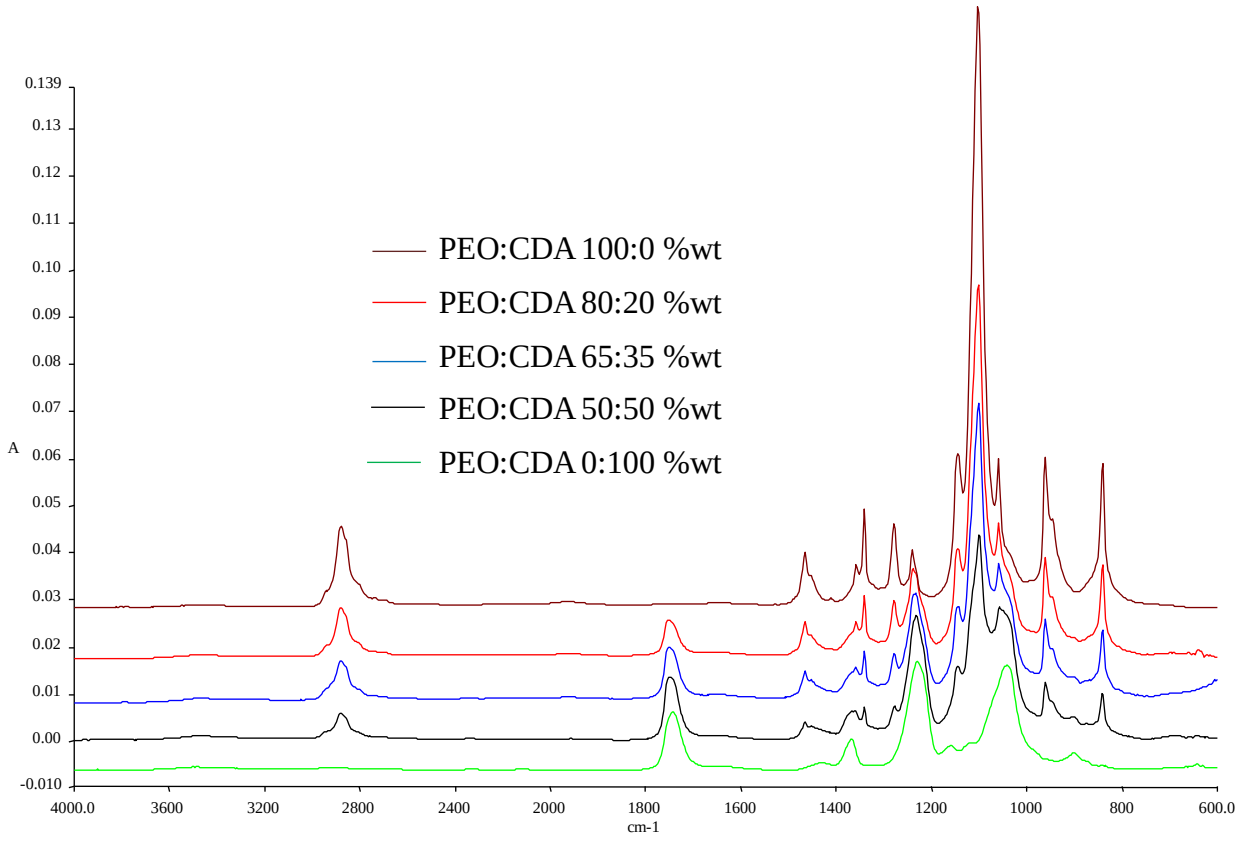

Figure A32: FTIR analysis (full spectrum 600 to 4000 cm^{-1})of the various PEO/CDA (100:30 k M_n) polymer blend electrospun fibres.